INJECTION MOLDING OF FLAX FIBER BIOCOMPOSITES BY SIMULATION AND OPTIMIZATION

A Thesis Submitted to the College of Graduate and Postdoctoral Studies

in Partial Fulfillment of the Requirements

for the Degree of Master of Science

in the Division of Biomedical Engineering

University of Saskatchewan

Saskatoon, Saskatchewan

Canada

By

Dong He

PERMISSION TO USE

In presenting this thesis in partial fulfillment of the requirements for a Postgraduate degree from the University of Saskatchewan, I agree that the Libraries of this University may make it freely available for inspection. I further agree that permission for copying of this thesis in any manner, in whole or in part, for scholarly purposes may be granted by the professor or professors who supervised my thesis work or, in their absence, by the Head of the Department or the Dean of the College in which my thesis work was done. It is understood that any copying or publication or use of this thesis or parts thereof for financial gain shall not be allowed without my written permission. It is also understood that due recognition shall be given to me and to the University of Saskatchewan in any scholarly use which may be made of any material in my thesis.

Requests for permission to copy or to make other use of material in this thesis in whole or part should be addressed to:

Head of the Division of Biomedical Engineering
57 Campus Drive
University of Saskatchewan
Saskatoon, Saskatchewan, S7N 5A9, Canada

ABSTRACT

Flax (*Linum usitatissimum)* fibers have the advantages of low density, low cost, and recyclability and are considered as a potential material to reinforce plastic materials. Though Canada is one of the largest seed flax growing countries in the world, the utilization of flax fibers as reinforcement in composites is not as developed as in Europe. Indeed, in Canada, a large amount of flax straws are left in the fields and burned by farmers each year. Therefore, development of technologies to make use of flax straws for reinforcement in composites and for other purposes has huge benefits to both the material industries and flax farmers in Canada.

This thesis presented a study of flax fibers reinforced biocomposites by injection molding through modeling and optimization. The focus of the study was to understand the relationships between the properties of biocomposites and the processing conditions through the experiment and improve the qualities of biocomposites by optimizing the processing conditions.

In this thesis, biocomposites were successfully produced by injection molding with a proposed processing scheme. The influence of flax fiber loading and processing conditions, including injection temperature and pressure on the mechanical properties (tensile properties and flexural properties), and water absorption of biocomposites was investigated. The study also experimentally investigated the effect of the processing conditions (fiber content and temperature) on the rheological properties of biocomposites. In order to implement the simulation analysis of injection molding for biocomposites, the Cross-WLF model was employed to obtain the rheological information of biocomposites. Further, a systematic approach on simulation analysis and optimization of injection molding was proposed to minimize the shrinkage and warpage of biocomposites.

Several conclusions are drawn from this study:

1) With respect of the influence of the processing conditions on the properties of biocomposites, (a) Fiber content is the most significant impact factor influencing the mechanical properties of

biocomposites compared with the other two processing conditions and the tensile properties and flexural properties of biocomposites dreamingly increased with flax fiber content; (b) lower injection temperature led to higher tensile properties and flexural properties; (c) Water absorption of biocomposites was significantly dependent on fiber content and injection temperature; (d) Injection pressure had no significant effect on either mechanical properties or water absorption.

2) In the study on the rheological characteristics, (a) The shear viscosity of biocomposites increased with fiber content, but at very high shear rates (from 5,000 to 10,000 S−1), the shear viscosities of biocomposites with various fiber content (from 0 to 30%) tended to be the same; (b) The shear viscosity of biocomposites decreased with temperature, and at higher shear rate, all the shear viscosity variations as function of shear rates followed the same rate for different temperatures; (c) At high shear rate, the shear viscosity mostly depended on the shear rate rather than fiber content and temperature; (d) A method was presented to determine the seven parameters of the Cross-WLF model for biocomposites.

3) For minimizing the shrinkage and warpage of injection molded biocomposites, (a) The significant factors on the shrinkage and warpage of biocomposites by injection molding were injection temperature, packing time, and packing pressure; (b) The optimization of the injection molding of biocomposites for reducing the shrinkage and warpage of biocomposites was successful by integrating design of experiment (DOE) and simulation technique.

The contribution of this thesis includes:

1) In the field of biocomposites reinforcement, the study has shown a great promise to use flax fibers to enhance the mechanical properties of thermoplastics, in particular an increase of 41.83% in tensile strength and an increase of 47.13% in flexural strength. In addition, this work has provided a mathematical relationship between the processing condition of injection molding and the mechanical properties of biocomposites, which would be important to control the manufacturing process to reach desired mechanical properties.

2) In the field of optimal design and manufacturing of flax fiber biocomposites, this work has provided: (a) an effective method to determine the parameters in the rheology model of the

biocomposites melt, which has been an important step in simulating the process, and this method has a generalized implication to other types of biocomposites; and (b) a systematic approach to optimize the injection molding process for minimizing the shrinkage and warpage of biocomposites, which are the two most important quality issues in biocomposites.

ACKNOWLEDGEMENTS

I would like to express my sincere gratitude to my supervisor Professor W.J. (Chris) Zhang, who provided me with dedicated guidance, broad knowledge, and continuous encouragement through my master study. His enthusiasm and dedication on his work has impressed and influenced me greatly. I would also like to acknowledge his moral and financial support. I appreciate all what he has provided me during my whole life.

I would also like to thank my co-supervisor Professor R. Lal Kushwaha for giving his guidance and help. I am also deeply thankful to my CNH industrial research advisor Dr. Satya Panigrahi, and appreciate his expertise and guidance on this research. Appreciation also goes to other members of my advisory committee, Professor Assem Hedayat, and Professor Duncan Cree for providing me valuable suggestions and ideas which greatly improved my research.

Thanks to Jim Henry in CNH for supporting my project. Special thanks go to Louis Roth and Jimmy Fung for helping me set up the test-bed and guiding me for all of my experiments. Without their help, I could not have finished this thesis.

Many thanks to my friends for their help and support in my study. They are Dr. Bing Zhang, Dr. Xiaohua Hu, Dr. Jun Liu, Dr. Yu Zhao, Hu Wang, Jialei Huang, Ang Chen, Fan Fan and Xu Wang.

I would also like to acknowledge the financial support from the Developed Scholarship in Division, NSERC grant by Professor R. Lal Kushwaha, and DG grant by Professor W.J. (Chris) Zhang.

Last but not the least, I want to express my deepest gratitude to my family in China. My parents Yanxin He and Jingui Li and my brother Xi He have been very supportive and understanding for every decision I have made over the years.

TABLE OF CONTENTS

LIST OF TABLES

LIST OF FIGURES

LIST OF ABBREVIATIONS

DOE	design of experiments
CAE	computer aided Engineering
RSM	response surface method
GA	genetic algorithm
ANN	artificial neural network
ANOVA	analysis of variance
PP	polypropylene
HDPE	high-density polyethylene
ASTM	American Society for Testing and Materials
CCD	central composite design
BBD	Box–Behnken design

CHAPTER 1 INTRODUCTION

1.1 Motivation

Conventional fiber reinforced composites are made of polymer matrixes with synthetic fibers. These have largely been applied to modern industries such as aerospace, ship, automotive, sport equipment, and civil infrastructure (Mallick, 2007) because they can offer better strengths and stiffness, compared with the pure polymers. The synthetic fibers are usually glass fiber, carbon fiber, and aramid fibers. They are expensive, non-renewable and non-recyclable. In recent decades, natural fibers as an alternative reinforcement in fiber reinforced composites have received ever increasing attention, both from the academic world and from industries due to their advantages of low density, low price, specific properties, non-toxic, recyclability and renewability over traditional synthetic fibers (Saheb & Jog, 1999; Mohanty et al., 2000; Monteiro et al., 2009).

Natural fibers are subdivided into groups in terms of their origins and sources from plants, animals, or minerals. For the purpose of reinforcements, the fiber is extracted from plant fibers such as cotton, flax, hemp, jute, ramie, coir, and sisal. Among them, the bast fibers (flax, hemp, jute, etc.) are commonly used due to their suitable properties and readily availability. As one of the bast fibers, flax fibers are of particular significance to this study.

Flax (*Linum usitatissimum)* fibers are originated from flax, and flax is an annual crop which is usually used for edible seed. Flax fibers have widely been used as reinforcement in composites in the industries of Europe (Bos, 2004). Though Canada is one of the largest seed flax growing countries in the world, the utilization of flax fiber as reinforcement in composites in Canada is not as developed as in Europe. Indeed, in Canada, a large amount of flax straw is left in the fields and burned by farmers each year. Therefore, development of technologies to make use of flax straws for reinforcement in composites will have huge benefits to both the material industries and flax farmers in Canada.

Natural fiber reinforced composites, also referred to as biocomposites, are usually manufactured with the injection molding technology. Injection molding is one of the most important manufacturing processes for polymeric products and biocomposites. In injection molding, both the quality of the part and performance of the production depend not only on material properties, the shape of the part but also on how the material is processed during molding.

In short, there are two categories of parameters: process parameters and design parameters. The process parameters refer to the parameters such as fiber content, temperature and pressure. The design parameters refer to the parameters such as the product geometrical shape and size. Processing of materials to particular shapes of parts will lead to the parts with the desired properties, which then would meet particular needs of applications (e.g., agricultural machinery).

General research questions are raised as follows:
Question 1: What would be the best injection modeling process to make flax fiber composites (or biocomposites) given a class of parts?

Question 2: What are the scientific reasons behind the aforementioned best injunction molding process?

1.2. Objectives with their scope

This study attempted to generate answers to the above questions. The overall objective of the study was to develop injection molding technologies for biocomposites to achieve their best geometrical and mechanical properties and to maximize their usage in machinery (e.g., agricultural machinery and automotive machinery). To achieve this overall objective, the following specific objectives were defined for this study.

Objective 1: Establish a test-bed with an effective method to process flax fiber reinforced biocomposites with injection molding such that all the factors or parameters in the process can be covered

Objective 2: Understand and build the relationship between the process or operating parameters including the material composition of parts and the properties of the parts

Objective 3: Identify the main factors influencing the rheological properties of biocomposites during the processing

Objective 4: Develop an effective approach to improve the quality of injection molded biocomposites

Remark 1: In this study, the design parameters of parts are usually assumed to be known and their influence to the injection modeling process and the properties of parts is not concerned. However, whenever possible, the influence of the design to manufacturing will be observed to give some general guidelines to the design.

Remark 2: The properties of parts include geometrical property (shape and dimension), mechanical property (tensile strength and flexural strength, and water absorption).

1.3 Organization of the thesis

This thesis consists of six chapters. The remaining five chapters are outlined as follows:

Chapter 2 provides a literature review to further confirm the need and significance of the research objectives as described before. The literature review is focused on the effect of on the properties and the qualities of injection molded biocomposites.

Chapter 3 establishes a test-bed with an effective method to produce flax fiber reinforced biocomposites by injection molding and investigate the effect of processing conditions on the properties of injection molded biocomposite products.

Chapter 4 investigates the factors influencing the rheological properties of biocomposites and presents a method to determine the parameters of the Cross-WLF model (a rheological model used for the simulation of the injection molding process) for biocomposites.

Chapter 5 proposes a systematic approach on simulation analysis and optimization of injection molding for minimizing the shrinkage and warpage of biocomposites.

Chapter 6 concludes the thesis with discussion of the research results, contributions, and future work.

CHAPTER 2 BACKGROUND AND LITERATURE REVIEW

2.1 Background

Nature fibers are more and more often applied as the reinforcement of biocomposites. Their availability, sustainability, low density, and price as well as satisfactory mechanical properties make them an attractive ecological alternative to synthetic man-made fibers used for the manufacturing of biocomposites.

Lower specific density and reinforcement characteristics of the natural fibers lead to weight savings and high strength in composites, which has direct advantages for various industrial applications. The use of biocomposites has reduced the impacts on the environment. Lightweight structures have increased fuel efficiency in cars, buses, ships and some others. The biocomposites containing natural fibers are more environmentally friendly and are used in transportation, building and construction industries. Houses may be built in earthquake zones (e.g., BC in Canada) using lightweight biocomposites and therefore, may help in reducing the impact on human life when disaster strikes. Biocomposites have already proven their worth as weight-saving materials; the current challenges are to make their properties match to conventional plastic and be cost effective according to market needs.

Agricultural based biocomposites have a great future all around the World. Canada has a strong potential to contribute agricultural straws (e.g., flax, industrial hemps, and switch grass wheat straws.) for biocomposite industries each year. Biocomposites can be easily recycled and also disposed of or composted without harming the environment at the end of their life. It is essential that there be an integrated effort in design, material, process, tooling, quality assurance, manufacturing, and even program management for biocomposites to become competitive with petroleum based plastic and its composites. According to the report of Flax Council of Canada (FCC, 2015), Canada has been the world's leading producer and exporter of flax since 1994. More than half of Canadian flax is produced in Saskatchewan, with the remainder grown in Manitoba and Alberta. Overall in the Canadian Prairie Provinces, the amount of potential salvageable oilseed

flax straws is annually 400,000 to 1,000,000 tones and Saskatchewan has the largest producer to oilseed flax, regularly exceeding 500,000 tonnes in 2015 (FCC, 2015). But not a single industry is engaged in processing high quality flax fiber-based commercial products. Thus, flax straw has been burned by most of the farmers across the prairies. Hence, there is a need of research for developing value-added flax fibers and along with other bast fibers and straws.

It is important to investigate how flax fibers can be used and optimized for their loading in the polymer matrix to enhance the properties of the composite materials such that it can be used to develop the injection molded product for agricultural equipment manufacturer such as CNH Saskatchewan.

2.2 Material properties

2.2.1 Flax fiber

The basis for the strength and stiffness of the flax fibers is their composition of cellulose, hemicellulose and lignin. Among these, the cellulose is the import part because it has the high strength and stiffness, while the hemicellulose and lignin form a sort of "glue", holding the cellulose units (microfibrils) together and allowing them to work in combination. The amount of cellulose and non-cellulosic proportion in a fiber determines the structural properties. Typical compositions of cellulose fibers are listed in Table 2.1 (Liholt & Madsen, 2012). It is noted that flax fibers have the highest cellulose content, and thus they have the best potential to form strong and stiff fibers for composites.

Table 2.1 Composition of cellulose fibers (Liholt & Madsen, 2012).

Fiber	Cellulose (mass%)	Hemicellulose (mass%)	Lignin (mass%)
Flax	80	15	5
Hemp	75	20	5
Wheat straw	40	30	20
Soft wood	40~50	20~30	25~35
Hard wood	40~50	25~40	20~25

The flax fibers have great strength, fineness and durability. The increasing application of natural fiber-reinforced plastic offers advantages in the density, cost, availability, degradability, biodiversity (Kromer, 2009). The cost of flax fibers is nearly three time cheaper than that of glass fibers that are often used in the composite application. One of the outstanding properties of flax fibers is that these can withstand processing temperatures up to 250ºC (Sreekala et al., 2000) and this makes them suitable for making biocomposites with polymers. Because of the relatively low density of flax fibers, their specific mechanical properties (i.e., the properties divided by the density) can even be comparable to those of glass fibers; see Table 2.2 (Bos, 2004). For the automotive industry, weight reduction is always an issue and this is the primary reason that more and more automotive parts use flax fibers instead of man-made fibers as reinforcements in composites.

Table 2.2 Mechanical properties and specific properties between flax fiber and glass fiber (Bos, 2004).

Property	Glass fibers	Flax fibers
Diameter [μm]	8-14	10-80
Density [g/cm^3]	2.56	1.4
Young's modulus [GPa]	76	50-70
Tensile strength [GPa]	1.4-2.5	0.5-1.5
Elongation to fracture [%]	1.8-3.2	2-3
Specific Young's modulus [GPa / (g/cm^3)]	30	36-50
Specific tensile strength [GPa/ (g/cm^3)]	0.5-1	0.4-1.1

Flax fibers show very good tensile mechanical properties; however, during processing of the fibers, the good mechanical properties may be lost with the formation of dislocations of flax fibers. It has been shown that these defects can lower the stiffness of the fiber (Davies & Bruce, 1998) and lead to non-linear tensile deformation behavior (Baley, 2004). When flax fibers are used as reinforcement in thermosetting polymer matrix composites, the presence of dislocations can lead to stress concentrations at the interface and in the matrix, resulting in the microstructural damage

(Hughes et al., 2000) and this in turn can lead to yielding behavior at low levels of stress and strain (Hughes et al., 2007) and to lower composite toughness. Clearly, these will have a direct impact on the application of natural fiber reinforced composites.

Another significant factor that can affect the properties of flax fibers is moisture absorption. Accessible hydroxyl groups present in the cell wall polymers of plant fibers are able to attract water molecules and bind them through hydrogen bonds, rendering the fibers hydroscopic (Thakur at el., 2014). Water molecules can continue to be adsorbed by the polymers in the cell wall, to a point where the cell wall becomes saturated. The total amount of water in the plant fiber is known as its moisture content. When placed in certain conditions of relative humidity and temperature, the fiber would establish an equilibrium moisture content with those surroundings, so the moisture content of the fibers always varies with those surroundings.

Changes in the fiber's moisture content lead to dimensional changes occurring mainly in the transverse direction; when the moisture is lost, the fiber shrinks, and when the moisture content increases, it swells. This can be problematic when the fiber is used as composite reinforcement, since the dimensional changes can lead to tensile stresses normal to the interphase, which can result in fiber-matrix debonding if the adhesion between fiber and matrix is not sufficiently strong. Another effect of the moisture is to alter the mechanical properties of the fiber (this is partly the reason why wood is dried prior to use: dried wood is stronger and stiffer than "green" wood). In general, an increase in moisture content leads to a decrease in mechanical properties. High moisture contents, close to the fiber saturation point, can result in biological degradation of the fiber and to a rapid loss in its mechanical properties.

Recent studies on flax fiber biocomposites have shown that the effect of water sorption on the mechanical properties of biocomposites limits their outdoor applications (Stamboulis at el., 2001; Assarar at el., 2011). To reduce moisture sorption, to enhance fiber-matrix adhesion and to reduce biodegradation, flax fibers are often modified by chemical or physical treatments in order to render them more suiTable As composite reinforcement. Common treatments include mercerization/alkali treatment, silane treatment, acylation, esterification, enzymatic treatment,

peroxide treatment, coatings, and impregnation with a dilute epoxy. Some typical treatment methods from published articles are collected in Table 2.3.

Table 2.3 Different treatments of flax-reinforced composites.

Fiber/matrix	Treatment	Conditions	Effect on properties	Ref.
flax/PP	esterification	10 wt % MA, 25h, 50 ℃	highest flexural and tensile strength	(Cantero at el., 2003)
flax/phenolic	esterification	25 wt % MMA, 30min, 210 W	more moisture retardant	(Kaith & Kalia, 2007)
flax/epoxy	alkali treatment	5 wt % NaOH, 30 min	tensile strength 21.9%; flexural strength 16.1%	(Yan at el., 2012)
flax/epoxy	alkali treatment	4 wt % NaOH, 45 s	transvers strength, 30% increment	(Van de W. at el., 2006)
flax/polyester	silane treatment	0.05 wt %, 24 h	hydric fiber/matrix interface	(Alix at el., 2011)
flax/pp	esterification	MA-PP coupling agent	interphase compatibility	(Bledzki at el., 2004)

In this study, flax fibers will be modified by using the silane treatment. This treatment method has been proved to be effective for improving the adhesion between fiber and matrix by the literature investigation and the previous experiment studies in our group.

2.2.2 Matrix

A composite material can be defined most simply as a two-phase assembly consisting of a matrix and its reinforcement (flax fibers in this study). Flax fibers bring high mechanical properties, and the role of the matrix is to distribute external loads between fibers and to protect them. According to the types of matrices used in flax fiber reinforced composites, they can be divided into the two main categories: thermoplastic polymers and thermosetting polymers.

The early natural fiber composites use thermosetting matrices because during heat processing thermosets can form cross-linking bonds, which extremely improve the mechanical properties of the composites when applying the thermosets as the matrices in natural fibers composites. But they are not capable of being re-melted since the cross-link is an irreversible chemical bond. While the process for thermoplastics is completely reversible without the formulation of chemical bonds, which allows thermoplastics to be re-melted and recycled. Thus, more recently, thermoplastics are being used in natural fibers reinforced composites, because they are more ecological, have better impact behavior and shorten process cycle time of composites.

In this study, one of the most frequently used thermoplastic matrices is considered, namely polypropylene (PP) because PP has the advantages of low density, good mechanical properties, excellent process ability, good dimensional stability and recyclability (Van de Velde & Kiekens, 2001). In the literature, many researches (Joshi et al., 2004; Andersons et al., 2006; Modniks & Andersons, 2010) have studied the suitability and capabilities of flax fibers embedded in PP. In order to get the composites with the better properties, the studies for the flax fiber PP composites are mainly concentrated on the points of the materials, which include the fiber the ratio of constituents (fibers and matrix) and the compatibility of fiber and matrix.

Modniks & Andersons (2010) and Andersons et al. (2011) inverstigated the effect of fiber content and length on the mechanical properties of flax fiber reinforced PP biocomposite. Flax fiber content had a significant effect on the final mechanical properties of biocomposites. The critical length of flax fibers was concluded to be reduced by the addition of MAPP in PP matrices. Van den Oever et al. (2000) studied the influence of physical structure of flax fibers on mechanical properties. The results stated that the hackled flax fiber removed some weak lateral bonds and with reduced tensile and flexure strength of biocomposites. To improve the adhesion between flax fiber and PP, Arbelaiz at el. (2005) and Arbelaiz at el. (2006) investigated the influence of the modification of both flax fiber and PP, fiber content, water uptake and recycling. Boiling of flax fiber and chemicals treatment for flax fiber or PP were proven to be good for adhesion modification in order to increase mechanical properties of biocomposites. Chabba & Netravali (2005) studied moisture absorption and environmental durability of flax fiber reinforced PP biocomposites. At

room temperature, composites absorbed water towards an equilibrium and then became time-independent.

According to the above review on studies of flax fiber reinforced PP biocomposites, most of the researchers focused on the effect of constituents on the composites. There were limited researches about influence of processing biocomposites. Thus, this study proposes to investigate how to make a better biocomposite through optimizing the processing conditions.

2.2.3 Application of natural fiber reinforced biocomposites

Environmental concerns, the limited resource of the Earth, and the end of cheap petrol are creating opportunities for the use of natural fibers as reinforcement in polymer composites. Natural fibers can offer not only good mechanical properties but also other specific advantages such as renewable cultivation, CO2 storage, low energy consumption during production, durability, biodegradability and incineration potential (Pervaiz & Sain, 2003). Therefore, the applications of natural fiber reinforced biocomposites are growing fast in numerous engineering fields such as automotive, aerospace, boats, sport equipment and construction. Above all, automotive companies are most interested in this new biomaterial and first expanded it to the market (Bledzki et al., 2006).

In last decade, the automotive market has been undergoing massive changes in Europe. Under growing pressure from environmental regulations, builders are tightening specifications for their equipment manufacturers. To reduce CO_2 emissions and shrink the environmental footprint of transportation, the market is demanding more lightweight materials that are recyclable at end of life. In the studies of Le Duigou et al. (2011) and Le Duigou et al. (2012), flax fiber biocomposites are evaluated to be the environment-friendly meterials from the environmental impact analysis of both production of flax fibers and manufacturing biocomposite by the tool of life cycle analysis. Therefore, flax fiber biocomposites can help to meet these new requirements, and have special appeal for builders. In addition, the micro-structural morphology and high modulus of elasticity of the hollow flax fibers impart good sound and vibration damping properties. The fibers can absorb vibrations without deterioration of their mechanical properties, and their morphology also attenuates noise, giving good acoustic comfort.

In current automotive industries, there are mainly two type of car parts which are either already being produced or under development by using natural fiber reinforced biocomposites (Holbery & Houston, 2006; Yan et al., 2014; Pickering et al., 2015): 1) hidden interior parts such as door panels, rear seat shells, sound insulation for bulk heads, rear window shelves, and dashboards; 2) structural parts such as floors, under-the-hood parts, degas tank caps, air ducts for center and side ventilators, and rear-view mirror support flames.

2.3 Injection molding for natural fiber biocomposites

Ho et al. (2012) performed extensive literature review on the fabrication of natural fiber composites. They reported that natural fiber composites are mostly manufactured by conventional composite manufacturing processes, which include compression molding, resin transfer molding, vacuum infusion molding, direct extrusion and injection molding. Injection molding is one of the most common methods of shaping plastic resin. It is widely used for manufacturing a variety of parts, from the smallest component to entire body panels of cars. Compared with other traditional molding processes, it has the advantages of fast cycle times, molding accuracy, relatively low labor of large scale production runs, and a wide range of products (Rosato & Rosato, 2012).

2.3.1 Pre-processing flax fiber for injection molding

For the purpose of producing flax fiber biocomposites, long flax fibers should be chopped into short fibers. In a short fiber composite, there is a certain critical fiber length that represents the optimum effective length of short fibers (Nyström at el., 2007). According to the critical fiber length criterion (Nyström at el., 2007), tensile load should be fully transferred from the matrix to the fiber and the fiber can be loaded to its full capacity. During the process of injection molding, the fiber length is usually shorter than the predicted fiber length because of the fiber attrition. This fiber attrition results in the fiber below length the predicted length, and the actually shorter fibers cannot carry their maximum load effectively. Furthermore, the shorter fiber rather acts as a defect in the biocomposites not only because of the effect of its length, but also of the poor bonding properties. Therefore, it is necessary to carefully predict the critical length of the flax fiber before conducting injection molding.

A certain critical fiber length is defined such that a fiber with this length is loaded to its failure stress at its midpoint, and the expression is:

$$\frac{L_C}{d} = \frac{Q_{fu}}{2T_i} \tag{2.1}$$

Where L_C is the critical fiber length, d is the fiber diameter, $Q_{fu}$is the fiber failure stress and T_i is the interface shear stress between fiber and matrix. Fibers with lengths below the critical length cannot be loaded to failure in a composite. At fiber lengths shorter than the critical length, the composite strength depends strongly and linearly on the fiber length, while at longer fiber lengths the composite strength approaches the strength value for very long (infinite) fiber lengths. According to Lilholt and Madsen (2012), the critical length of flax fiber is very short (0.4 mm for cellulose). In this study, by considering the existed experimental conditions, flax fibers will be processed into 2mm, which is longer than the critical fiber length.

2.3.2 The effect of processing parameters on the properties of biocomposites

There have been many studies on the potential of using injection molding to process natural fiber reinforced biocomposites (Serizawa et al., 2006; Huda et al., 2005; Huda et al., 2006; (Li et al., 2006). The injection molding deals with processing the mixture of natural fibers and polymer into final product based on time, pressure and temperature. Usually the mixture of chopped fibers and polymers is first fed into the screw zone. Then the mixture is heated until melted and the melted biocomposite is forced into an unyielding mold under high pressure. Once the mold is filled with the melt, the biocomposite is shaped and cooled at certain pressure and temperature. After sufficient cool, the mold is opened and the final product is ejected. The sequence of events during the injection molding of a biocomposite part is called the injection molding cycle. The cycle begins when the mold closes and injection of the melts into the mold cavity. Once the cavity is filled a holding pressure is maintained to compensate for material shrinkage.

The properties of final biocomposite are influenced by many factors including type of material, shape of molded product, and processing conditions (i.e. temperature and pressure). In this study, the mold is determined to be used in injection molding, and thus the processing temperature and pressure are mainly considered in the process. The temperature must be high enough to melt the

polymer but not too high to cause thermal degradation. The pressure must be high enough to avoid partially filled cavities of the injection mold, but not too high to cause flash at the surfaces. Usually when temperature is increased, the pressure decreases a little bit. This can be found from the surface of the product when pressure is not high enough or too high. For each new product, a particular pressure and a particular temperature need to be developed for manufacturing of the product within a given tolerance range.

In the current literature, studies on how injection molding parameters influence the properties of natural fiber reinforced biocomposites are very limited. This research will investigate the effect of processing parameters on the performance of flax fiber biocomposites based on trial and error.

2.3.3 Shrinkage and warpage of injection molded biocomposites

In the current market, natural fiber reinforced biocomposite is an emerging material due to their environmental and economic benefits. To make the market of biocomposites more competitive, producing higher quality products with more accurate dimension is critical (Bledzki et al., 2015; Qatu, 2011). In the process of injection molding, the shrinkage and warpage are two major attributes determining the final dimensions of the product. Natural fiber reinforced biocomposites by injection molding often experience discrepancies in part dimensions or shape due to the shrinkage and warpage defects (Guo et al., 2011). Therefore, it is very important to reduce and minimize the shrinkage and warpage of the final product before under-the-hood application of biocomposites (Guo et al., 2011; Dhakal et al., 2013).

The shrinkage is a geometric size reduction of the injection molded product. If the shrinkage is uniform, the product does not deform and only simply becomes smaller. The warpage causes the product to deform or change its shape when shrinkage is not uniform. The shrinkage and warpage of injection molded parts are often affected by the factors such as material properties, product shape, mold design and processing conditions. This study aimed to reduce the shrinkage and warpage of biocomposites by optimization of processing conditions. Many researchers have investigated the effect of processing conditions on the shrinkage and warpage of injection molded parts (Chang & Tsaur, 1995; Kramschuster et al., 2005; Fischer, 2012). Accoding to these studies, the injection temperature and the packing pressure are the most important process variables

affecting shrinkage and warpage of injection molded parts. In the injection molding for most ploymers, higher injection temperature and packing pressure can reduce the shrinkage and warpage. However, because of enforcement of natural fibers, biocomposites have different theromal properties from pure polymers. So far there is rare literature on the shrinkage and warpage of injection molded biocomposites. Therefore, for the biocomposites, the effect of processing conditions on the shrinkage and warpage needs to be inverstigated. This study aimed to reduce the shrinkage and warpage of biocomposites by optimization of processing conditions.

Traditionally, in the process of injection molding, the selection of processing parameters was based on trial and error and technicians' experience and intuition (Cheng et al., 2013). Such a manual process often required a lot of time and costs as the effects of various underlying parameters could not be predicted beforehand. Nowadays, many studies state that design of experiments (DOE), computer aided engineering (CAE) and optimization methods can be employed to optimize the shrinkage and warpage of injection molded products. Kusić et al. (2013) investigate the influence of six injection moulding process parameters on the post-moulding shrinkage and warping of parts made from polypropylene filled with calcium carbonate by carrying out experimental tests using the Taguchi method. The optimal set of parameters that provides minimal post-moulding shrinkage and warpage, was determined by the Taguchi method, together with nominally-the-best (type II) quality characteristic. Chen et al. (2009) proposed the use of CAE to replace a traditional DOE approach for reducing the warpage of a thin-shell injection molded plastic part. A predictive model of warpage, based on RSM and Moldflow analyses, was developed and simulation results are then validated with physical experiments. Various optimization methods such as Taguchi (Barghash & Alkaabneh, 2014; Hajiha et al., 2014), integrated response surface method (RSM) (Jou et al., 2014), genetic algorithm (GA) (Rocha et al., 2014) and artificial neural network (ANN) (Halimin et al., 2015) have been employed to improve process, product and design in injection molding.

However, so far there is rare literature on the shrinkage and warpage of injection molded products made of natural fiber reinforced biocomposites. Additionally, the current methods rarely consider the influence of the rheological behavior of melts in injection molding and inhibits its effective optimization because of the lack of integration between practical experience, DOE approach and CAE process simulation. This study aimed to develop a more effective method which involves the

analysis of the rheological behavior of biocomposites and integrates DOE and CAE to analyze and optimize the effect of the injection molding process conditions on the shrinkage and warpage of biocomposites.

2.4 Rheology of biocomposites

Rheology is the study of the deformation and flow of matter. The rheological properties of a melt govern the way it deforms and flows in response to applied forces, as well as the decay of stresses when the flow is halted. These rheological properties are of central importance in the injection molding process. In mold filling, it is viscosity, along with thermal properties, that determines the ability of the melt to fill the mold, that is, the pressure required to force the melt through the runner and gate and into the cavity. After filling, the relaxation of stress in the melt affects the residual stresses in the finished part, which has an important effect on its mechanical properties. For these reasons, it is important to know something about the rheological behavior of polymers. Lack of the information about rheological behavior of biocomposites leads to difficulty in analysis and simulation of injection molding by using CAE software. To employ CAE to analyze and simulate the injection molding of biocomposites, it is necessary to investigate their rheological behavior first.

The studies of natural fiber reinforced biocomposite rheology are scarce despite the importance of understanding and predicting the flow and viscoelastic properties of molten biocomposites. The exception is wood fiber reinforced biocomposites and their rheological behaviors are extensively investigated (Li & Wolcott, 2005; Kim et al., 2008; Godard et al., 2009). However, fiber aspect ratio in wood fiber reinforced biocomposites is very low when compared with other natural fibers, which limits the overall understanding of the rheology of natural fiber reinforced biocomposites. Few studies have been focused on the rheology of composites reinforced with natural fibers such as sisal, jute, and hemp fibers (Van Den Oever & Snijder, 2008; Twite-Kabamba et al., 2009; Ogah et al., 2014).

For the viscoelastic characteristics of biocomposites, the mathematical explanation of their viscoelastic fluid is much more complex than Newtonian fluid. For modeling the rheology of biocomposites, in addition to the conservation equations of mass and momentum, the constitutive

equation or rheological equation is required, and this equation relates the relationship between stress and deformation (Cherizol et al., 2015). For the biocomposite fluid, this relationship is nonlinear and there is no universal standard form valid for each fluid in different flow situations. This reality results that modeling biocomposite rheology is so challenging. The constitutive equation should not only describe the rheological characteristic of the polymer melt but also give the final fiber orientation of biocomposite.

In most rheological studies of natural fiber biocomposites, the constitutive equations found in the literature that adequately describe polymer melt will be explored to model the rheological characteristics of biocomposites. The power-law, Cross WFL, Casson, Bird-Carreau and Hershel Bulkley models are among the most preferred rheological models because of their ability to predict velocity and pressure distributions in polymer composite flows (Owens & Phillips, 2002; Marynowski, 2006; Ansari et al., 2010; Dealy & Wissbrun, 2012; Ansari et al., 2012).

The software of injection processing simulation, such as Moldflow, use values of the parameters from the Cross-WLF model. The Cross-WLF model is a combination of two different models, which are a “Cross” model (Cross, 1979) that describes the viscosity dependence on the shear rate and a “WLF” model (Williams, Landel, & Ferry, 1955) that describes the viscosity dependence on the temperature. This model has become widely implemented in various process simulations due to its intuitive form and excellent predictive capability across a relatively wide range of shear rates and temperatures. Accordingly, this model is implemented in this investigation for modeling of the viscous component of the melt rheology. In this study, the Cross-WLF model will be employed to describe the Rheology of biocomposites.

2.5 Conclusion

The literature showed that natural fibers are more and more often applied as the reinforcement in biocomposites due to their availability, sustainability, low density, and price as well as satisfactory mechanical properties. As Canada has been the world's leading producer and exporter of flax since 1994, the research on flax fiber biocomposites has the potential benefit for the Canadian agricultural industry and environment.

First, this chapter reviewed the properties of flax fibers and matrix materials as well as the application of natural fiber composites.

Second, the manufacturing methods of biocomposites were also discussed and among these methods, injection molding is a widely-used technique to manufacture biocomposites due to its fast cycle times, molding accuracy, relatively low labor of large scale production runs, and a wide range of products. However, there were no comprehensive studies on injection molding for natural fiber biocomposites, especially on the factors affecting the properties of biocomposites. This chapter reviewed the effect of the size of flax fibers on properties of biocomposites during the injection molding and determined the size of fiber used in the experiment. The factors affecting the properties of injection molded biocomposites were then investigated and this study will focus on the effect of processing temperature and pressure on the properties of biocomposites.

Third, the shrinkage and warpage are two major attributes determining the final dimensions and quality of the injection molded product. This chapter introduced the factors that affect the shrinkage and warpage and reviewed the methods of reducing the shrinkage and warpage in the current literature. However, there were rare researches on the shrinkage and warpage of injection molded biocomposites, and additionally, the current methods rarely consider the influence of the rheological behavior of melts during injection molding. This study will develop an effective method which involve the analysis of the rheological behavior of biocomposites and integrates DOE and CAE to analyze and optimize the effect of the injection molding process conditions on the shrinkage and warpage of biocomposites.

Finally, the discussion in this chapter has provided a further justification of the need and urgency of the proposed research.

CHAPTER 3 PROPERTIES OF BIOCOMPOSITES VERSUS PROCESSING CONDITIONS

3.1 Introduction

This chapter presents a work in which flax fiber reinforced PP biocomposites were manufactured by injection molding. The materials, processing scheme and equipment were discussed. The mechanical properties and water absorption of biocomposites manufactured by injection molding were measured. The influence of flax fiber loading and processing conditions including injection temperature and pressure on the properties of biocomposites were also investigated. According to the investigation, the relationships between the properties of biocomposites, particularly tensile properties, flexural properties and water absorption, and processing conditions, particularly flax fiber content, injection temperature and injection pressure, were built by polynomial linear regression.

3.2 Materials and methods

3.2.1 Materials

It is obvious that flax fiber and polypropylene (PP) are the basic materials to process biocomposites. PP resin was purchased from Nexeo Solutions, LLC. (Richmond, BC, Canada) and Flax fiber grown in Saskatchewan was obtained from Biofiber Industries LTD. (Canora, SK, Canada). Other chemicals include Vinyltrimethoxysilane ($C_8H_{18}O_3Si$) (Alfa Aesar, Heysham, United Kingdom), sodium hydroxide (EM Industries, Inc., Gibbstown, NJ, United State) and wax (Conros Corp. North York, ON, Canada).

3.2.2 Processing procedure and experimental equipment

The schematic overview of processing composites is shown in Fig. 3.1, where there are several critical steps including pretreatment of flax fiber, extrusion, and injection molding.

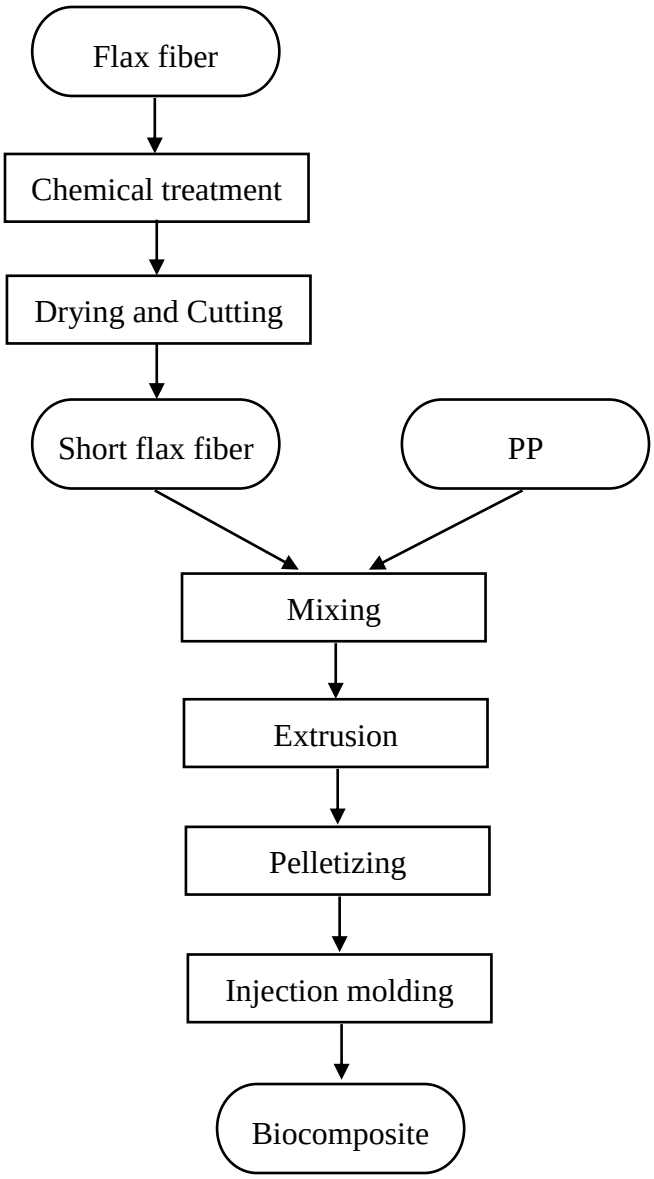

Fig. 3.1 Processing scheme of flax fiber reinforced PP Biocomposites.

1. The pre-treatment of flax fiber

In this experiment, the chemical treatment of flax fiber was silane treatment. The flax fiber was first washed three times with hot water at 70 ºC and then was immersed in 5% NaOH for 24 hours, which can make the OH group in cellulose activated. After this the flax fiber was washed with distilled water. The pretreated flax fiber was submerged in the solution containing 1% triethoxyvinylsilone coupling agent for 24 hours. Last, the flax fiber was washed properly with distilled water again.

The treated fiber was dried at 70 ℃ in air oven for 24 h. It is one of the important processes for making a biocomposite because the moisture inside the fiber forms bubbles during the mixing process of making biocomposites. The dried fiber was then grounded to the short fiber with 2 mm. The size reduction of flax fiber will be done to ensure a homogeneous mixing of fiber and PP resin.

2. Extrusion

The mixture of short flax fiber and PP was fed into the twin-screw extruder shown in Fig. 3.2. Extrusion was conducted in order to avoid the separation of fiber from the PP during the later injection molding process. The extruder parameters were the temperature of 200 ℃ and the screw speed of 60 rpm.

Fig. 3.2 Twin-screw extruder for compounding the mixture.

Prior extrusion compounding is necessary for the processing biocomposites before injection molding, because the screws of injection molding machine are much shorter than those of extruders and the lower ratio of length to diameter of the screws in injection molding makes it less efficient in mixing and non-homogenous melt comparison with extruders.

3. Pelletizing

In order to be fed into the injection molding machine, the extrudates were pelletized into small particles (as shown in Fig. 3.3). The process of pelletizing was conducted by a grinding mill (as shown in Fig. 3.4). The pellets were dried 24 h at 70 ˚C under vacuum before injection molding.

Fig. 3.3 The pellets of extruding the mixture of flax fibers and PP.

Fig. 3.4 Grinding mill machine for pelletizing the extrudates.

4. Injection molding

Then the pellets were fed into the injection molding machine (as shown in Fig. 3.5) to produce biocomposites. There are four controlled temperature zones in the heater barrels for this injection molding machine, as shown in Fig. 3.6. Temperature increases from zone D to A and zone A was close to the injection chamber where the melt is injected into the mold. The operating temperature must lie in the range between the melting point temperature and the degradation temperature of the material. The recommended processing temperature for PP is 210-290℃ (Hindle, 2015), and flax fiber can withstand processing temperatures up to 250ºC according to Sreekala et al. (2000). Thus, for the injection molding of biocomposites, the characteristic temperatures both of PP and flax fiber should be considered.

Fig. 3.5 Injection molding machine for producing biocomposites.

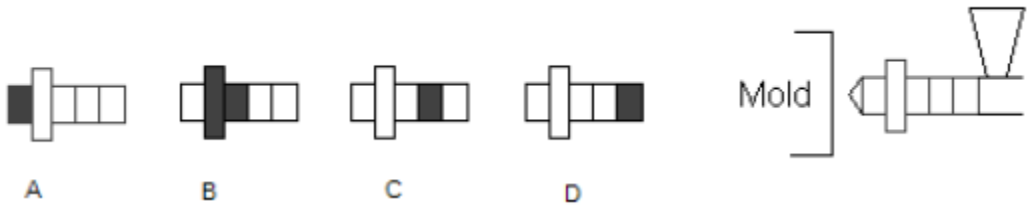

Fig. 3.6 Temperature zones in the heater barrels for this injection molding machine.

In this experiment, the injection mold was also designed for facilitating the testing of the mechanical properties of biocomposites. The molded product includes two parts, as shown in Fig. 3.5, which are a dog bone for tensile and flexural testing with shape and dimensions by following ASTM D638 method (ASTM International, 2014) and ASTM D790 method (ASTM International, 2015), and a rectangular card for water absorption testing.

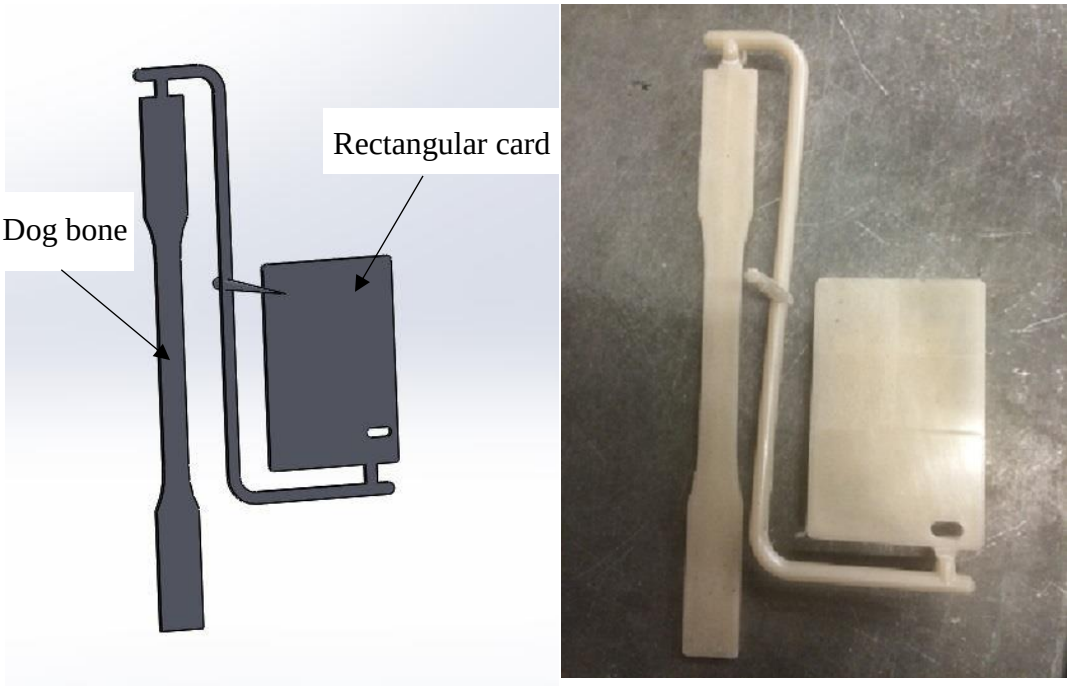

Fig. 3.7 Molded biocomposite product by injection molding (Dog bone is for tensile and flexural testing. Rectangular card is for water absorption testing).

3.2.3 Experimental design

The processing temperature and pressure play important roles in the mechanical property and water absorption property of biocomposites. The processing temperature must be high enough to melt the polymer but not too high to cause degradation of flax fibers. The processing pressure must be high enough to avoid short shots (i.e. partially filled cavities), but not too high to cause flash at the surfaces. Thus, the processing temperature and pressure are potentially significant factors.

In general, increasing fiber loading in biocomposites would improve the stiffness and the strength of biocomposites. However, in practice, the injection modelling process would limit the amount

of fibers to be injected because of the fiber cluttering, narrow gate and sprue, and viscosity of the fiber-polymer mixture. In addition, biocomposites with different fiber contents may require different injection molding conditions. As such, fiber loading potentially a significant factor.

Three factors experiments were conducted to study the effects on the properties of biocomposites: 1) fiber content; 2) injection temperature; 3) injection pressure. The complete experimental design is shown in Table 3.1.

Table 3.1 The design of the three factors experiment.

Trial	Fiber Content (wt%)	Injection Temperature (℃)	Injection Pressure (MPa)
1	0	210	4.8
2	0	210	5.9
3	0	210	7.0
4	0	220	4.8
5	0	220	5.9
6	0	220	7.0
7	0	230	4.8
8	0	230	5.9
9	0	230	7.0
10	10	210	4.8
11	10	210	5.9
12	10	210	7.0
13	10	220	4.8
14	10	220	5.9
15	10	220	7.0
16	10	230	4.8
17	10	230	5.9
18	10	230	7.0

Table 3.1 continued.

19	20	210	4.8
20	20	210	5.9
21	20	210	7.0
22	20	220	4.8
23	20	220	5.9
24	20	220	7.0
25	20	230	4.8
26	20	230	5.9
27	20	230	7.0
28	30	210	4.8
29	30	210	5.9
30	30	210	7.0
31	30	220	4.8
32	30	220	5.9
33	30	220	7.0
34	30	230	4.8
35	30	230	5.9
36	30	230	7.0

In Table 3.1 it is shown that fiber loading used were 10 wt%, 20 wt%, 30 wt% fiber content by mass to reinforce the PP biocomposites and the pure PP (with 0 wt% flax fiber) was the control group. Three injection temperatures (210 ℃, 220 ℃, 230 ℃) and three injection pressures (4.8 MPa, 5.9 MPa, 7.0 MPa) were selected. It is noted that for a full factorial experimental design, there would be 36 trials in total. Tensile and flexural properties, and water absorption of injection molded biocomposites were measured. SPSS (SPSS Inc., Chicago, IL) were used to analyze and compare the effects of the three factors on the properties of biocomposite properties.

3.2.4 Measurement of the properties of biocomposites

The various ASTM tests adopted for testing the mechanical and physical properties (i.e. tensile properties, flexural properties and water absorption) of the injection molded biocomposites are given below.

1. Tensile testing

Tensile tests were conducted using an Instron Universal testing machine, Instron 3366 (Instron Corp., Canton, MA, USA), as shown in Fig. 3.6, following the standard ASTM D638 method (ASTM International, 2014). Testing samples were conditioned at the temperature of 20 ℃and the relative humidity of 50 for 24 hours, prior to testing. Each test was performed at a cross head speed of 10 mm/min and repeated five times. The maximum (peak) load F_{max} (N) was recorded by the instrument. The tensile strength σ_t (Pa) was calculated from the following equation (ASTM International, 2014):

$$\sigma_t = \frac{F_{max}}{A} \tag{3.1}$$

where, A is the area of cross-section (m^2).

Young's modulus E (MPa) was determined by using the following equation (ASTM International, 2014):

$$E = \frac{\Delta\sigma}{\Delta\varepsilon} \tag{3.2}$$

where, $\Delta\sigma$ (MPa) is the change of tensile stress before the material yields, and $\Delta\varepsilon$ is the change of tensile strain before the material yields.

2. Flexure testing

Flexure testing was also conducted by Instron 3366 (Fig. 3.8) according to the standard ASTM D790 method (ASTM International, 2015). Using a three-point testing method, the testing samples rest on two supports and were loaded by means of a loading nose midway between the supports. The samples were deflected until a breaking point occurs in the outer surface of the samples. Testing samples were conditioned at the temperature of 20 ℃and the relative humidity of 50 for 24 hours, prior to testing. Each test was performed at a cross head speed of 10 mm/min and

repeated five times. Flexural strength and modulus were recorded from the software in the computer connected to the testing machine.

Flexural strength σ_f (MPa) is calculated from the following equation (ASTM International, 2015):

$$\sigma_f = \frac{3PL}{2bd^2} \tag{3.3}$$

where:

P = load at a given point on the load-deflection curve, N;

L = support span, mm;

b = width of beam tested, mm; and

d = depth of beam tested, mm.

Flexural modulus is determined from Equation 3.4 (ASTM International, 2015):

$$E_B = \frac{L^3 m}{4bd^3} \tag{3.4}$$

where:

E_B = modulus of elasticity in bending, MPa;

L = support span, mm (in.);

b = width of beam tested, mm;

d = depth of beam tested, mm; and

m = slope of the tangent to the initial straight-line portion of the load-deflection curve, N/mm.

Fig. 3.8 Instron testing machine 3366 (Instron Corp., Canton, MA, USA).

3. Water absorption

The water absorption test followed ASTM D570 method (ASTM 1998). The test sample was the rectangular card with 88.2 mm long, 57.5 mm wide and 3.2 mm thick. Prior to testing, the sample was dried in an air oven at 50 ℃for 24 hours, in order to remove any initial water. After drying the sample was immediately weighed, which is taken as the dry weight of the sample, M_0. Then the sample was immersed in distilled water for 24 hours. After immersion, the sample was taken out from water and the water on the surface of the sample was wiped off. Last, the sample was immediately weighed again, which is considered as saturation weight, M_1. Three specimens for each sample were tested. The water absorption of the sample was calculated as percent weight change $M\%$, as follows:

$$M\% = \frac{M_1 - M_0}{M_0} \tag{3.5}$$

3.3 Results and discussion

In the injection molding of biocomposites, injection temperature and injection pressure are the two most important variables to be controlled. However, biocomposites with different fiber contents may vary in their physical and rheological properties, and thus might require different processing conditions. In this section, three factors with three levels: 1) fiber content; 2) injection temperature; and 3) injection pressure were investigated and analyzed as to their influence on properties of the flax fiber reinforced PP biocomposites. The 36 biocomposites (including 9 control groups) were manufactured, and their physical and mechanical properties (i.e. tensile properties, flexural properties and water absorption) were measured and analyzed.

3.3.1 The effect of processing conditions on tensile properties of biocomposites

The tensile properties of biocomposites were characterized by the tensile strength σ_t and Young's modulus E. Table 3.2 shows the tensile strength σ_t and Yong's modulus E of biocomposites at various fiber content and processing conditions.

Table 3.2 Tensile properties of biocomposites at different processing conditions.

Trial	Fiber Content (wt%)	Injection Temperature (℃)	Injection Pressure (MPa)	Tensile Strength σ_t (MPa)		Young's Modulus E (MPa)	
				Mean	St.dev.	Mean	St.dev.
1	0	210	4.8	34.47	0.38	1288	33
2	0	210	5.9	34.81	0.22	1265	27
3	0	210	7.0	35.33	0.43	1233	41
4	0	220	4.8	33.65	0.34	1317	30
5	0	220	5.9	33.87	0.43	1320	36
6	0	220	7.0	33.82	0.50	1301	39
7	0	230	4.8	32.27	0.71	1364	49
8	0	230	5.9	32.19	0.38	1369	45
9	0	230	7.0	32.24	0.47	1382	67
10	10	210	4.8	42.27	0.69	1533	49
11	10	210	5.9	42.84	0.34	1556	37
12	10	210	7.0	43.63	0.34	1603	69
13	10	220	4.8	41.23	0.60	1701	34
14	10	220	5.9	41.77	0.73	1713	47
15	10	220	7.0	41.52	0.52	1682	70
16	10	230	4.8	39.58	0.60	1841	22
17	10	230	5.9	39.86	0.32	1889	24
18	10	230	7.0	39.21	0.32	1839	24
19	20	210	4.8	44.39	0.39	1941	55
20	20	210	5.9	45.66	0.77	2025	28
21	20	210	7.0	46.12	0.21	2054	42
22	20	220	4.8	43.22	0.72	2117	75
23	20	220	5.9	43.76	0.58	2099	39
24	20	220	7.0	44.43	0.39	2023	78
25	20	230	4.8	41.94	0.59	2187	29
26	20	230	5.9	41.45	0.71	2175	69

Table 3.2 continued.

27	20	230	7.0	41.20	0.56	2182	55
28	30	210	4.8	47.47	0.67	2235	38
29	30	210	5.9	48.90	0.70	2319	42
30	30	210	7.0	50.11	0.25	2395	14
31	30	220	4.8	46.28	0.29	2412	24
32	30	220	5.9	46.77	0.32	2433	77
33	30	220	7.0	47.03	0.48	2454	63
34	30	230	4.8	45.02	0.27	2567	65
35	30	230	5.9	45.21	0.43	2541	75
36	30	230	7.0	45.96	0.27	2550	26

From Table 3.2, the highest tensile strength is in the biocomposite with 30 wt% flax fibers and processed at injection temperature 210 ℃ and injection pressure 7.0 MPa, and flax fiber reinforcement contributed to an increase of 41.83% in tensile strength compared with the tensile strength of the pure PP at the same processing conditions. The highest Young's modulus was found in the biocomposite with 30 wt% flax fibers with processing conditions of injection temperature 230 ℃ and the injection pressure 4.8 MPa, and flax fiber reinforcement contributed to an increase of 88.20% in Young’s modulus.

Analysis of variance (ANOVA) of experimental data (refer to Tables A.1 and A.2 in Appendix A) showed that the tensile strength and Young's modulus of biocomposites were significantly dependent on fiber content and injection temperature. The injection pressure had no significant influence on the tensile properties and Young’s modulus of biocomposites. The effects of these three factors on tensile properties of biocomposites are discussed as follows.

3.3.1.1 Fiber content

ANOVA (Tables A.1 and A.2 in Appendix A) showed that fiber content was the most significant impact factor on the tensile strength and Young’s modulus of biocomposites. The results are in accordance with the studies of Facca et al. (2007) and Facca et al. (2006). Facca et al. (2007)

studied the effect of fiber content on the tensile strength of natural fiber reinforced thermoplastics by measuring the tensile strength of the various composite specimens with the reinforcements of hemp fibers, hardwood fibers, rice hulls, and E-glass fibers, and the tensile strength of all types of fiber reinforced high-density polyethylene (HDPE) composites increased with their fiber contents. Facca et al. (2006) also used hemp fibers, hardwood fibers, rice hulls, and E-glass fibers reinforced HDPE composites to investigate the influence of fiber content on the Young's modulus of the biocomposites, and the results showed that Young's modulus of the various composite specimens increased with the fiber content.

Fig. 3.9 to Fig 3.11 show the variation of tensile properties with the variation of fiber contents and the variation of injection temperatures, respectively, at the three levels of injection pressures. It can be seen from these figures that the tensile strength of biocomposites increased with the increase fiber contents at the same processing conditions (i.e., injection temperature and injection pressure). The average tensile strength of the biocomposites with 10 wt%, 20 wt% and 30 wt% flax fibers, respectively, increased by 22.88%, 29.58% and 39.68% compared with the tensile strength of the pure PP.

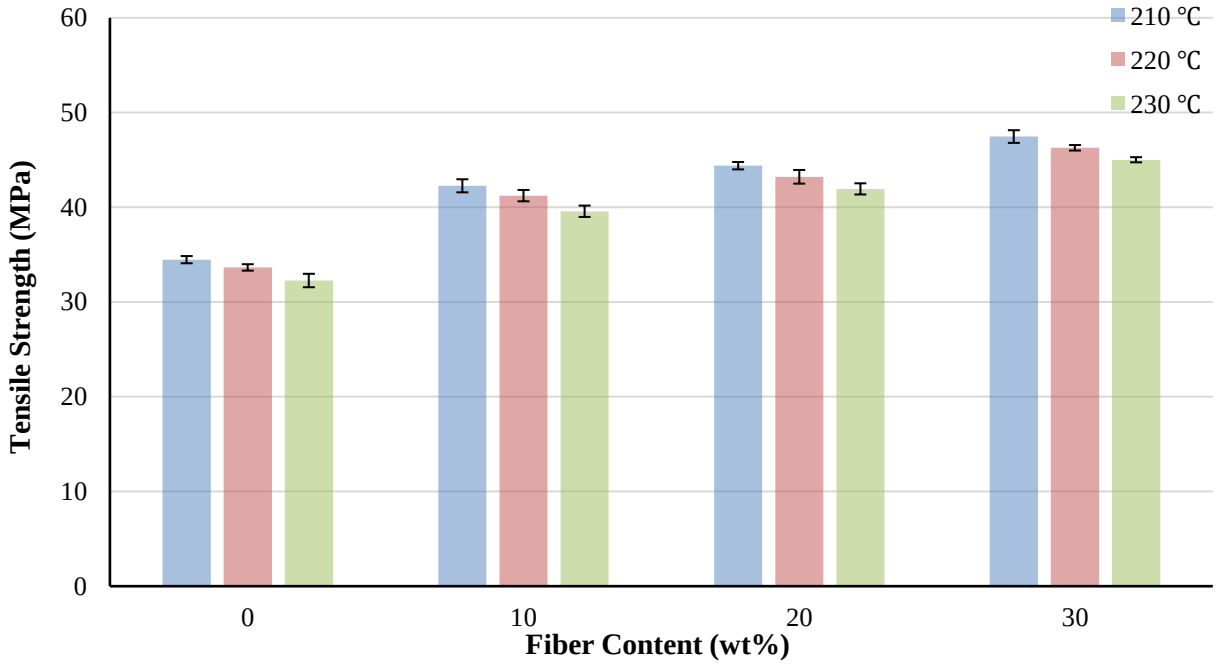

Fig. 3.9 The variation of tensile strength of biocomposites with fiber contents and injection temperatures at injection pressure 4.8 MPa.

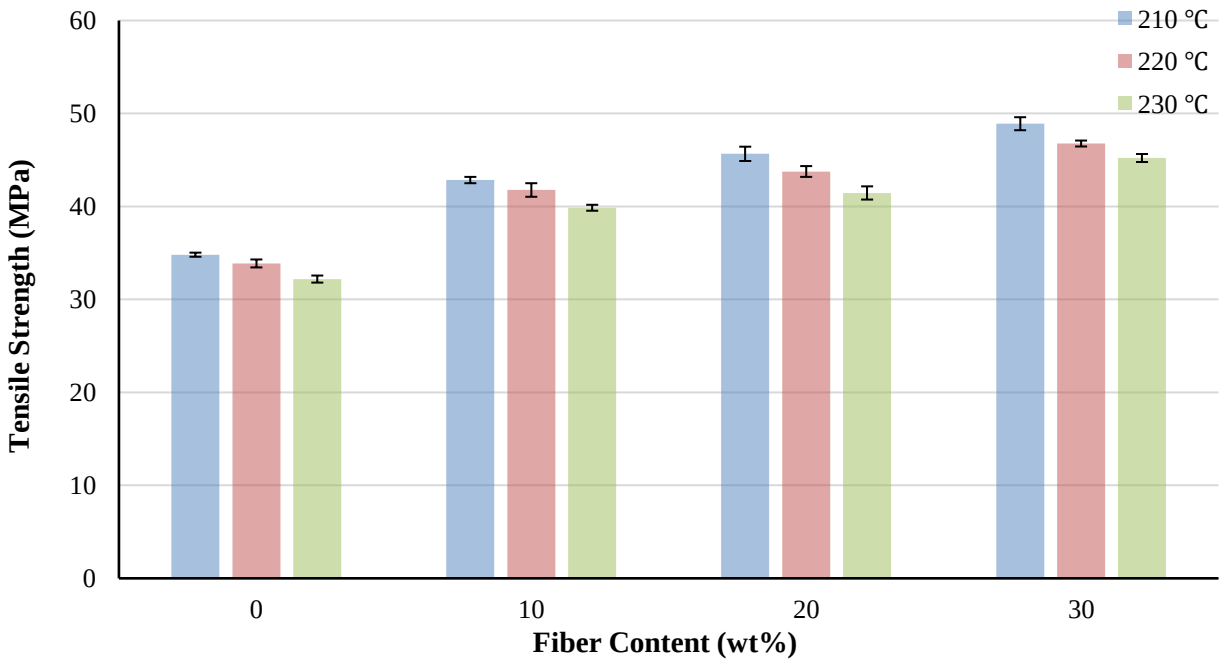

Fig. 3.10 The variation of tensile strength of biocomposites with fiber contents and injection temperatures at injection pressure 5.9 MPa.

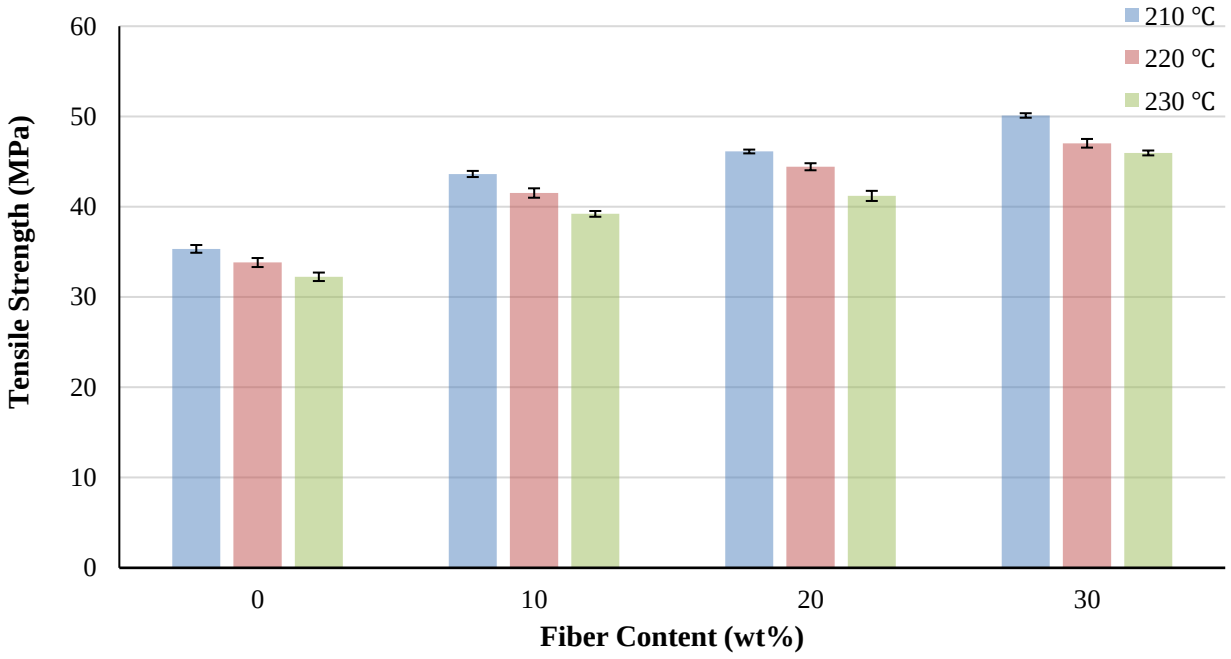

Fig. 3.11 The variation of tensile strength of biocomposites with fiber contents and injection temperatures at injection pressure 7.0 MPa.

Fig 3.12, Fig. 3.13 and Fig 3.14 showed the variation of Young's modulus of biocomposites with different fiber contents and different injection temperatures, respectively, at the three levels of injection pressures (4.8 MPa, 5.9 MPa, 7.0 MPa). It was concluded that the Young's modulus of biocomposites dramatically increased with fiber contents, which indicated that if the same stress is applied in the injection molded products, the biocomposites with higher fiber content will produce a smaller amount of strain. The average Young's modulus of the biocomposites with 10 wt%, 20 wt% and 30 wt% flax fibers respectively increased by 29.72%, 58.82% and 85.03% compared with the pure PP.

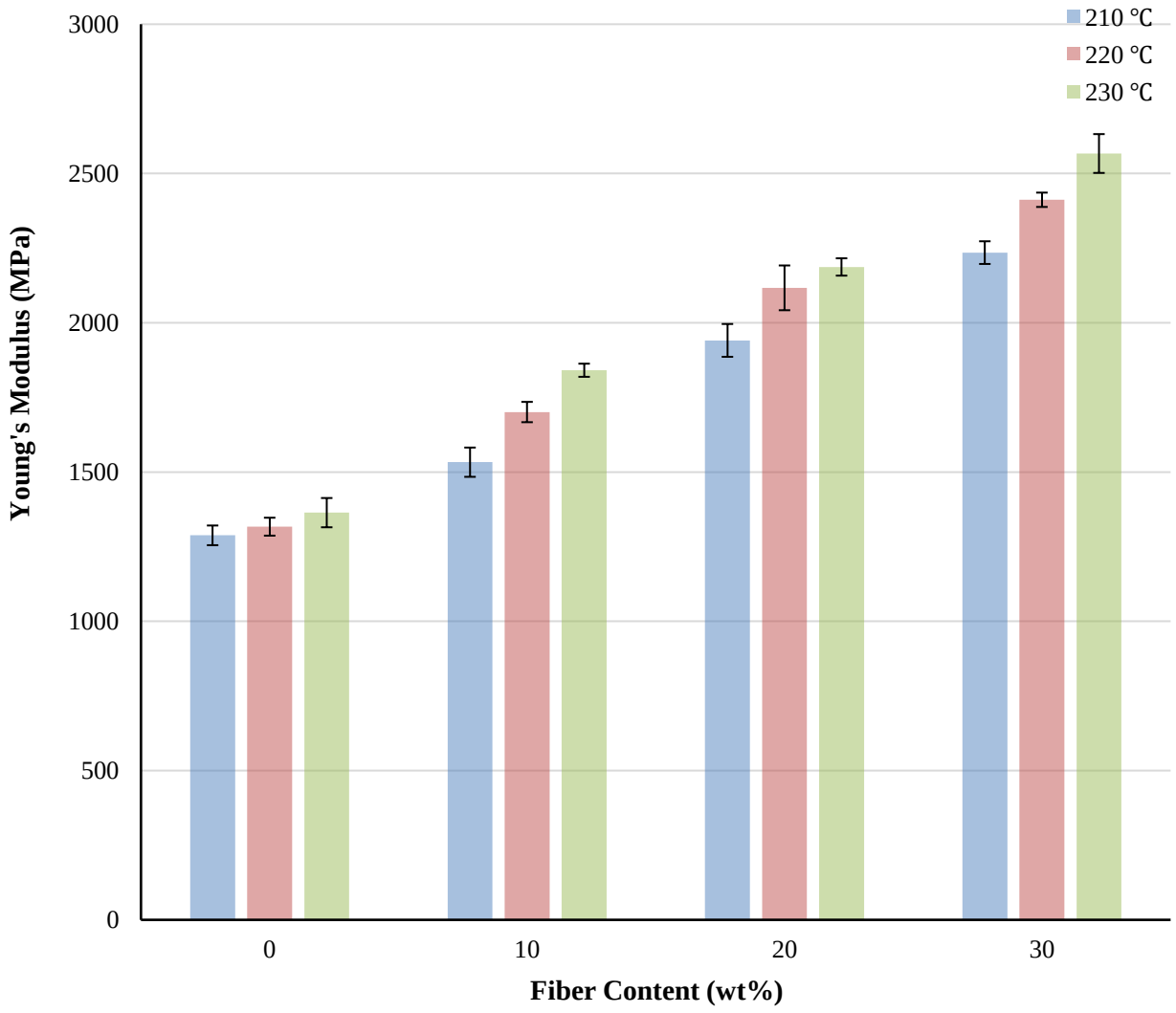

Fig. 3.12 The variation of Young's modulus of biocomposites with fiber contents and injection temperatures at injection pressure 4.8 MPa.

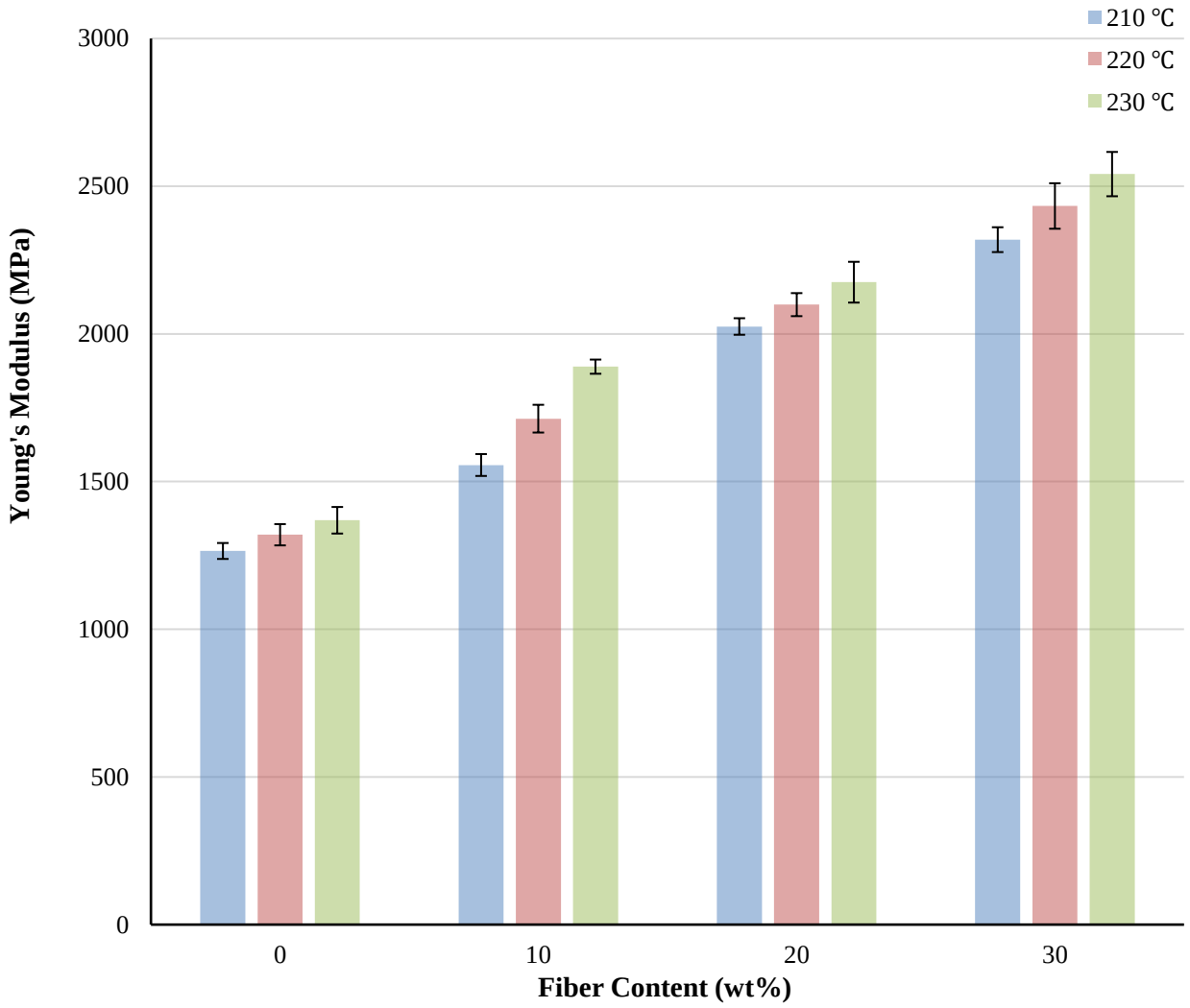

Fig. 3.13 The variation of Young's modulus of biocomposites with fiber contents and injection temperatures at injection pressure 5.9 MPa.

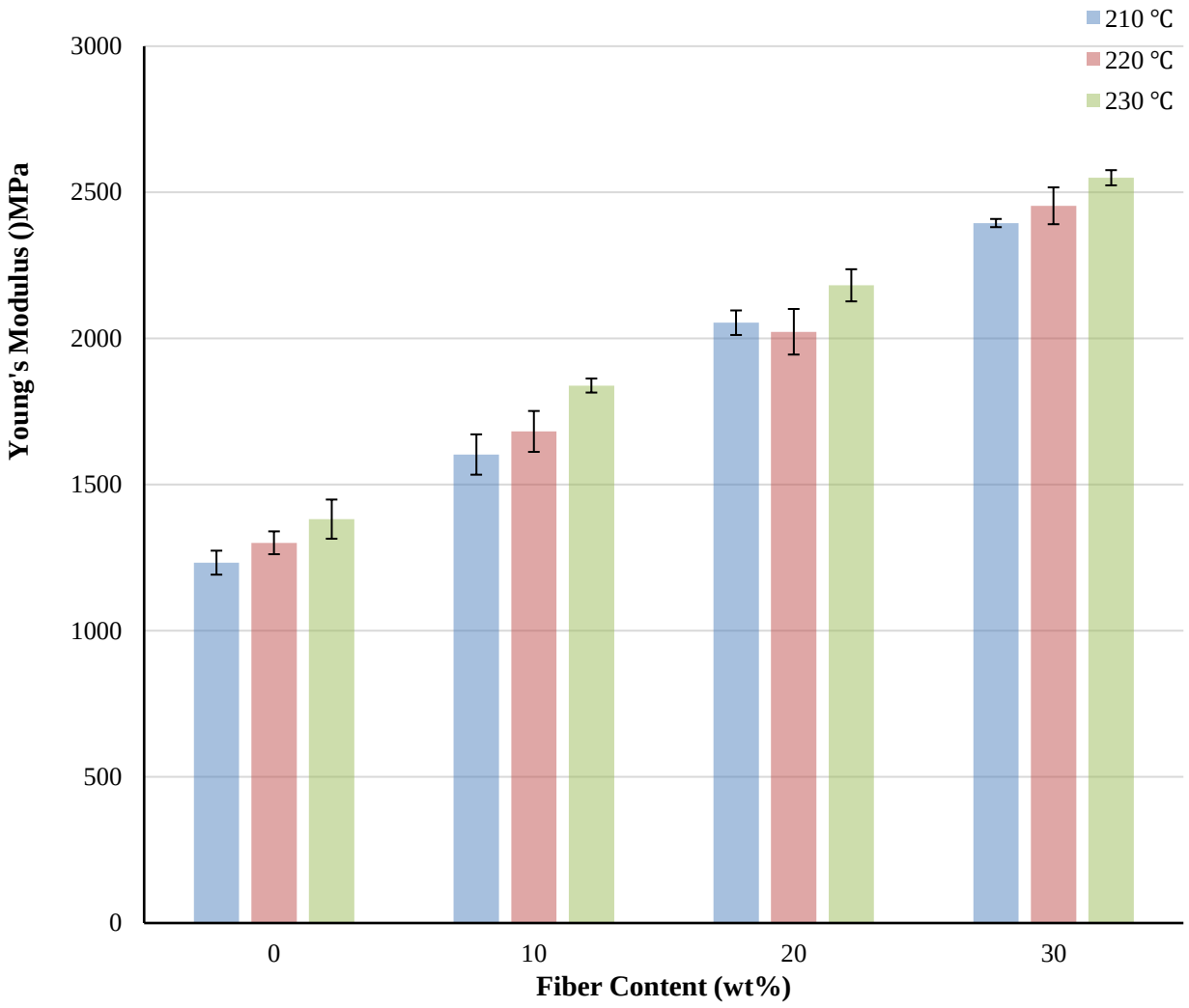

Fig. 3.14 The variation of Young's modulus of biocomposites with fiber contents and injection temperatures at injection pressure 7.0 MPa.

3.3.1.2 Injection temperature

From Fig. 3.9 to Fig 3.11, it can also be seen that biocomposites with fiber contents (from 0 to 30 wt%) manufactured at the lower injection temperature (210 ℃) had a higher tensile strength than the other two injection temperatures (220 ℃ and 230 ℃). As an example of the biocomposite with 20 wt% flax fibers, the lowest injection temperature (210 ℃) resulted in the highest tensile strength regardless of the injection pressures. Ota et al. (2005) studied the influence of injection temperature on the tensile strength of glass fiber reinforced PP composites, and their results showed that there

was a slightly decrease of tensile strength with the increase of injection temperature, which suggested the same tendency of the effect of injection temperature on tensile strength of PP composites.

The effect of the injection temperature on the tensile strength of biocomposites could be explained by the thermal properties of PP and flax fiber. PP can be processed at temperature of 210 to 290ºC (Hindle, 2015). In general, the degradation of natural fibers involves two main steps: the first one is the thermal depolymerisation of the hemicellulose and the cleavage of glycosidic linkages of cellulose and the second one is related to the decomposition of the α-cellulose (Albano et al., 1999; Nair et al., 2001). According to Manfredi et al. (2006), flax fibers start to degrade at around 230 ºC. The higher injection molding temperatures (220 ºC and 230 ºC) might cause the decomposition of flax fibers, which resulted in the fiber loss and reduce the reinforcement effect. Therefore, a higher injection temperature usually resulted in a lower tensile strength.

In the case of Young's modulus (Fig. 3.12 to Fig. 3.14), it is shown that Young's modulus of biocomposites increased with the injection temperature, respectively, at the three levels of injection pressures, regardless of the different groups of fiber content (0 to 30wt%).

3.3.1.3 Injection pressure

ANOVA (Tables a.1 and a.2 in Appendix A) shows that the influence of injection pressure on tensile strength is not significant. But the higher injection pressure (p = 7.0 MPa) resulted in higher tensile strength when at lowest injection temperature (i.e., T = 210 ºC). This may be because the melt of the biocomposite at a lower temperature has a higher viscosity, which resulted in the biocomposite melt needed more pressure to be injected into the mold. It was also found that injection pressure did not significantly influence Young's modulus.

3.3.1.4 Predicted models for tensile properties

The predicted models were aimed to develop the relationship between the tensile properties (tensile strength and Young's modulus) of biocomposites and processing conditions (fiber content, injection temperature and injection pressure) by statistical tools based on the experimental data.

From the foregoing discussion on the effect of processing conditions on tensile properties, it can be concluded that processing pressure had no significant influence on either tensile strength or Young's modulus of biocomposites. So the injection pressure was excluded for consideration in the mathematical model of the injection molding process for the biocomposites. A linear regression model can be developed between the tensile strength and fiber content and injection temperature, and the Young's modulus and fiber content and injection temperature, respectively, using the commercial software MINITAB as follows:

Tensile strength:

$$\sigma_t = 14.001 + 1.062F + 0.327T - 0.011F^2 - 0.001T^2 - 0.001FT \qquad (3.6)$$

where, σ_t is Tensile strength (MPa);

F is flax fiber weight content (wt%);

T is Injection temperature (°C).

Young's modulus:

$$E = 3317 + 12.0F - 26.5T - 0.1153F^2 + 0.079T^2 - 0.1312FT \qquad (3.7)$$

where E is Young's modulus (MPa).

F is flax fiber weight content (wt%);

T is Injection temperature (°C).

The above two equations revealed the relationship between the tensile properties (tensile strength and Young's modulus) and the two main factors (fiber content and injection temperature). The detailed result of the linear regression can be seen from the tables in Appendix B (refer to Table B.1 to B.8). Further, from the R-square = 95.63% for tensile strength (shown in Table B.3) and R-square = 98.77% for Yong's modulus (shown in Table B.7), the two equations were in a very good fit to tensile strength and Young's modulus.

From Equations 3.6 and 3.7, Fig. 3.15 and 3.16 can be produced, which show the variations of tensile strength and Yong's modulus of biocomposites with respect to fiber content and injection temperature. The surface responses in the two figures approved the previous discussion about the

effect of flax fiber content and injection temperature on the tensile strength and Young's modulus of biocomposites.

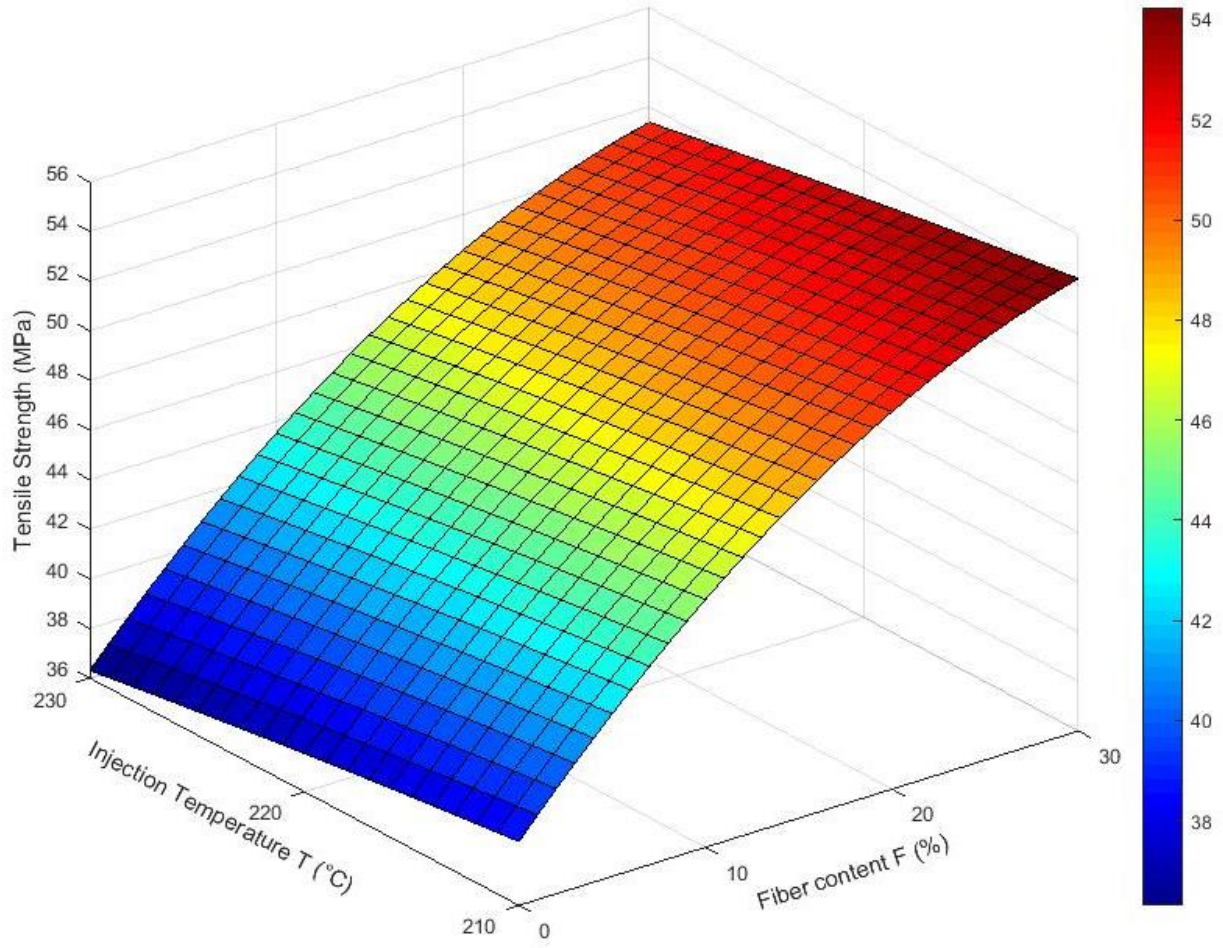

Fig. 3.15 The variation of tensile strength of biocomposites with flax fiber content and injection temperature by the predicted model of tensile strength.

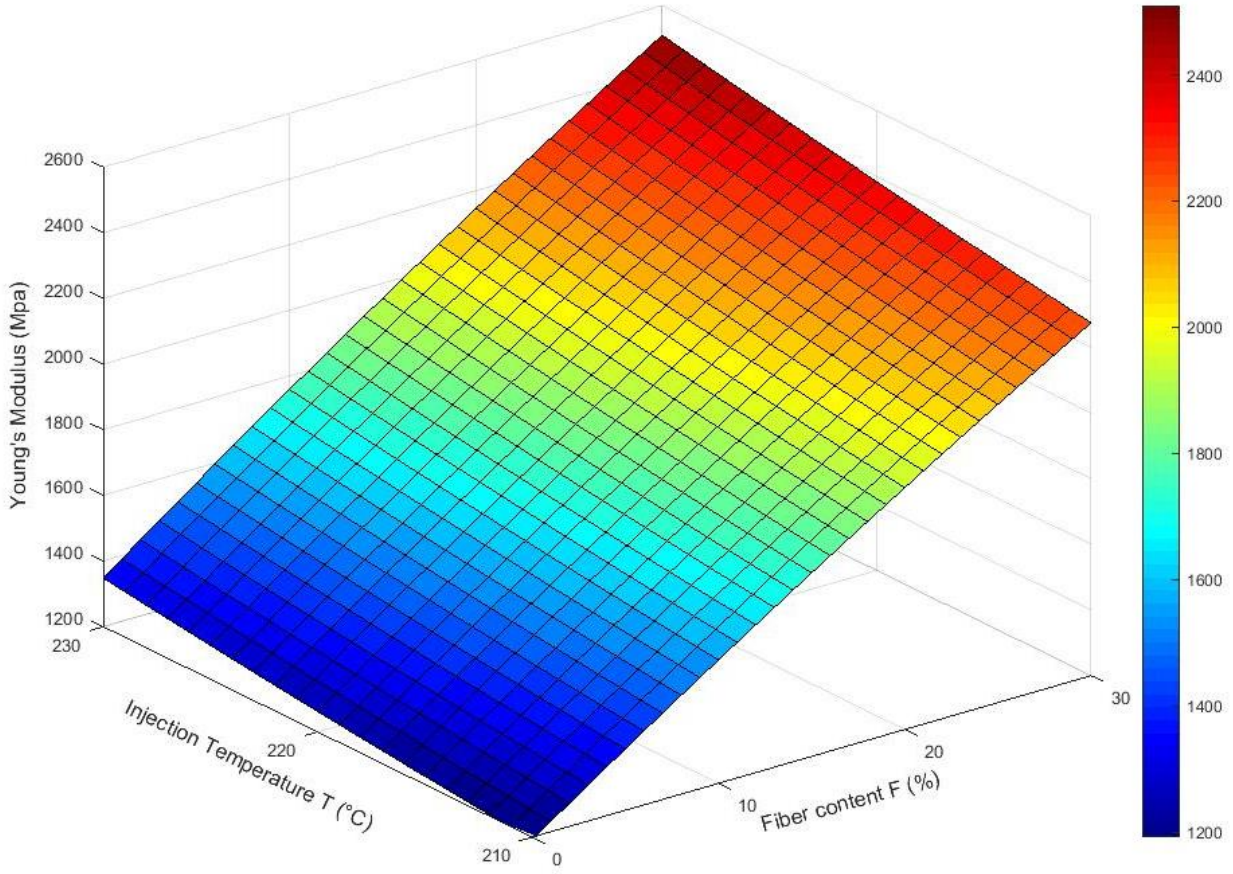

Fig. 3.16 The variation of Young's modulus of biocomposites with flax fiber content and injection temperature by the predicted model of Young's modulus.

3.3.2 The effect of processing conditions on flexural properties of biocomposites

The flexural properties of biocomposites were characterized by the flexural strength σ_f and flexural modulus E_B. Table 3.3 shows the flexural strength and flexural modulus of biocomposites with different flex fiber weight contents (from 0 to 30 wt%) at various injection temperature (210 ℃, 220 ℃, 230 ℃,), and three levels of injection pressure (4.8 MPa, 5.9 MPa, 7.0 MPa).

Table 3.3 Flexural properties of biocomposites at different processing conditions.

Trial	Fiber Content (wt%)	Injection Temperature (℃)	Injection Pressure (MPa)	Flexural Strength σ_f (MPa)		Flexural Modulus E_B (MPa)	
				Mean	St.dev.	Mean	St.dev.
1	0	210	4.8	48.26	0.98	1241	65
2	0	210	5.9	48.19	0.61	1249	37
3	0	210	7	48.33	0.70	1267	74
4	0	220	4.8	47.08	1.30	1117	79
5	0	220	5.9	47.03	0.73	1125	35
6	0	220	7	47.17	0.66	1129	65
7	0	230	4.8	45.98	0.93	991	65
8	0	230	5.9	45.91	0.61	1001	61
9	0	230	7	45.87	0.91	1015	65
10	10	210	4.8	62.51	0.96	1754	69
11	10	210	5.9	62.39	1.34	1798	42
12	10	210	7	62.47	1.04	1761	84
13	10	220	4.8	60.42	0.85	1632	87
14	10	220	5.9	60.77	1.08	1607	55
15	10	220	7	61.09	1.35	1641	53
16	10	230	4.8	58.67	1.35	1507	46
17	10	230	5.9	58.86	1.08	1491	85
18	10	230	7	59.24	1.34	1511	77
19	20	210	4.8	65.34	1.36	2243	31
20	20	210	5.9	65.86	1.35	2257	75
21	20	210	7	66.11	1.13	2287	89
22	20	220	4.8	63.52	0.81	2106	62
23	20	220	5.9	63.71	1.24	2115	85
24	20	220	7	63.8	1.00	2068	38
25	20	230	4.8	61.94	1.17	1987	52
26	20	230	5.9	61.91	0.62	2016	83

Table 3.3 continued.

27	20	230	7	61.73	1.16	1991	79
28	30	210	4.8	70.38	0.85	2621	37
29	30	210	5.9	70.91	1.09	2669	70
30	30	210	7	71.59	1.35	2702	34
31	30	220	4.8	69.07	0.92	2455	89
32	30	220	5.9	68.14	1.33	2458	48
33	30	220	7	68.35	0.74	2482	68
34	30	230	4.8	66.57	0.70	2361	78
35	30	230	5.9	66.62	0.63	2347	38
36	30	230	7	66.73	0.99	2350	65

As shown in Table 3.3, the highest flexural strength and flexural modulus were both from the biocomposite with 30 wt% flax fibers and processed at injection temperature 210 ℃ and injection pressure 7.0 MPa. In the same processing conditions, flax fiber reinforcement contributed to an increase of 47.13% in flexural strength and 113.26% in flexural modulus comparing with the pure PP.

ANOVA (refer to Tables A.3 and A.4 in Appendix A) showed that the flexural strength and flexural modulus of biocomposites were significantly dependent on flax fiber content and injection temperature. The fiber content was the most significant impact factor on the flexural strength and flexural modulus of biocomposites. The injection pressure had no significant influence on the flexural properties. The variation of flexural properties (flexural strength and flexural modulus) with various fiber contents and different injection temperatures respectively at the three levels of injection pressures is illustrated by Fig. 3.17 - Fig.3.22.

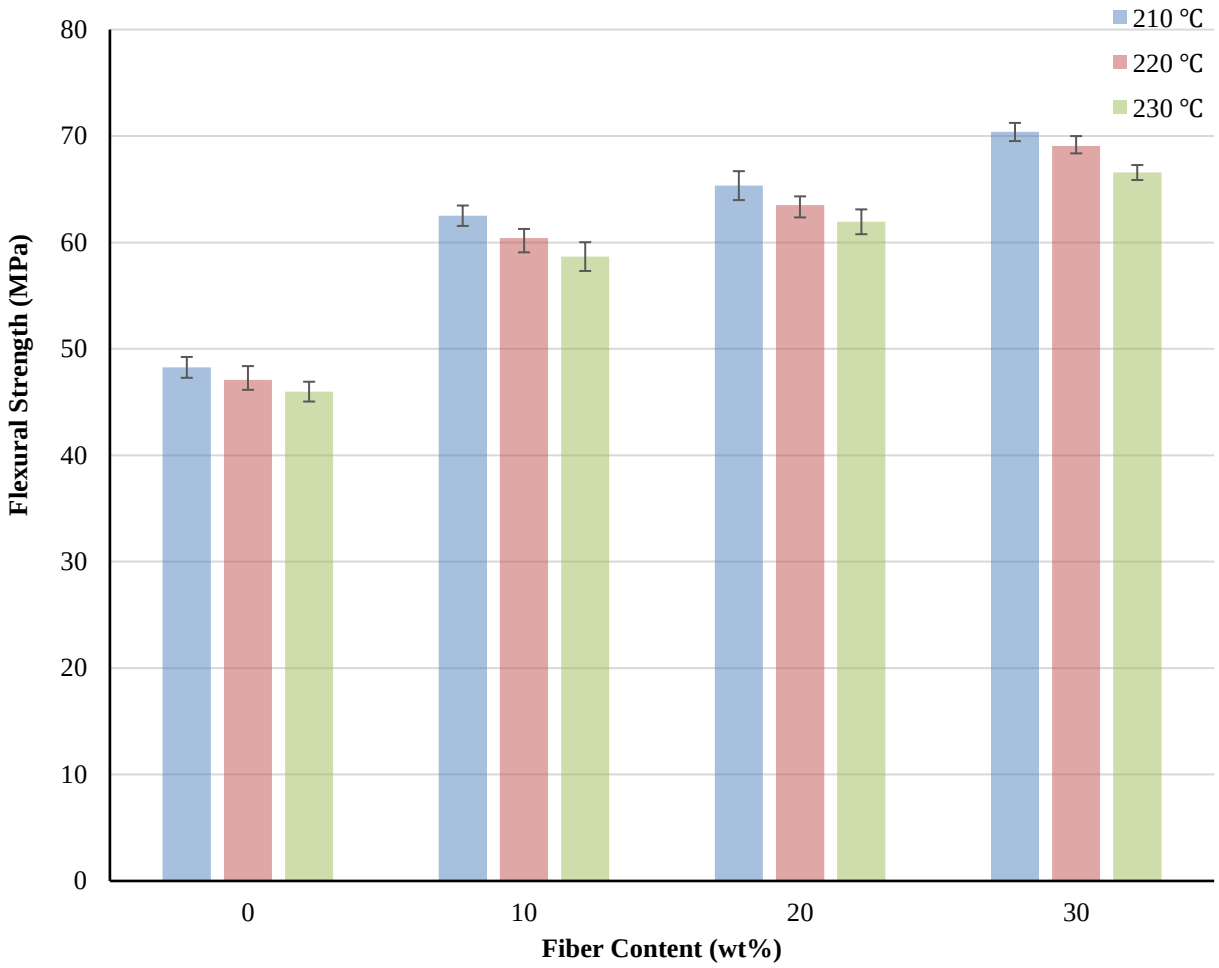

Fig. 3.17 The variation of flexural strength of biocomposites with fiber contents and injection temperatures at injection pressure = 4.8 MPa.

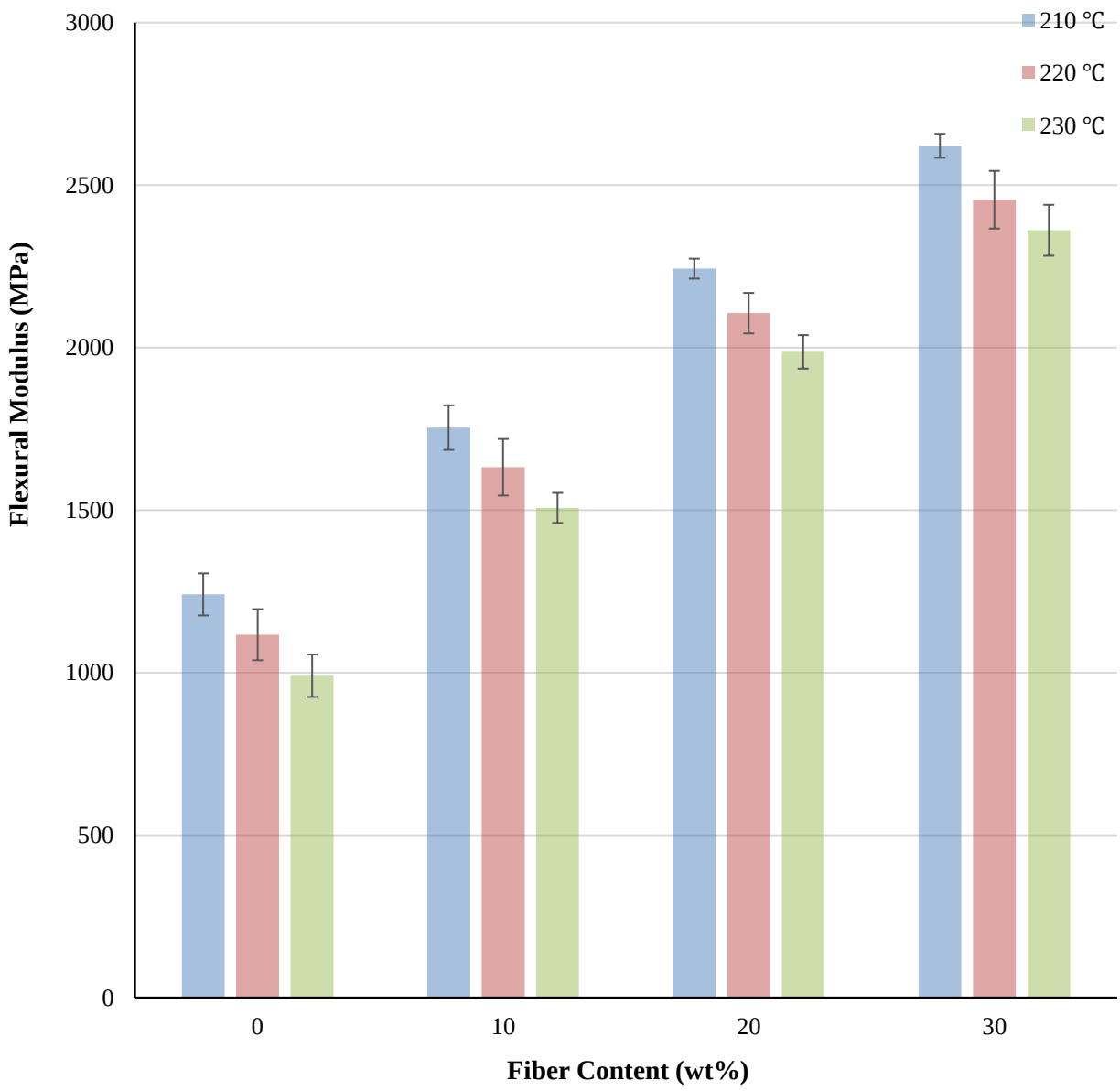

Fig. 3.18 The variation of flexural modulus of biocomposites with fiber contents and injection temperatures at injection pressure = 4.8 MPa.

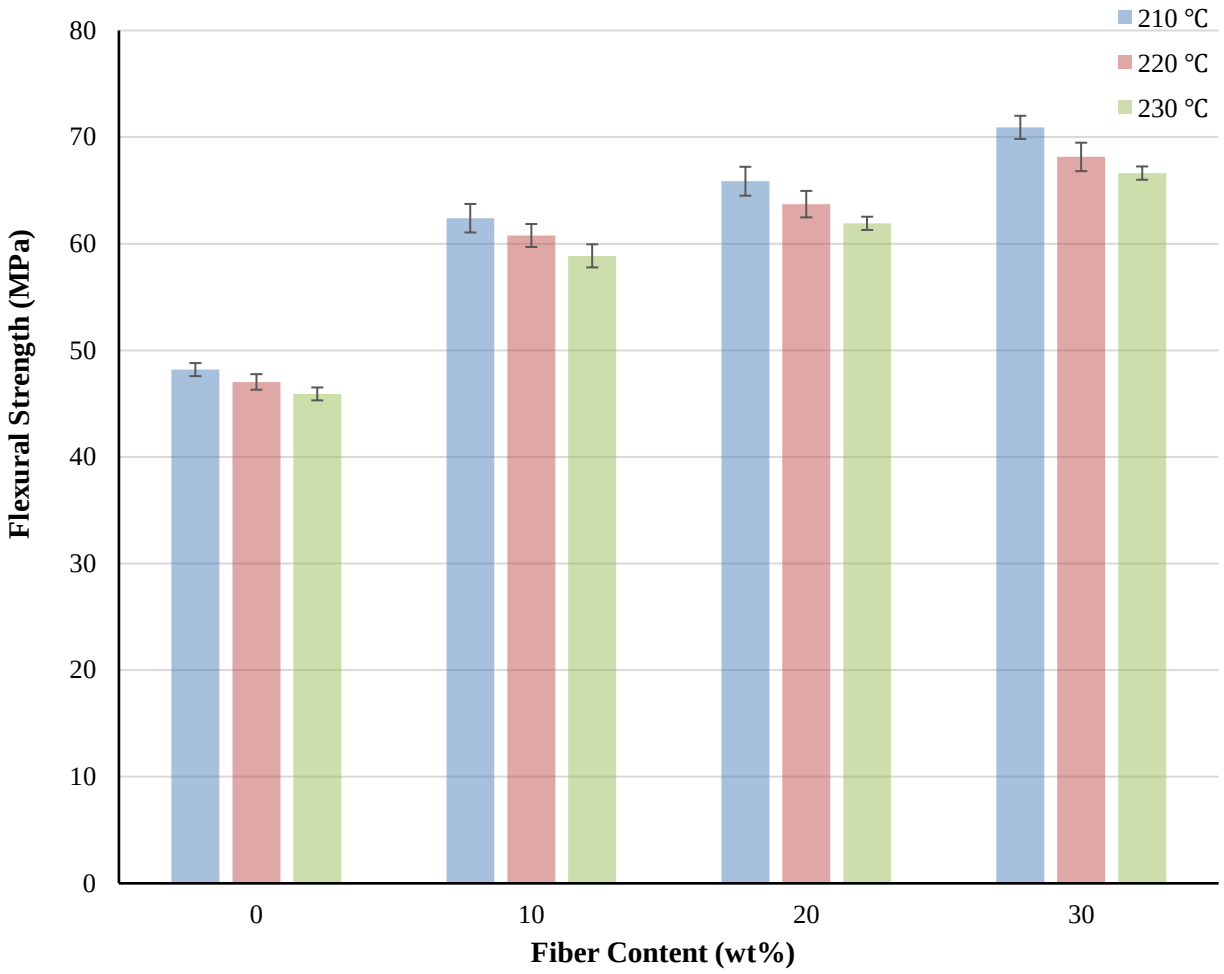

Fig. 3.19 The variation of flexural strength of biocomposites with fiber contents and injection temperatures at injection pressure = 5.9 MPa.

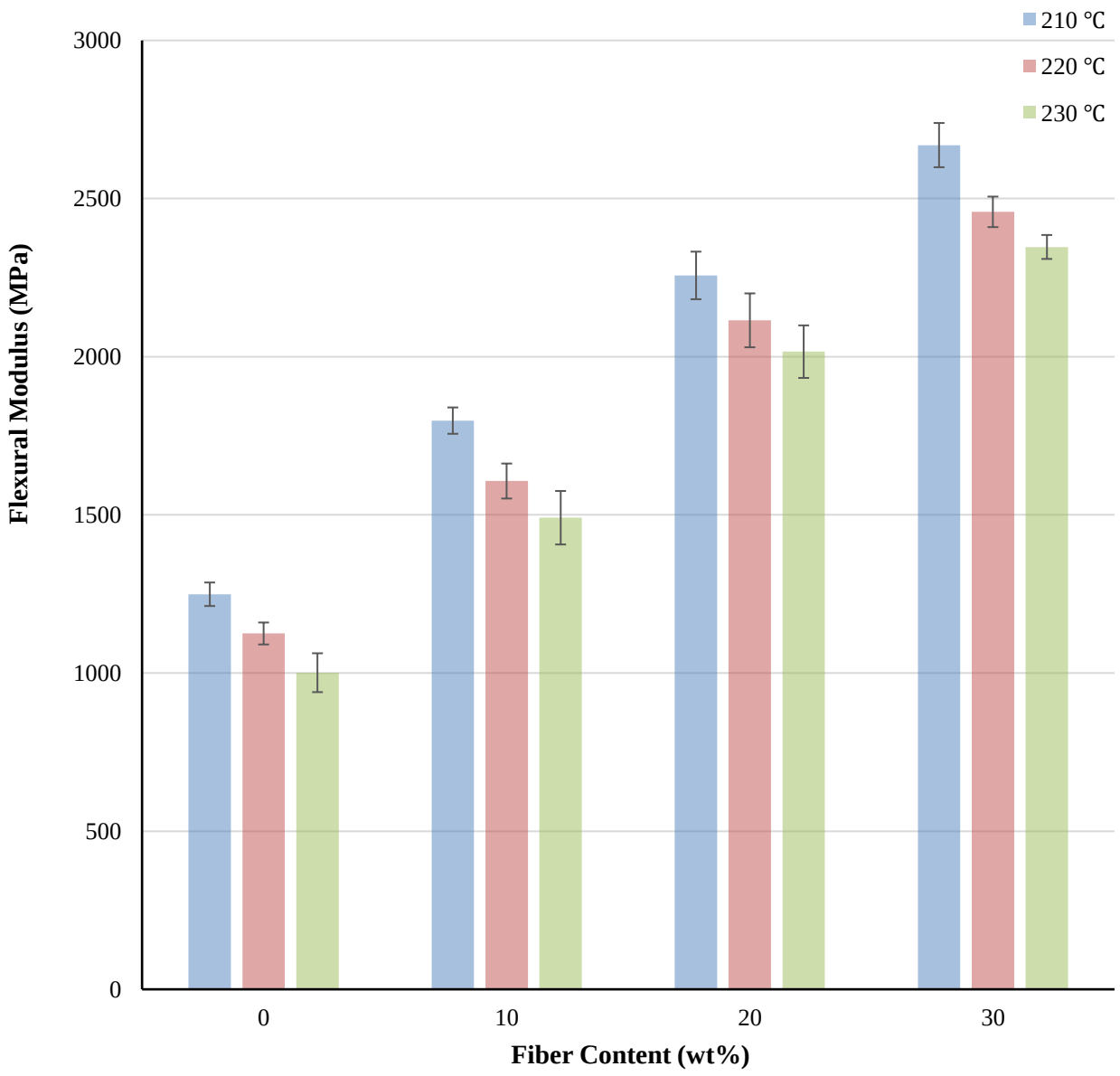

Fig. 3.20 The variation of flexural modulus of biocomposites with fiber contents and injection temperatures at injection pressure = 5.9 MPa.

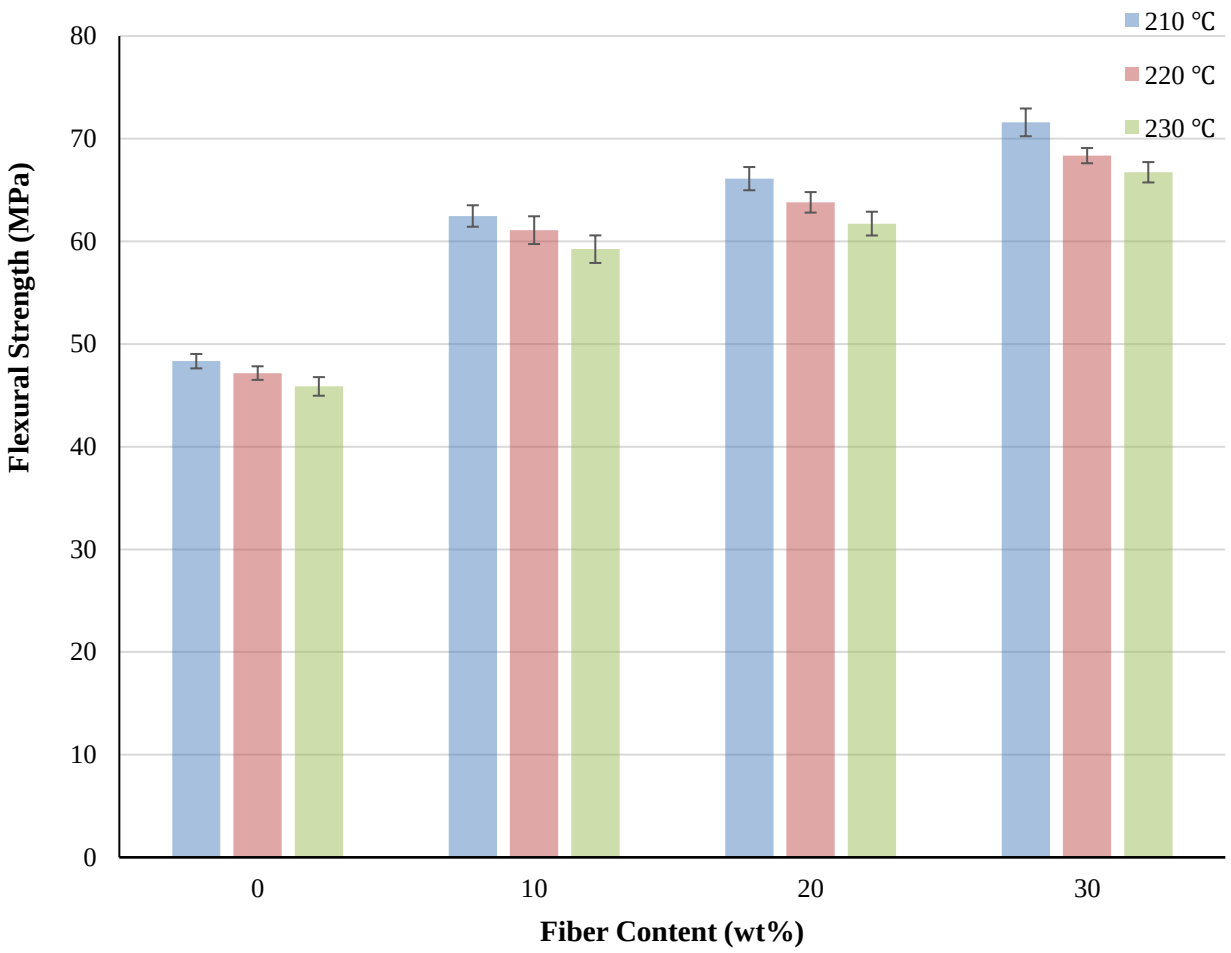

Fig. 3.21 The variation of flexural strength of biocomposites with fiber contents and injection temperatures at injection pressure = 7.0 MPa.

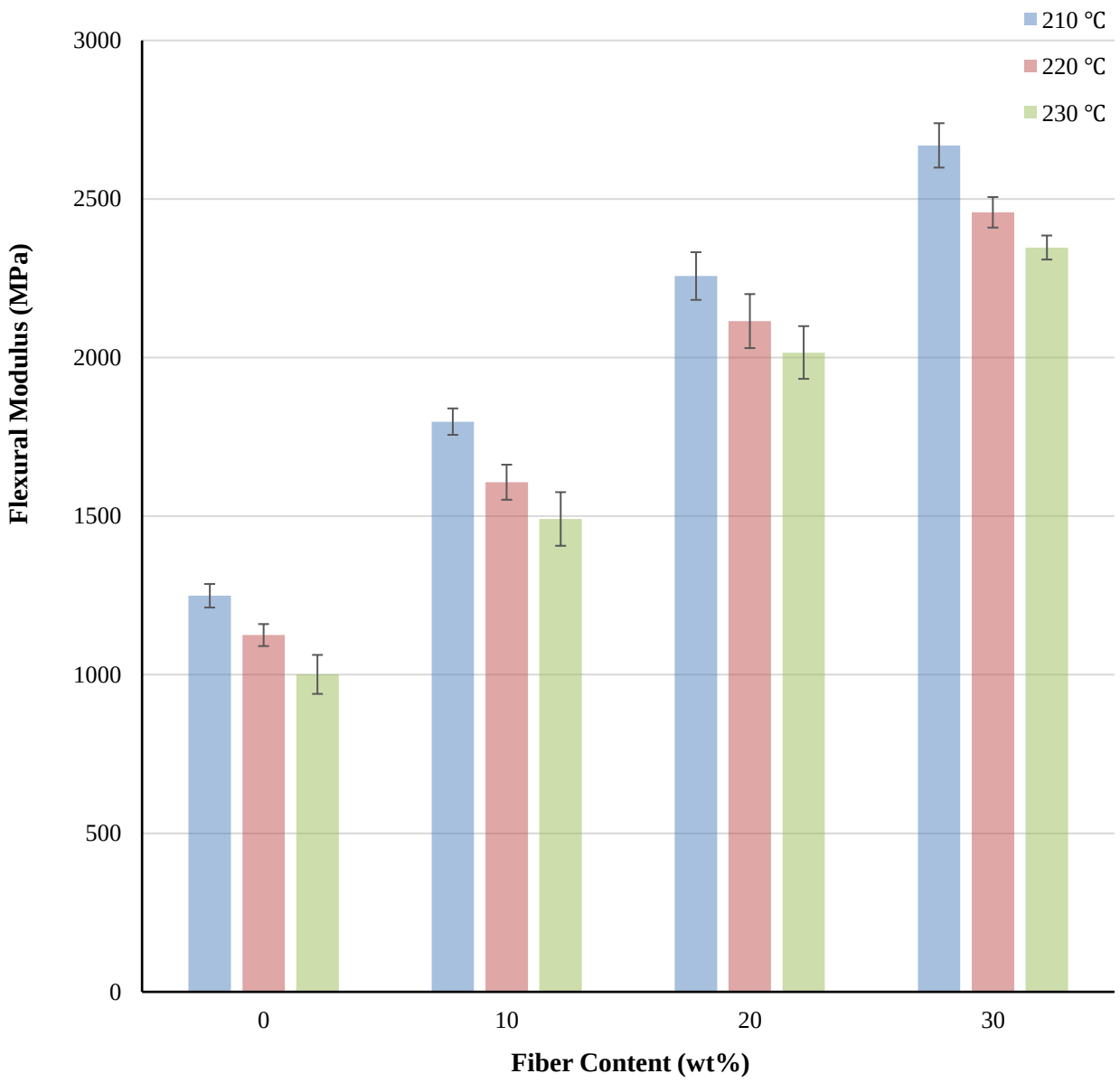

Fig. 3.22 The variation of flexural modulus of biocomposites with fiber contents and injection temperatures at injection pressure = 7.0 MPa.

According to the above figures, the flexural strength and flexural modulus of biocomposites increased dreamingly with increasing fiber content at the same processing conditions (i.e., injection temperature and injection pressure). The average flexural strength of biocomposites with 10 wt%, 20 wt% and 30 wt% flax fibers respectively increased by 28.92%, 35.42% and 45.90% compared with the pure PP. The average flexural modulus of biocomposites with 10 wt%, 20 wt%

and 30 wt% flax fibers respectively increased by 45.06%, 88.16% and 121.46% compared with the pure PP. It was also found the lower injection temperature led to higher flexural strength and modulus for the pure PP and biocomposites with fiber contents of 10 to 30 wt%.

It can also be found that biocomposites with various fiber contents (from 0 to 30 wt%) manufactured at lower injection temperature had higher flexural strength and flexural modulus. As an example of the biocomposite with 30 wt% flax fibers, the lowest injection temperature (T = 210 ℃) led to the highest flexural strength and flexural modulus.

Predicted models of flexural properties

According to the above analysis for the effect of processing condition on flexural properties, the injection pressure had no significant influence on flexural strength and flexural modulus of biocomposites. The injection pressure was excluded in the predicted model. A linear regression model can be developed between the flexural strength and fiber content and injection temperature, and the flexural modulus and fiber content and injection temperature, respectively, using the commercial software MINITAB as follows:

Flexural strength:

$$\sigma_f = 118 + 2.025F - 0.510.327T - 0.02171F^2 + 0.00086T^2 - 0.00316FT \qquad (3.8)$$

where, σ_t is Tensile strength (MPa);

F is flax fiber weight content (wt%);

T is Injection temperature (ºC).

Flexural modulus:

$$E_B = 14848 + 75.66F - 112.6T - 0.3311F^2 + 2279T^2 - 0.0902FT \qquad (3.9)$$

where E_B is Young's modulus (MPa).

F is flax fiber weight content (wt%);

T is Injection temperature (ºC).

The above two equations revealed the relationship between flexural properties (flexural strength and flexural modulus) and the two main factors (fiber content and injection temperature). The

detailed result of the linear regression can be seen from the tables in Appendix B (refer to Table B.9 to B.19). According to the R-square = 95.97% for flexural strength (shown in Table B.11) and R-square = 99.78% for flexural modulus (shown in Table B.15), the two equations were very in a good fit of the predicted model of flexural strength and flexural modulus.

From Equations 3.8 and 3.9, Fig. 3.23 and 3.24 can be produced, which show the variations of flexural strength and flexural modulus of biocomposites with respect to fiber content and injection temperature. The surface responses in the two figures approved the previous discussion about the effect of flax fiber content and injection temperature on the flexural strength and flexural modulus of biocomposites.

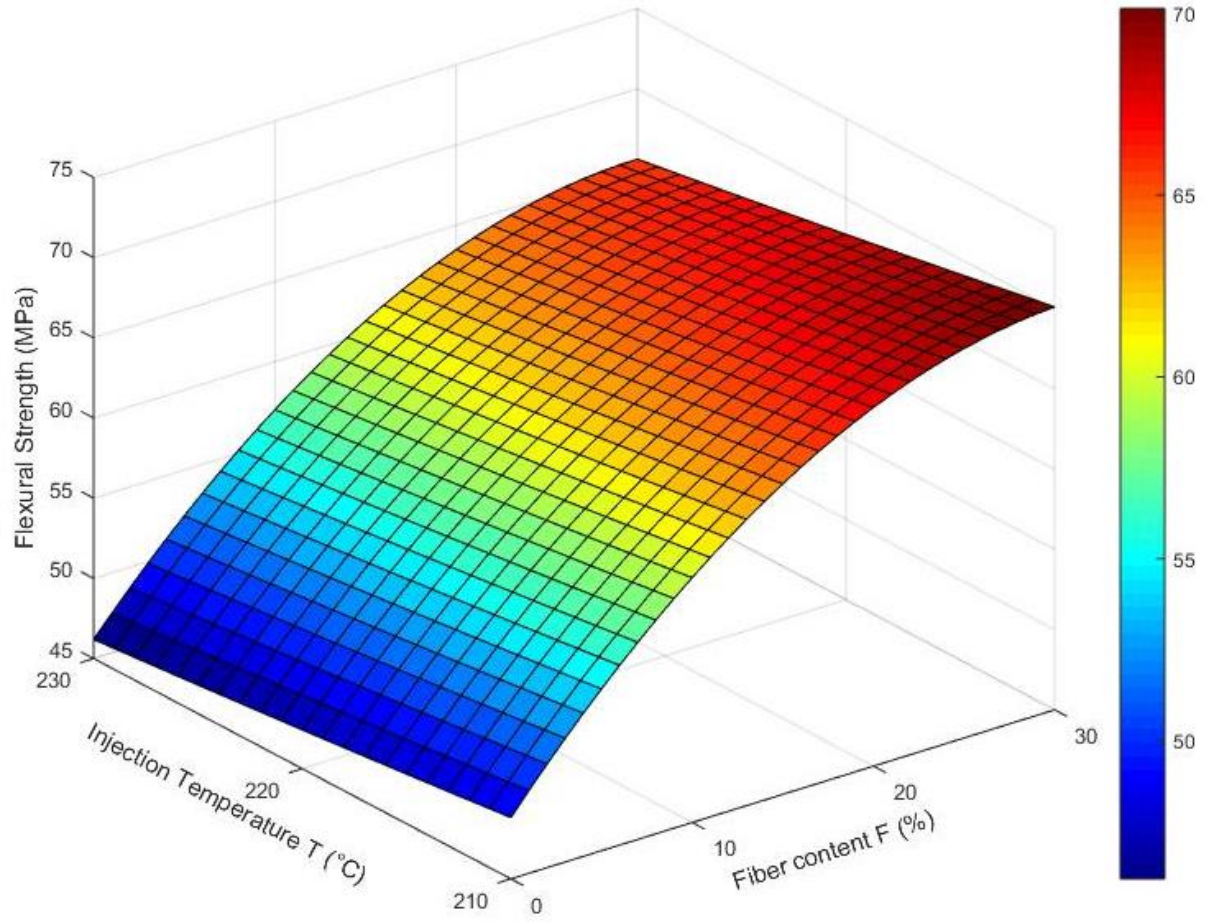

Fig. 3.23 The variation of flexural strength of biocomposites with flax fiber content and injection temperature by the predicted model of flexural strength.

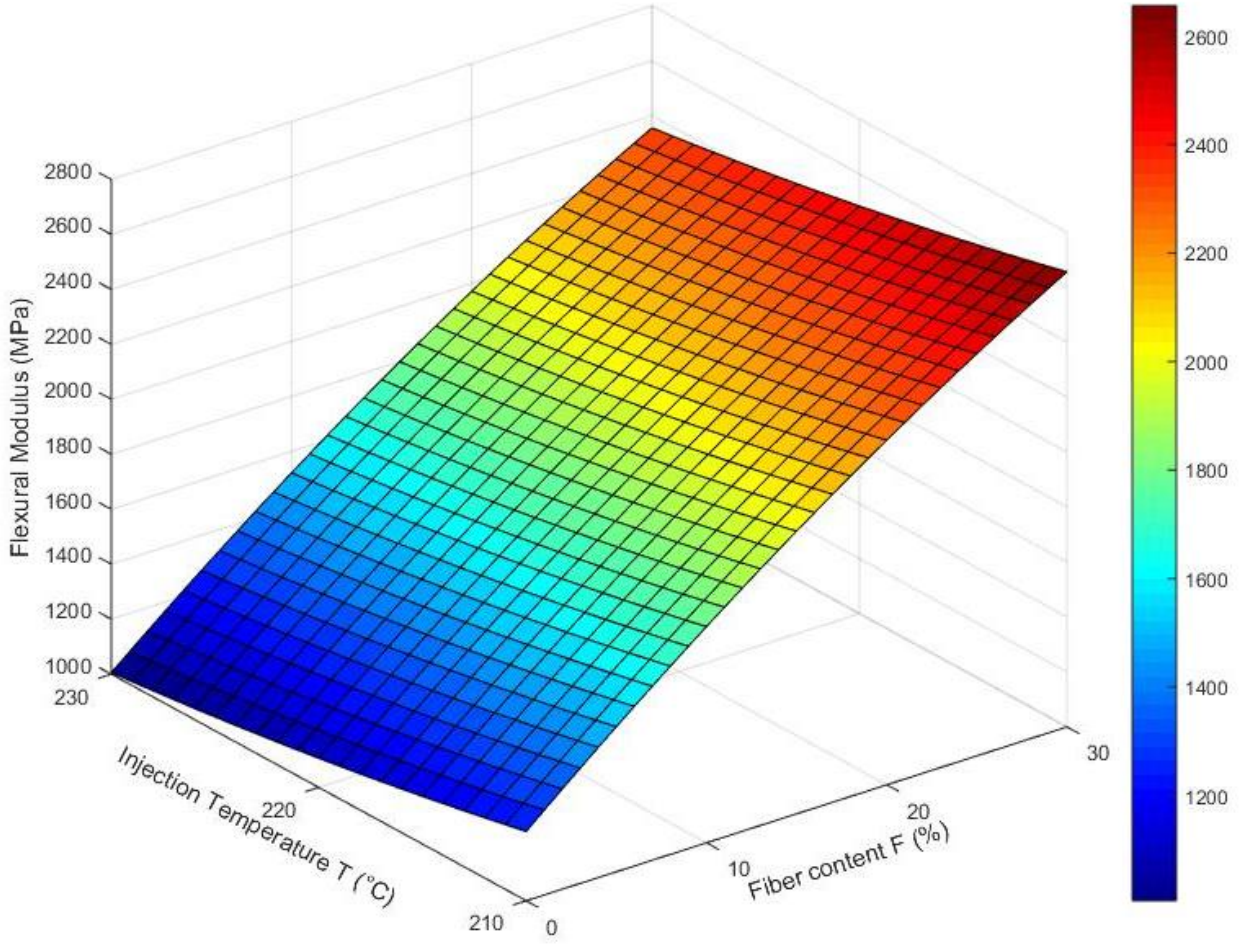

Fig. 3.24 The variation of flexural modulus of biocomposites with flax fiber content and injection temperature by the predicted model of flexural modulus.

3.3.3 The effect of processing conditions on water absorption of biocomposites

Hygroscopicity is the property of a small particle system – particularly the ability to take up moisture from the atmosphere (Winterkorn, 2008). Hygroscopicity of biocomposites is an obstacle in the applying natural fibers as reinforcements. Higher water absorption leads to poor dimensional stability of final product and water inside the biocomposites may affect their physical and mechanical properties. The water absorption of natural fibers can be reduced through chemical

treatments, but little understanding on how water absorption of natural fiber reinforced biocomposites may be affected by the processing conditions. This thesis study has advanced the understanding.

Table 3.4 shows the property of water absorption of biocomposites with different fiber contents at several processing conditions, and these conditions cover the workable range of operation.

Table 3.4 Water absorption of biocomposites at different processing conditions.

Trial	Fiber Content (wt%)	Injection Temperature (℃)	Injection Pressure (MPa)	Water absorption (%)	
				Mean	St.dev.
1	0	210	4.8	0.0234	0.0035
2	0	210	5.9	0.0241	0.0046
3	0	210	7.0	0.0237	0.0049
4	0	220	4.8	0.0345	0.0062
5	0	220	5.9	0.0368	0.0041
6	0	220	7.0	0.0347	0.0040
7	0	230	4.8	0.0451	0.0062
8	0	230	5.9	0.0446	0.0037
9	0	230	7.0	0.0424	0.0057
10	10	210	4.8	0.1712	0.0099
11	10	210	5.9	0.1729	0.0084
12	10	210	7.0	0.1693	0.0066
13	10	220	4.8	0.1841	0.0132
14	10	220	5.9	0.1850	0.0177
15	10	220	7.0	0.1869	0.0032
16	10	230	4.8	0.1972	0.0065
17	10	230	5.9	0.1987	0.0068
18	10	230	7.0	0.2001	0.0127
19	20	210	4.8	0.1771	0.0158
20	20	210	5.9	0.1756	0.0191

Table 3.4 continued.

24	20	220	7.0	0.1862	0.0107
21	20	210	7.0	0.1721	0.0105
22	20	220	4.8	0.1881	0.0165
23	20	220	5.9	0.1887	0.0050
25	20	230	4.8	0.2007	0.0176
26	20	230	5.9	0.2012	0.0109
27	20	230	7.0	0.2017	0.0036
28	30	210	4.8	0.1809	0.0147
29	30	210	5.9	0.1807	0.0106
30	30	210	7.0	0.1823	0.0067
31	30	220	4.8	0.1931	0.0119
32	30	220	5.9	0.1947	0.0121
33	30	220	7.0	0.1936	0.0059
34	30	230	4.8	0.2034	0.0195
35	30	230	5.9	0.2042	0.0186
36	30	230	7.0	0.2057	0.0085

As shown in Table 3.3, compared with pure PP, all biocomposites have a higher water absorption, which result from a high hydrophilicity of flax fiber and a high hydrophobicity of the matrix PP. The highest water absorption can be found from the table, with the biocomposite with 30 wt% flax fibers at injection temperature 230 ℃ and injection pressure 7.0 MPa. In the same processing conditions, flax fiber contributed to a huge increase of 385.14% in water absorption compared with the pure PP.

In term of the above analysis, biocomposites had totally different water absorption from pure PP, and thus data from pure PP was excluded when doing ANOVA. The result of ANOVA (refer to Table A.5 in Appendix A) showed that water absorption of biocomposites was significantly dependent on flax fiber content and injection temperature, and the effect of fiber content on water

absorption was almost the same as the effect of injection temperature. The injection pressure had no significant influence on water absorption.

The variation of water absorption of biocomposites with various fiber contents (from 0 to 30 wt%) and different injection temperatures, respectively, at the three levels of injection pressures is illustrated by Fig. 3.25 - Fig.3.27.

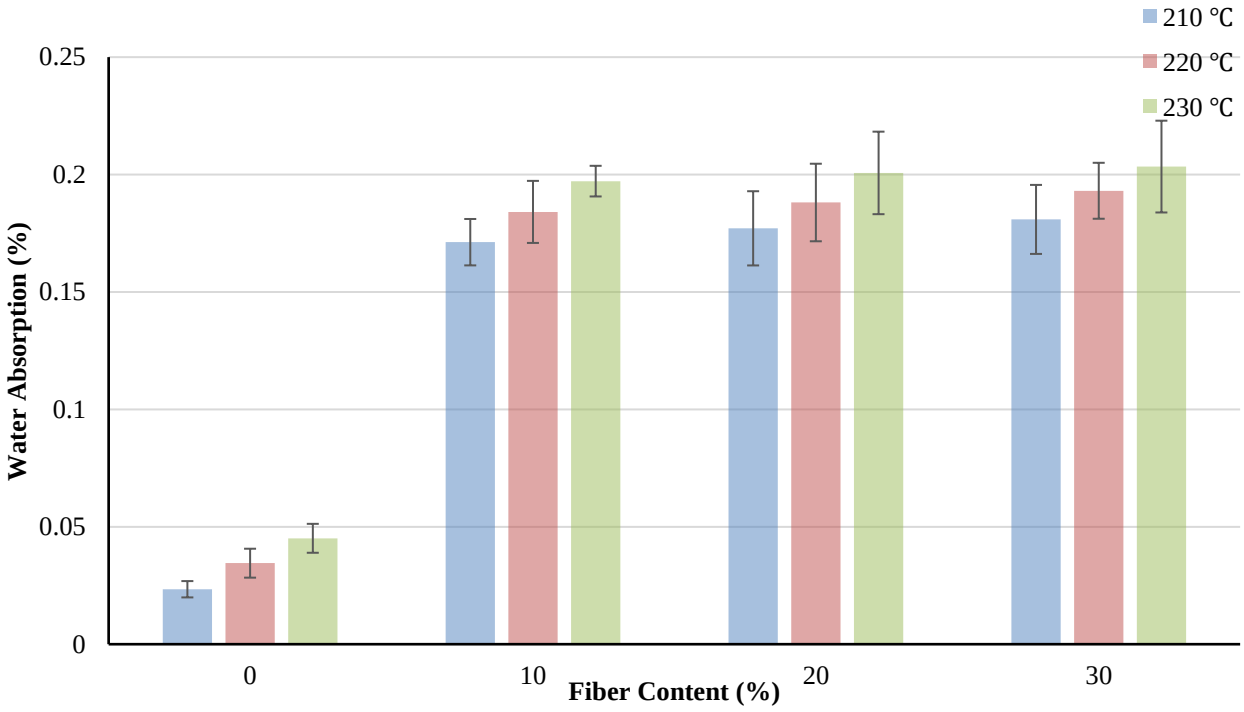

Fig. 3.25 The variation of water absorption of biocomposites with fiber contents and injection temperatures at injection pressure = 4.8 MPa.

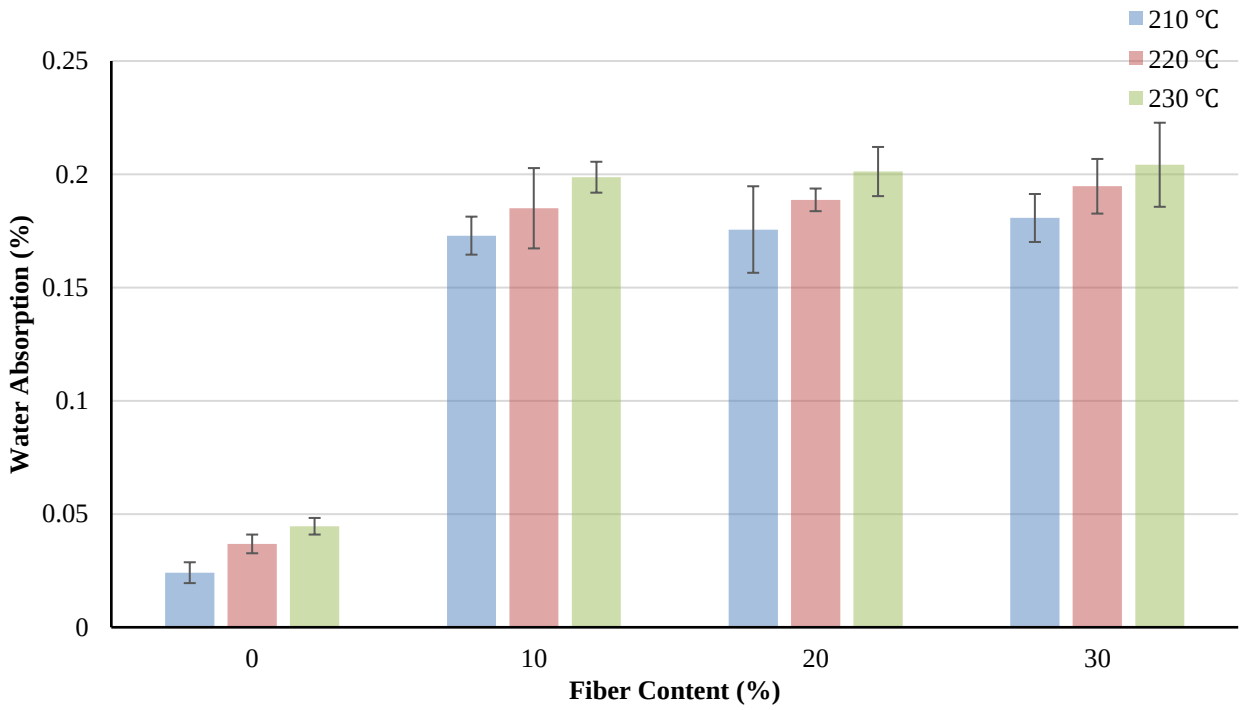

Fig. 3.26 The variation of water absorption of biocomposites with fiber contents and injection temperatures at injection pressure = 5.9 MPa.

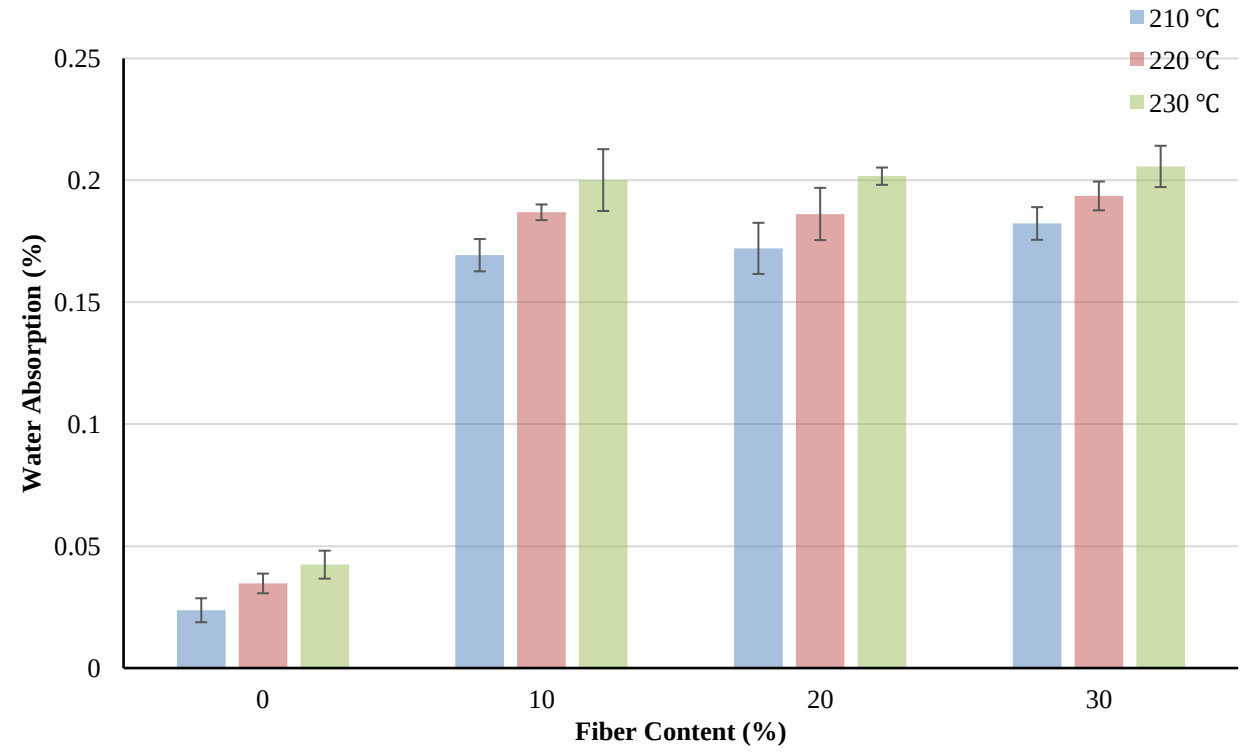

Fig. 3.27 The variation of water absorption of biocomposites with fiber contents and injection temperatures at injection pressure = 7.0 MPa.

Based on the above analysis for the effect of processing conditions on water absorption, it was concluded that injection pressure had no significant influence on water absorption of biocomposites. The injection pressure was excluded in the predicted model. Additionally, the data from pure PP was excluded when doing regression. A linear regression model can be developed between water absorption of biocomposites and fiber content and injection temperature, using the commercial software MINITAB as follows:

Water absorption:

$$W = -0.302 + 0.002356F + 0.00292T + 0.000012F^2 - 0.000003T^2 + 0.000011FT \quad (3.10)$$

where, W is water absorption (%);

F is flax fiber weight content (wt%) (from 10 to 30);

T is Injection temperature (ºC).

The above equation revealed the relationship between water absorption and the two main factors (fiber content and injection temperature). The detailed result of the linear regression can be seen from the tables in Appendix B (Table B.17 to B.20). Further, the R-square = 98.01% for water absorption (shown in Table B.19), the equation was in a very good fit of the model of water absorption of biocomposites with experimental data.

From Equation 3.10, Fig. 3.28 can be produced, which shows the variations of water absorption of biocomposites with respect to fiber content and injection temperature. The surface responses in the two figures approved the previous discussion about the effect of flax fiber content and injection temperature on water absorption of biocomposites.

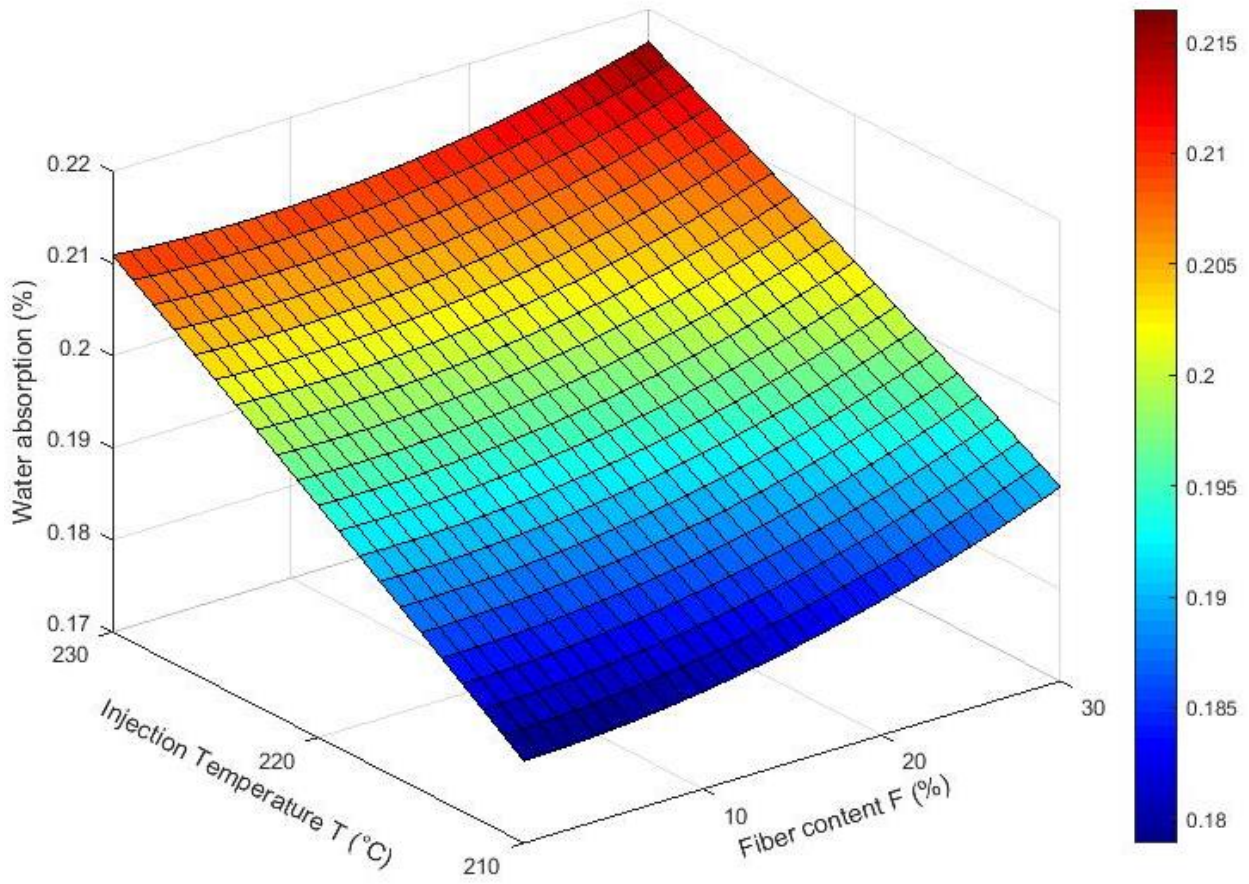

Fig. 3.28 The variation of water absorption of biocomposites with flax fiber content and injection temperature by the predicted model of water absorption.

3.4 Conclusion with discussion

In this chapter, biocomposites were successfully produced by injection molding and the processing scheme was presented. The influence of flax fiber loading and processing conditions including injection temperature and pressure on the mechanical properties (tensile properties and flexural properties) and water absorption of biocomposites were investigated.

The results showed that fiber content was the most significant factor to change the mechanical properties of biocomposites compared with the other two processing conditions (injection temperature and injection pressure), and the tensile properties (tensile strength and Young's modulus) and flexural properties (flexural strength and flexural modulus) of biocomposites dreaming increased with flax fiber content. Biocomposites with different fiber contents (from 0 to 30 wt%) processed by lower injection temperature had higher tensile properties and flexural properties. Water absorption of biocomposites was significantly dependent on fiber content and injection temperature and their effects on water absorption of biocomposites were almost the same. Injection pressure had no significant effect on either mechanical properties or water absorption.

Additionally, the relationships between the properties of biocomposites (i.e., tensile properties, flexural properties and water absorption) and the two main factors (flax fiber content and injection) were built by polynomial linear regression. These models approved the understanding of the effect of processing conditions on the mechanical properties and water absorption of biocomposites. It was also concluded that biocomposites could have the highest mechanical properties and relatively low water absorption when adding 30 wt% flax fibers and processing at 210 ℃ by injection molding.

CHAPTER 4 RHEOLOGY

4.1 Introduction

This chapter experimentally studied the rheological characteristics of flax fiber reinforced PP composites, and the effect of the processing conditions (fiber content and temperature) on rheological properties of biocomposites was also investigated. In order to widen the simulation analysis of injection modeling of biocomposites by CAE (Computer Aided Engineering), it was necessary to determine the viscosity using a mathematical model. The Cross-WLF model is the most common model used by injection molding simulation software, because it offers the best fit to most viscosity data (Hieber & Chiang, 1992). Because of biocomposites as a new type of materials, the relevant parameters of the Cross-WLF for biocomposites could not be found in the simulation software, and thus it was necessary to determine the relevant parameters so that the simulation of injection molding could be successfully conducted. In this chapter, a methodology on determining such parameters using rheological data measured by capillary rheometer was presented.

4.2 Experimental

4.2.1 Materials

The polymer matrix used in this experiment was the same in Chapter 3, and it was HIVAL® 2412 PP Homo-polymer from Nexeo Solutions with a melt flow rate (MFR) of 12 (g/10 min at 230 ˚C/2.16 kg). Flax fiber was treated by using the same processes of fiber pre-treatment in Chapter 3 and the fiber length was 2 mm.

4.2.2 Methods and Measurements

The experimental biocomposites were pellets of extruding the mixture of PP and short flax fibers

as described in chapter 3. The biocomposite pellets were dried 24 h at 70 ˚C under vacuum before the rheological experiments.

The rheological measurements of biocomposites were carried out in a twin-bore Rosand Capillary Rheometer RH2000 as shown in the Fig. 4.1. The capillary rheometer measures the viscosity of a material by controlling its temperature in the bore, forcing the material to go through a capillary die inside the bore by a piston, and using a sensor called a pressure transducer to measure the pressure just above the die. According to RH2000 manual, the standard range of operation temperatures is from −40 ˚C to 500 ˚C and the maximum force loaded is 12 kN. The maximum shear rate produced by an RH2000 is approximately 10^7 s^{-1} and the minimum shear rate is 0.1 s^{-1}.

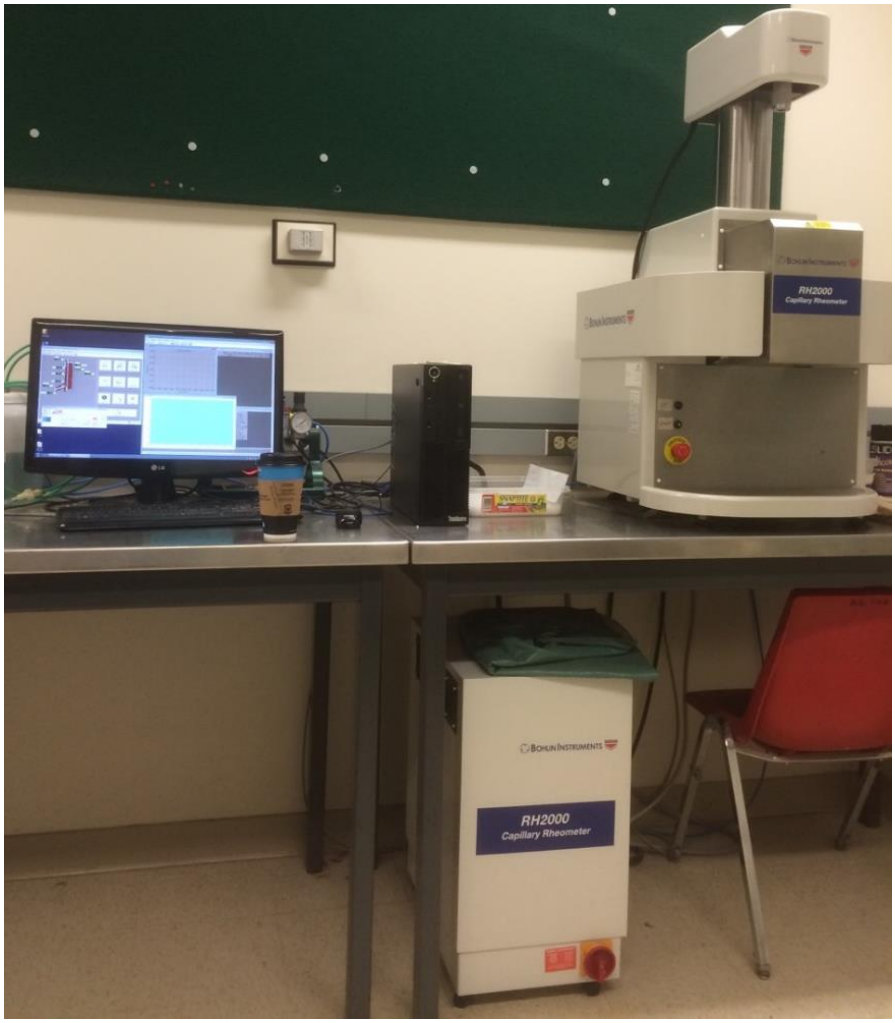

Fig. 4.1 Rosand Capillary Rheometer RH2000.

In this experiment, the viscosities of the melted PP and biocomposites with various fiber content (10, 20 and 30 wt%) were measured at temperatures of 220 ˚C, 230 ˚C and 240 ˚C in three replicates per sample. The shear rate used in the study were in the range 0 to 10,000 s^{-1}. The rheometer was equipped with a die with the length of 10 mm and the diameter of 1 mm. The flow viscosity data presented in this study represent an average value of three measurements.

4.2.3 Corrections on measured "raw" data

In general, there are pressure drops occurring at entry to and exit from a capillary die. The simple measure of shear viscosity does not take account of this pressure drop. As a result, it is termed the uncorrected shear viscosity. To obtain the true measure, a correction called the Bagley correction is normally applied. At the same conditions of material, temperatures and shear rates, a separate test on a zero length capillary die was used to correct the pressure data and determine the true shear stress occurring inside the capillary.

Since the biocomposite melt is pseudo-plastic non-Newtonian fluid, the velocity profile in the capillary die is frequently assumed to be plug-like. However, in practice, such velocity profiles vary, this being related to the shear rate being measured. The velocity profile or shear rate profile is suggested to be related to the power-law index. Therefore, it is necessary to obtain the true shear rate, normally by finding the power-law index as the flow properties of the melt is being determined. Rabinowitsch's correction was applied to obtain the true shear rate in such a case, i.e. for an arbitrary fluid. The correction is carried out by plotting log wall shear stress versus log apparent shear rate. If the curve is a straight line, the slope obtained is the power-law index and the corrected shear rate is expressed as:

$$\dot{\gamma}_c = \left(\frac{3n+1}{4n}\right)\dot{\gamma}_a \tag{4.1}$$

where $\dot{\gamma}_a$is the measured shear rate; $\dot{\gamma}_c$ is the corrected shear rate; and n is the corresponding flow index. The corrected viscosity η is defined as the ratio of the shear stress τ to the correct shear rate, as follows.

$$\eta = \frac{\tau}{\dot{\gamma}_c} \tag{4.2}$$

4.3 Mathematical model

4.3.1 General equation

In this study, the injection molded parts have three-dimensional (3D) configurations and the rheological response of polymer melt is non-Newtonian and non-isothermal. The generalized Hele-Shaw flow model introduced by Hieber and Shen (Hieber & Shen, 1980) is the most common approximation that provides the governing equations for non-isothermal, non-Newtonian and inelastic flows. To model the flow of an injected fluid in a mold, we start from the conservation equations for mass, momentum and energy (Gerhart & Gross, 1985).

Equation of mass conservation,

$$\frac{d\rho}{dt} + \rho \cdot (\nabla \cdot \vec{v}) = 0 \tag{4.3}$$

Equation of momentum conservation,

$$\rho \frac{d\vec{v}}{dt} = -\nabla \cdot p + \nabla \cdot \sigma_n + \rho g \tag{4.4}$$

Equation of conservation of energy,

$$\rho \frac{d}{dt}\left(e + \frac{1}{2}\vec{v}^2\right) = -\nabla \cdot \vec{q} + \nabla \cdot (\sigma \cdot \vec{v}) + \rho g \cdot \vec{v} \tag{4.5}$$

with ρ the density, $\vec{v}$ the velocity, p the pressure, σ_n the viscous stress tensor, e the internal energy, σ the stress tensor and $\vec{q}$ the heat flux.

The polymer melt is a high viscous fluid, and consequently, the inertial and gravitational terms will not be taken into account in the momentum equation. This simplification leads to the well-known Stokes equations (Girault & Raviart, 1979) from Equations 4.3 and 4.4:

$$\nabla \cdot \vec{v} = 0 \tag{4.6}$$

$$-\nabla \cdot p + \nabla \cdot \sigma_n = 0 \tag{4.7}$$

The above equations were on the assumption that it should describe the rheological behavior as a function of the rate of deformation according to different conditions (like fiber contents, temperature). In addition, the flow of biocomposite melts is assumed to be an incompressible fluid during the measurement.

During the filling phase, the flow into the mold cavity is very similar to a laminar flow between two plates with a very thin gap (seen in Fig 4.2).

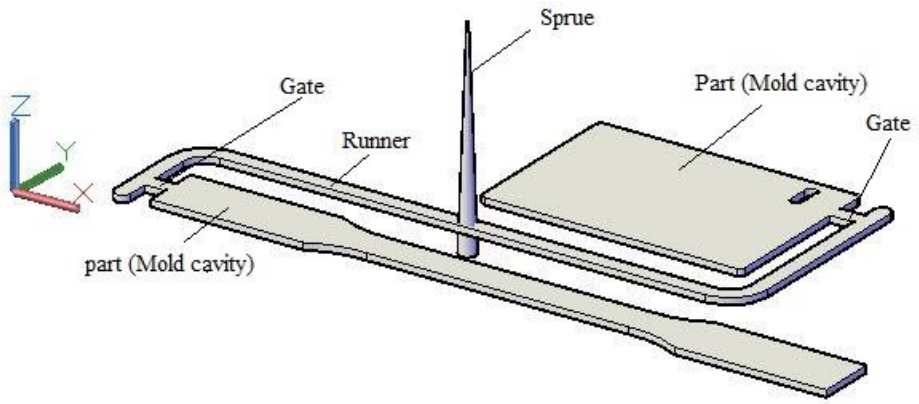

Fig. 4.2 Injection mold used in experiments including the delivery system and molded parts.

Assuming a Cartesian coordinate system (shown in Fig. 4.2), the z-axis is in the thickness direction and the x-y plane is on the mid plane of the cavity, and the velocity components u, v and w, are respectively taken in the x, y and z directions. The Hele-Shaw flow model has the following assumptions (Courbebaisse, 2005):

1) The w component of the velocity is neglected with respect to the others components;
2) The pressure constant in thickness, is a function of x and y;
3) The velocity gradient in the x and y directions is negligible with respect to z direction.

Applying the Hele-Shaw assumptions to the Stokes's equation leads to the following simplified equations:

$$\frac{\partial p}{dx} = \frac{\partial}{dz}\left(\eta \frac{\partial u}{dz}\right) \tag{4.8}$$

$$\frac{\partial p}{dy} = \frac{\partial}{dz}\left(\eta \frac{\partial v}{dz}\right) \tag{4.9}$$

$$\frac{\partial p}{dz} = 0 \tag{4.10}$$

where η is the viscosity. By integrating the mass and the momentum equations with respect to the thickness direction, we obtain a single equation for pressure which combines mass conservation

and momentum conservation. The final result gives the following Laplace's equation (Hieber & Shen, 1980):

$$\frac{\partial}{\mathrm{dx}}\left(\mathrm{S}\frac{\partial \mathrm{p}}{\mathrm{dx}}\right)+\frac{\partial}{\mathrm{dy}}\left(\mathrm{S}\frac{\partial \mathrm{p}}{\mathrm{dy}}\right)=0 \tag{4.11}$$

$$\mathrm{S}=\int_0^{\mathrm{h}}\frac{\mathrm{z}^2}{\eta}\mathrm{dz} \tag{4.12}$$

Equation 4.11 means that the pressure field is the solution of Equation 4.12 with a zero pressure at each time step.

4.3.2 Cross-WLF model

To implement the simulation and analysis of injection molding for new biocomposites by computer aided engineering (CAE), it is necessary to determine the viscosity using a mathematical model. In this study, the analysis and simulation of injection molding process is conducted by Moldflow, which use values of the parameters from the Cross-WLF model. The Cross-WLF model is the most common model used by injection molding simulation software, because it offers the best fit to most viscosity data (Hieber & Chiang, Shear-rate-dependence modeling of polymer melt viscosity, 1992).

The Cross-WLF model is a combination of two different models, which are a "Cross" model that describes the viscosity dependence on the shear rate and a "WLF" model that describes the viscosity dependence on the temperature. The Cross-WLF model has become widely implemented in various process simulations due to its intuitive form and excellent predictive capability across a relatively wide range of shear rates and temperatures. Accordingly, this model is implemented in this investigation for modeling of the viscous component of the melt rheology. The mathematical expression of Cross model is the following (Cross, 1979):

$$\eta=\frac{\eta_0}{1+\left(\frac{\eta_0\dot{\gamma}}{\tau^*}\right)^{1-n}} \tag{4.13}$$

where:

η (Pa/s) is the melt viscosity;

η_0 (Pa/s) is the zero shear viscosity or the 'Newtonian limit' in which the viscosity approaches a constant at very low shear rates;

$\dot{\gamma}$ $(1/s)$ is the shear rate;

$\tau^*(Pa)$ is the model constant that shows the critical stress rate from which the pseudoplastic behavior of material starts; and

n is the power law index in the high shear rate regime, determined by curve fitting.

The effect of temperature on the viscosity can be described by the WLF model (Williams et al., 1955), which determines the zero shear viscosity, as follows:

$$\eta_0 = D_1 exp\left[-\frac{A_1(T-T^*)}{A_2+(T-T^*)}\right] \tag{4.14}$$

$$A_2 = A_3 + D_3 \cdot p \tag{4.15}$$

$$T^* = D_2 + D_3 \cdot p \tag{4.16}$$

where, T (K) is the operation temperature;

T^* (K) is the glass transition temperature of the material, depending on the pressure;

p (Pa) is the operation pressure;

τ^*, n, D_1 (Pa/s), D_2 (K), D_3 (K/Pa), $A_1$and A_3 (K) are the data-fitted coefficients which need to be determined.

4.4 Results and discussion

4.4.1 Analysis of rheological properties of biocomposites

Capillary rheology is the most widely used when high shear rates are required, for example in the processes like extrusion or injection molding. Fig. 4.2 to Fig. 4.5 show the shear viscosity of pure PP and biocomposites with various fiber content (10 wt%, 20 wt%, 30 wt%) at the different temperatures (210 ℃, 220 ℃, 230 ℃) as a function of the shear rate.

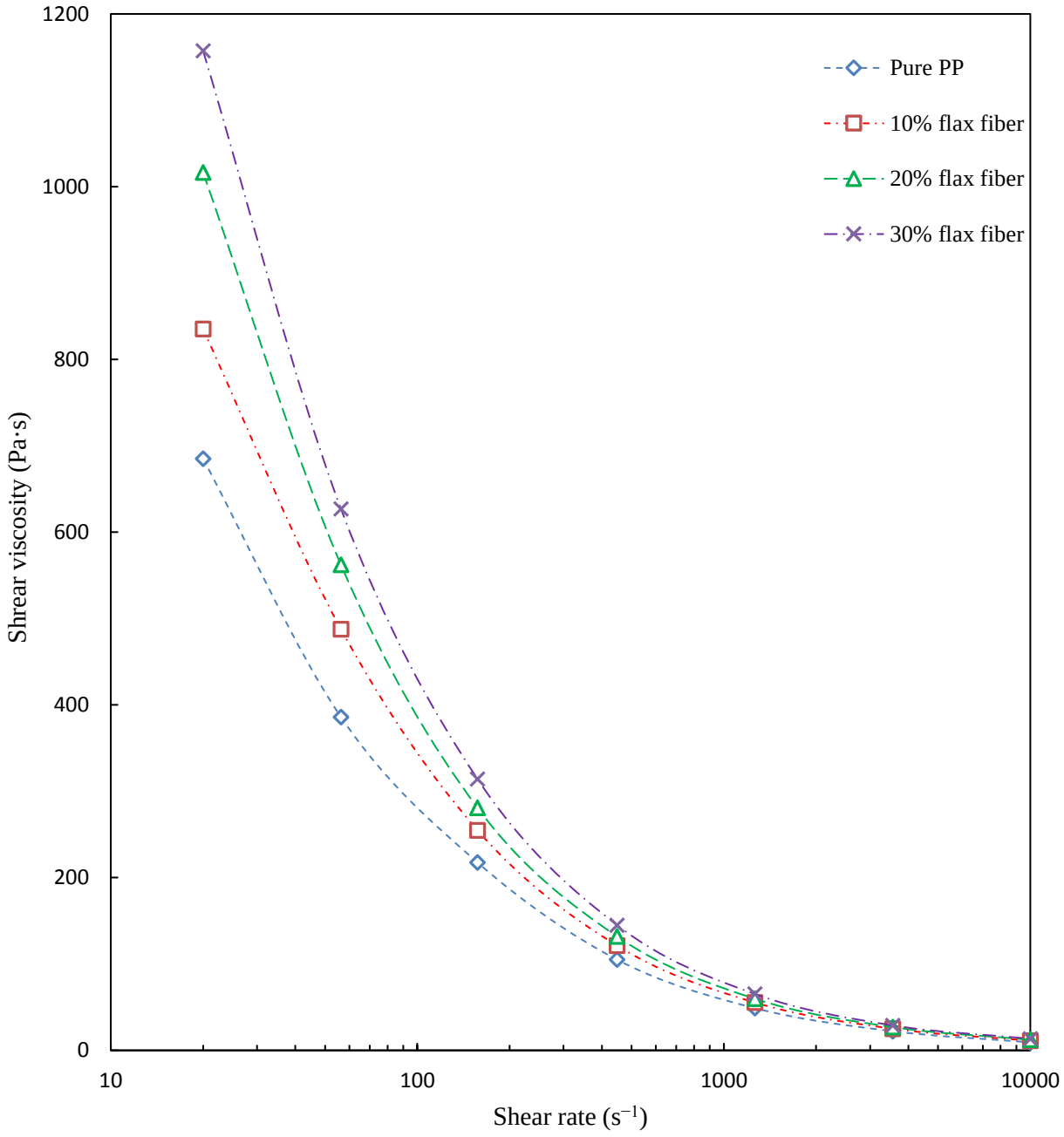

Fig. 4.3 Shear viscosity of pure PP and biocomposites at 210 ℃ as a function of the shear rate.

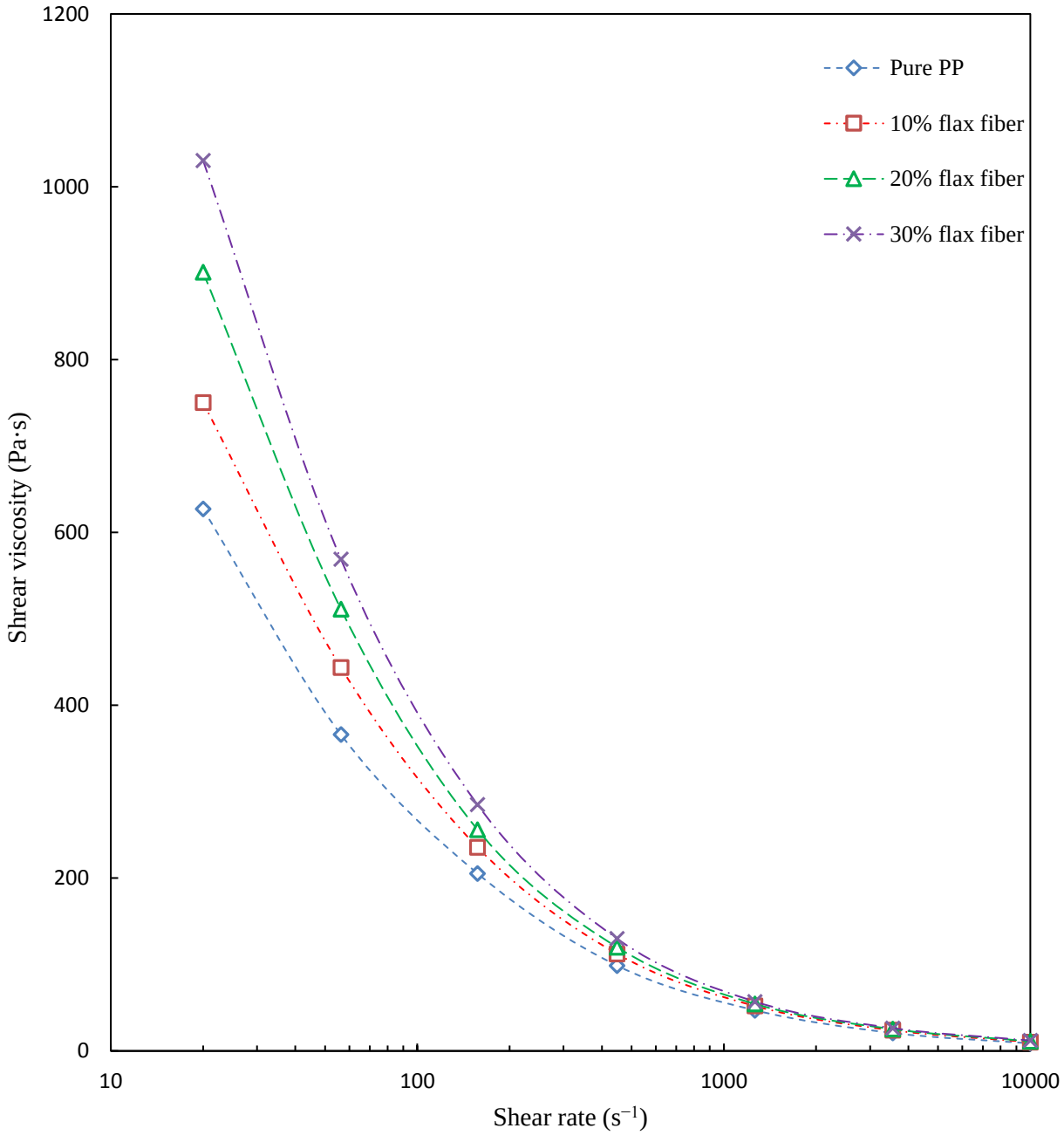

Fig. 4.4 Shear viscosity of pure PP and biocomposites at 220 ℃ as a function of the shear rate.

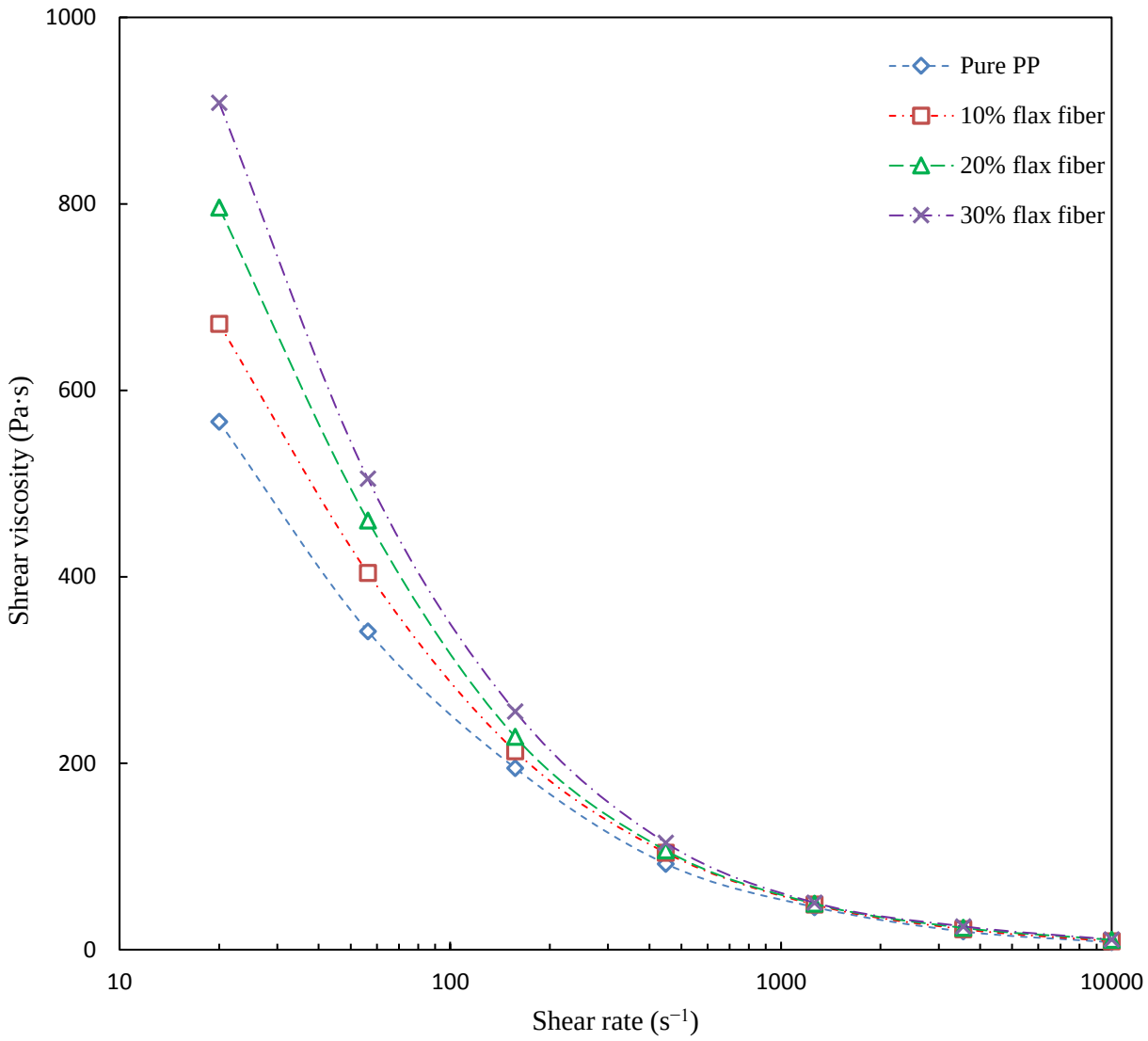

Fig. 4.5 Shear viscosity of pure PP and biocomposites at 230 ℃ as a function of the shear rate.

From the rheological behavior of pure PP or biocomposites at different temperatures (210 ℃, 220 ℃, 230 ℃) (shown in Fig. 4.3 to 4.5), they all showed that the shear viscosity of pure pp or biocomposites decreases with increasing shear rate. Such high decrease in the shear viscosity is associated with high shear-thinning behavior of the melt and biocomposites are more shear-thinning then the pure PP. The decrease of the shear viscosity with the increase of the shear rate is related to the high viscoelastic characteristics of biocomposite materials of the pure PP or biocomposite melt flow. However, at high shear rates (from 1,000 to 10,000 S^{-1}), the melt of biocomposites showed a less restrained decrease in shear viscosity.

It also showed that the shear viscosity of biocomposites increases with fiber content. This rheological behavior of biocomposites is associated with the alignment and the orientation of the flax fiber in the polymer chains. At low shear rates, flax fiber molecules are completely oriented due to the good dispersion in the PP matrix. The higher fiber content will result in increasing the fiber-fiber collisions, which leads to a higher decrease in the apparent viscosity. However, at very high shear rates (from 5,000 to 10,000 s^{-1}), the shear viscosities of biocomposites with various fiber content (from 0 to 30 wt%) all trend to be the same. This behavior mainly results from the higher shear rate leading to the orientation of the polymer molecules, the agglomeration of the flexible flax fiber, and the entanglements within the polymer chains in the capillary rheometer.

The variation of the shear viscosity in function of the shear rate of pure PP or biocomposites with different fiber contents at various temperatures was investigated and the rheological test results are presented in Fig. 4.6 to 4.9. The rheological conditions were kept constant while different tests were run for 210 ℃, 220 ℃, and 230 ℃.

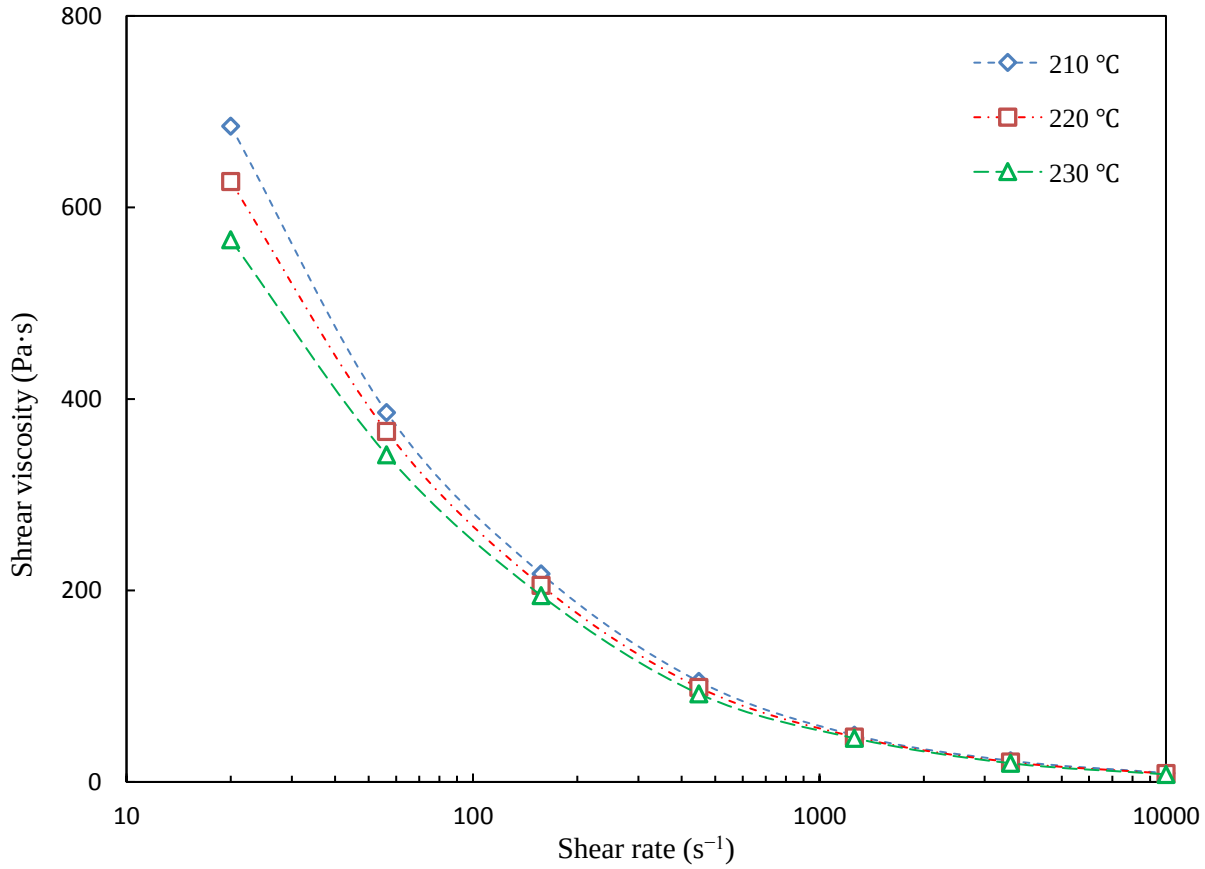

Fig. 4.6 Shear viscosity of pure PP at different temperatures.

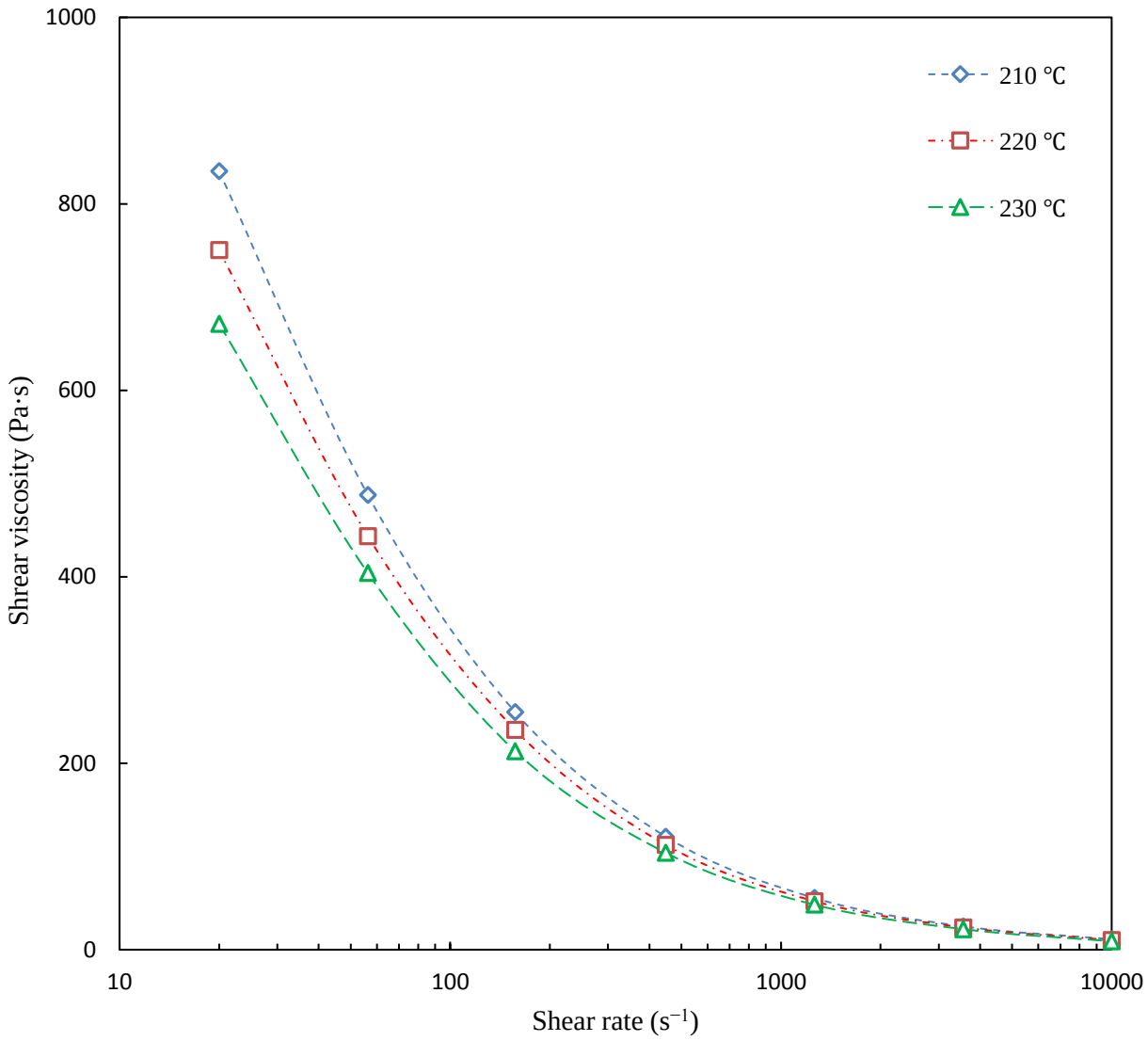

Fig. 4.7 Shear viscosity of the biocomposites with 10% flax fiber at different temperatures.

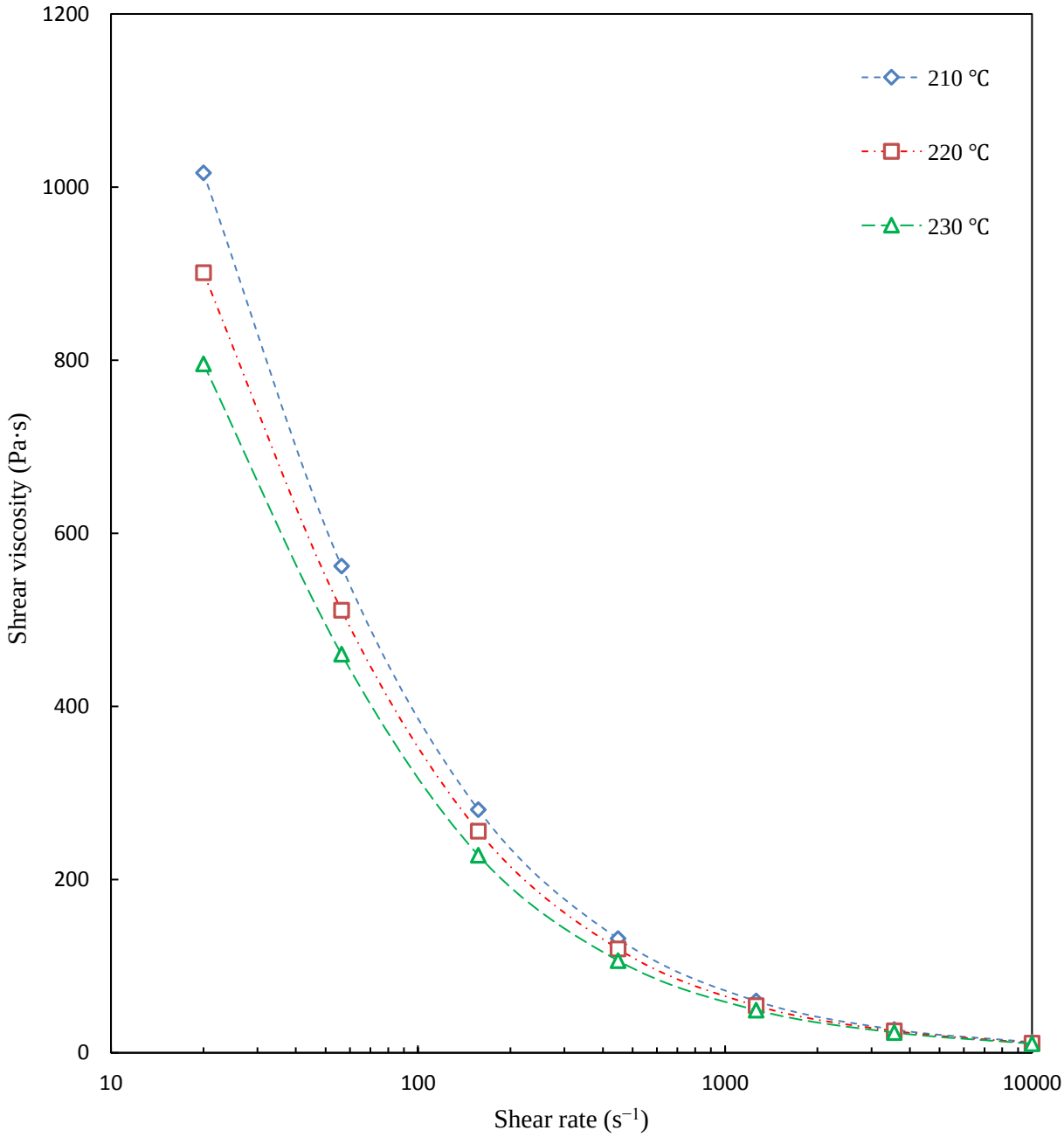

Fig. 4.8 Shear viscosity of the biocomposites with 20% flax fiber at different temperatures.

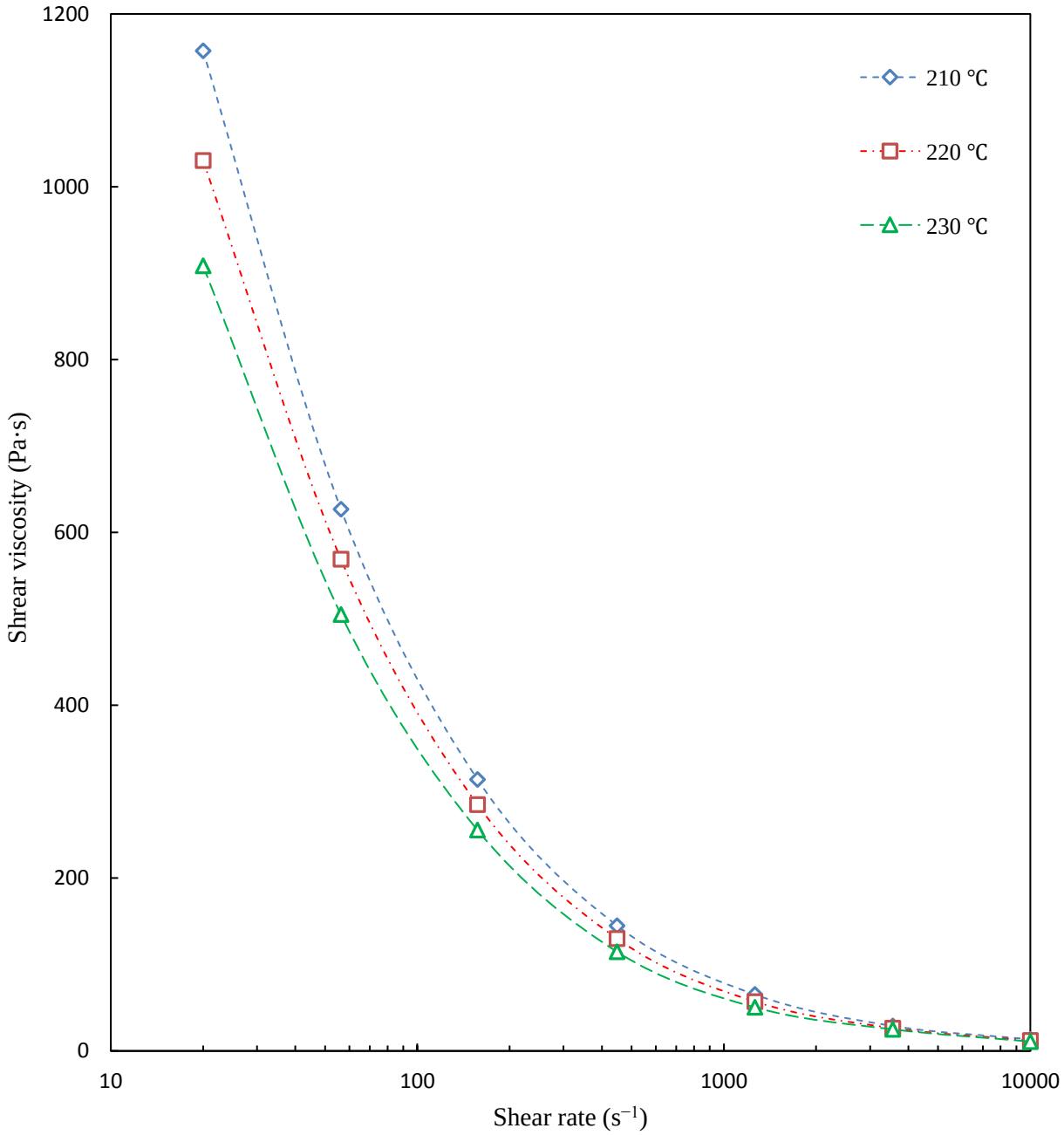

Fig. 4.9 Shear viscosity of the biocomposites with 30% flax fiber at different temperatures.

The shear viscosity decreased as the temperature increased and higher temperature led to a smaller non-Newtonian area. It means that lower temperature led to higher region for the reduction of the shear viscosity. This behavior is mainly caused by the agglomeration and entanglement of the flax fibers at low temperature and low shear rate, which made melt flow deformation. However, at a

higher shear rate, all the shear viscosity variations as function of shear rates followed the same rate for different temperatures, which corresponds to shear-thinning behavior of biocomposites. This is because the shear viscosity mostly dependents on the shear rate rather than the effect of temperature at high shear rate.

4.4.2 Assessment of the parameters in the Cross-WLF model

To implement the simulation and analysis of injection molding for biocomposites by computer aided engineering (CAE), the Cross-WLF model was selected to determine the rheological properties of biocomposites. The Cross-WLF model is a capable model for predicting the viscosity of the melt (η) as a function of shear rate ($\dot{\gamma}$), temperature (T) and pressure (p) (Carreau et al., 1968). There are 7 parameters ($\tau^*(Pa)$, n, D_1 (Pa/s), D_2 (K), D_3 (K/Pa), $A_1$and A_3 (K)) which need to be determined in this model. For those 7 coefficients, two groups can be classified in terms of their dependence on the material's physical characteristics. The first group of parameters are independent parameters, D_2 (K), D_3 (K/Pa), $A_1$and A_3 (K), which are only related to the type of the material. The other group is dependent parameters, $\tau^*(Pa)$, n, D_1 (Pa/s), which are dependent on the grade or the constituents of the material.

From the WLF model, the independent parameters (D_2 (K), D_3 (K/Pa)) are related to the glass transition temperature T^* of the material. Tajvidi et al. (2006) studied the effect of natural fibers on the thermal properties of natural fiber PP biocomposites an they concluded that the nature fibers don't affect the glass transition temperature of biocompsites and T^* of either pure PP or bicomposites are the same and around -10 ℃. In Equation 4.16, D_3 describes the pressure dependence of T^* and is often set at 0 (Ferry, 1980). Therefor,

$$D_2 = T^* = -10\ ℃ = 263.15\ \text{K};$$

$$D_3 = 0.$$

In the material database of Moldflow software, it appears that $A_1$and A_3 (K) values are either identical or approximate to the published "universal values" of 17.44 and 51.6, respectively (Gava & Lucchetta, 2012). In this project, it is assumed that $A_1 = 17.44, A_3\ (K) = 51.6\ (K)$.

The dependent parameters (τ^*, n, D_1 (Pa/s)) are dependent on the temperature and the fiber loading of biocomposites. First, the parameter n can be generated from the rheological data of biocomposites. In the Cross-WLF model, the relationship between the shear viscosity η and the shear rate $\dot{\gamma}$ is nonlinear. Based on the rheological data of biocomposites with various fiber contents (from 10 to 30 wt%) at different temperatures (from 210 ℃ to 230 ℃), the other two dependent parameters (τ^* and D_1 (Pa/s)) can be estimated by nonlinear regression. In this project, the process of nonlinear regression will be conducted by SPSS.

4.4.3 The results of the parameter estimation

Based on the previous discussion, the independent parameters (D_2 (K), D_3 (K/Pa), $A_1$and A_3 (K)) for biocomposites with various fiber contents (10 wt%, 20 wt%, 30 wt%) at different temperatures (210 ℃, 220 ℃, 230 ℃) could be determined as the four contents, as follows:

$$D_2 = T^* = 263.15 \text{ K},$$
$$D_3 = 0,$$
$$A_1 = 17.44,$$
$$A_2 = A_3 = 51.6\ K.$$

Then, Equation 4.14 was simplified into Equation 4.17.

$$\eta_0 = D_1 exp\left[-\frac{A_1(T-T^*)}{A_2+(T-T^*)}\right] = D_1 exp\left[-\frac{17.44(T-263.15)}{51.6+(T-263.15)}\right] \quad (4.17)$$

From the rheological data of biocomposites at various testing conditions, the power law index n could be determined as the experimental mean of the n_i parameters of each test. So the parameter n was calculated by Equation 4.18.

$$n = \frac{\sum_{i=1}^{m} n_i}{m} \quad (4.18)$$

where m is the number of all runs. The parameter n for all biocomposites at various testing conditions were shown in Table 4.1.

Table 4.1 The parameter n for different biocomposites at various testing conditions.

Fiber content (wt%)	Temperature (℃)	n	$1-n$
10	210	0.3392	0.6608
10	220	0.3512	0.6488
10	230	0.4245	0.5755
20	210	0.3143	0.6857
20	220	0.3477	0.6523
20	230	0.4041	0.5959
30	210	0.3004	0.6996
30	220	0.3217	0.6783
30	230	0.3871	0.6129

Based on the experimental data, the parameters $\tau^*(Pa)$ and η_0 were estimated through nonlinear regression by using SPSS (referred to Tables C.1 to C.18 and in Appendix C.). In the process of nonlinear regression, Equation 4.13 was considered as the model expression. The results of estimated parameters $\tau^*(Pa)$ and $\eta_0(Pa/s)$ were shown in the following Table 4.2.

Table 4.2 The estimated parameters $\tau^*(Pa)$ and $\eta_0\ (Pa/s)$ by nonlinear regression.

Fiber content (wt%)	Temperature (℃)	$\tau^*(Pa)$	$\eta_0\ (Pa/s)$
10	210	23313.9	2177.98
10	220	29998.7	2724.55
10	230	44077	2616.19
20	210	17312.8	1533.28
20	220	25177.6	2197.61
20	230	33587.7	2444.49
30	210	19756.6	628.515
30	220	20779	947.267
30	230	23076.1	864.609

Equation 4.17 at the different temperatures (210 ℃, 220 ℃ 230 ℃) was simplified respectively, as follows:

$$\eta_0 = 7.33 * 10^{-7} D_1 \ (at\ T = 210\ ℃) \quad (4.19)$$

$$\eta_0 = 6.51 * 10^{-7} D_1 \ (at\ T = 220\ ℃) \quad (4.20)$$

$$\eta_0 = 5.84 * 10^{-7} D_1 \ (at\ T = 210\ ℃) \quad (4.21)$$

Based on Table 4.2, the parameter D_1 was calculated from Equations 4.19 to 4.21. All seven parameters of different biocomposites at various testing conditions were shown in the following Table 4.3.

Table 4.3 The seven parameters of different biocomposites at various testing conditions.

Fiber content (wt%)	Temperature (℃)	$\tau^*(Pa)$	n	$D_1\ (Pa/s)$	$D_2\ (K)$	$D_3\ (K/Pa)$	A_1	$A_3\ (K)$
10	210	23313.9	0.3392	2.97E+09	263.15	0	17.44	51.6
10	220	29998.7	0.3512	4.18E+09	263.15	0	17.44	51.6
10	230	44077	0.4245	4.48E+09	263.15	0	17.44	51.6
20	210	17312.8	0.3143	2.09E+09	263.15	0	17.44	51.6
20	220	25177.6	0.3477	3.37E+09	263.15	0	17.44	51.6
20	230	33587.7	0.4041	4.19E+09	263.15	0	17.44	51.6
30	210	19756.6	0.3004	8.58E+08	263.15	0	17.44	51.6
30	220	20779	0.3217	1.45E+09	263.15	0	17.44	51.6
30	230	23076.1	0.3871	1.48E+09	263.15	0	17.44	51.6

4.4 Conclusion

In this chapter, the effect of the processing conditions (fiber content and temperature) on the rheological properties of biocomposites was investigated. Based on the analysis of the experimental data, the shear viscosity of biocomposites increases with increasing fiber content, and at very high shear rates (from 5,000 to 10,000 S^{-1}), the shear viscosities of biocomposites with various fiber content (from 0 to 30%) all tend to be the same. The shear viscosity of biocomposites

decreased with the increase of injection temperature, and at a higher shear rate, all the shear viscosity variations as function of shear rates followed the same rate for different temperatures. Therefore, at a high shear rate, the shear viscosity mostly depends on the shear rate rather than the effect of fiber content and temperature.

Among the seven parameters of the Cross-WLF model, the independent parameters, $D_2\ (K)$, $D_3\ (K/Pa)$, A_1 and $A_3\ (K)$, could be obtained by the thermal properties of this material. The parameter n could be generated from experimental data. The other two parameters ($\tau^*(Pa)$, $D_1\ (Pa/s)$) could be estimated through nonlinear regression based on the rheological data of biocomposites. This methodology presented could be used as guidelines to determine seven parameters of the Cross-WLF model for any new material.

CHAPTER 5 STUDY OF SHRINKAGE AND WARPAGE IN INJECTION MOLDED BIOCOMPOSITES

5.1 Introduction

Biocomposite, as a new material, has not been investigated on how it performs during injection molding. In the process of injection molding, the shrinkage and warpage are two major attributes determining the final quality of the product. In order to increase product quality and provide reliability for the future application in the market of biocomposites, the effects on the shrinkage and warpage of injection molded biocomposites need to be investigated. This chapter presents a systematic approach to analyze and optimize the simulation experiments of injection molding for biocomposites, aiming to investigate the optimal set of processing parameters with respect to shrinkage and warpage of biocomposites. Because of the reinforcement of nature fibers, biocomposites have different rheological properties with their matrix materials. While in the current market, the CAE software can only simulate the injection molding for some regular materials such as PP, PE, and ABS. Lack of information about rheological properties leads to difficulty in simulation of injection molding for natural fiber biocomposites. Based on the rheological model in Chapter 4, this approach can perform the simulation experiments of injection molded biocomposites.

5.2 Identifying significant factors for optimization

The systematic approach performs the identification of the factors on the research problem, selection of the significant parameters and determination of the optimal set of processing parameters by the integration of DOE, CAE simulation, statistical analysis and optimization methods.

The complete steps of the approach are generalized and described in Fig. 5.1. There are three steps in this approach showed in the following Fig. 5.1

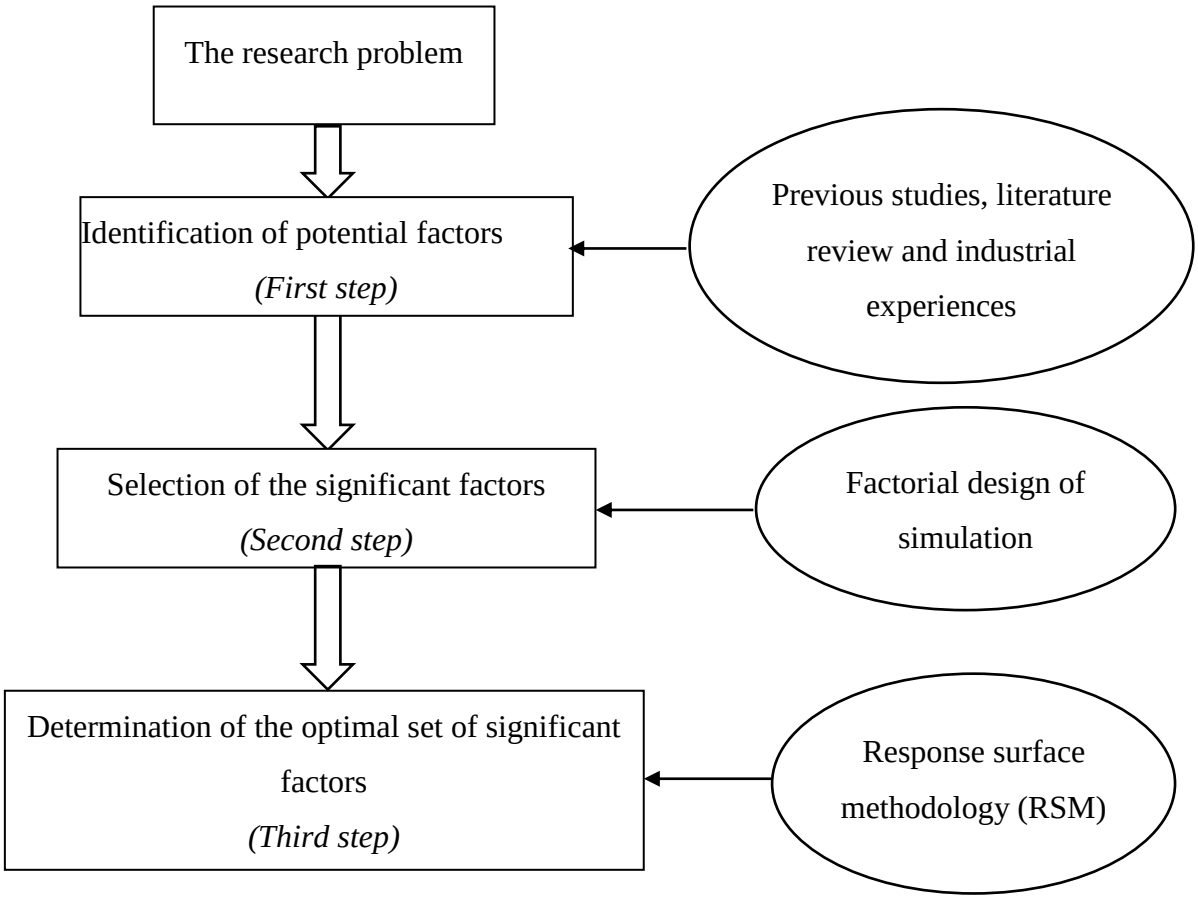

Fig. 5.1 The scheme of the approach.

5.2.1 Identification of potential factors – the first step

The problem is first clarified, and then the factors with respect to the problem are identified based on multi-sources of information such as literature and empirical knowledge of the author's team.

In this study, the research problem is to minimize the shrinkage and warpage of injection molded biocomposites. Although there is rare literature on the shrinkage and warpage of injection molded biocomposites, the studies on the shrinkage and warpage of thermoplastics in the process of injection molding is available in literature and was learned for biocomposites by considering the matrix materials of biocomposites as thermoplastics. Many studies (Chang & Tsaur, 1995; Jansen et al., 1998; Kramschuster et al., 2005; Fischer, 2012) have investigated the shrinkage and warpage of injection molded thermoplastics. For example, Jansen et al. (1998) investigated the effects of process conditions on the shrinkage of seven common thermoplastics. They found that the packing

pressure and melt temperature are the most important factors to the shrinkage of injection molded thermoplastics and the effects of injection time and mold temperature on the shrinkage are not very obvious. Based on the literature review of the effects of processing parameters on the shrinkage and warpage of injection molded parts, the potential factors include mold temperature, injection time, injection temperature, injection pressure, packing time, packing pressure and cooling time. Their value ranges need to be found. In this study, the potential factors and their value range are found, as shown in Table 5.1. The detailed process of finding them is given below.

Table 5.1 Potential factors and their value range.

Factors	Value Range
Mold temperature (℃)	40 – 50
Injection time (s)	1 – 3
Injection temperature (℃)	210 – 250
Injection pressure (MPa)	4.5 – 7.5
Packing time (s)	15 – 30
Packing pressure (% $P_{injection}$)	80 – 90
Cooling time (s)	10 – 20

5.2.2 Selection of the significant factors – the second step

The selection of the significant factors is to determine the main factors through an appropriate factorial design of simulation experiments. In general, a full factorial design is the most desirable design which can include all combinations of factors, second order interactions and other higher order interactions. But when many factors need to be considered, the full factorial design requires large number of the simulation runs and high computational resources. For example, a design of seven factors at two levels would have to run 128 simulation experiments.

The purpose of this step is to select the most important factors from many that may affect a specific response. This selection step is an initial screening stage in this study. Fractional factorial designs are good alternatives to a full factorial design. In the study (Kraber, 1998), a fractional factorial design with two-level factorial is suggested as a good choice for the initial screening. The same

seven factors could be tested in either 8 runs or 16 runs or 32 runs with the loss of certain information.

This step is based on such a fractional factorial design. Based on the fractional factorial design, the simulation experiments of injection molding for biocomposites were performed to test all combinations scheduled by design matrix. The design space refers to the number of all factors with their levels, which is determined from the factors and their value range in the first step.

5.2.3 Determination of the optimal set of significant factors – the third step

In this step, the response surface methodology (RSM) was employed to predict the multi-quality (i.e. shrinkage and warpage in this study) regression models. The significant factors selected in the second step are considered as input variables in the models. The problem finally can be generalized as a multi-objective optimization with multiple factors. Therefore, the third step of the proposed systematic approach includes the following two phases: 1) the prediction of the multi-quality regression models; 2) the optimization of the processing parameters.

RSM is a collection of mathematical and statistical techniques for building the relationship between variables and responses. The idea of RSM is using an appropriate mathematical model to predict the objective models through the appropriate design of experiments. According to Box and Wilson (1992), a second order function was widely used in RSM. So the response surface model is always described as follows:

$$y = a_0 + a_1x_1 + a_2x_2 + \cdots + a_ix_i + a_{11}{x_1}^2 + a_{22}{x_2}^2 + \cdots a_{ii}{x_i}^2 + a_{12}x_1x_2 + \cdots a_{i-1,i}x_{i-1}x_i \quad (5.1)$$

where y is response; x_i is the variable and i is the number of the variables.

The most frequently used second-order designs are central composite design (CCD) (Myers & Carter, 1973) and Box–Behnken design (BBD) (Box & Behnken, 1960). Ferreira et al. (2007) did a thorough review on two designs for RSM, and they found that BBD allows more efficient estimation of the first and second order cofficients, because BBD is less expensive than CCD with the same number of factors. BBD is a rotable second order design based on the construction of

balanced incompleted block designs and requires three levels for each factor (Box & Behnken, 1960). The number of experimental runs (N) required for BBD is defined as $N=2k(k-1)+C_0$ (where k is the number of factors and C_0 is the number of central points). In this study, BBD was chosen as simulation experimental designs to implement RSM.

Once the models between multi-quality and the significant factors are predicted, the problem is finally generalized to be the problem of optimization for multiple objectives. In the mathematical term, the problem can be formulated as (Miettinen, 2012)

$$\min(f_1(x), f_2(x), \dots, f_k(x)) \tag{5.2}$$

$$x \in X \tag{5.3}$$

where the integer $k \geq 2$ is the number of objectives and the set X is the feasible set of decision vectors.

5.3 Design of simulation experiments

5.3.1 Simulation analysis

Solidworks was used to model the testing part (dog bone), as shown in Fig. 5.2. The dimensions of the part were 240 mm × 20 mm × 3.2mm. According to Chapter 3, the biocomposite with 30 wt% flax fibers had the best mechanical properties and was thus selected as the simulation material. The shrinkage and warpage of the biocomposite were simulated and investigated using the software Autodesk Moldflow. It was noted that there is no rheological data for flax fiber reinforced PP biocomposite in Autodesk Moldflow. Before the simulation experiments, flax fiber reinforced PP biocomposite as a new type of material was added into the software based on the rheological information obtained in Chapter 4. Then, the simulation model was established with Moldflow based on standard design guidelines.

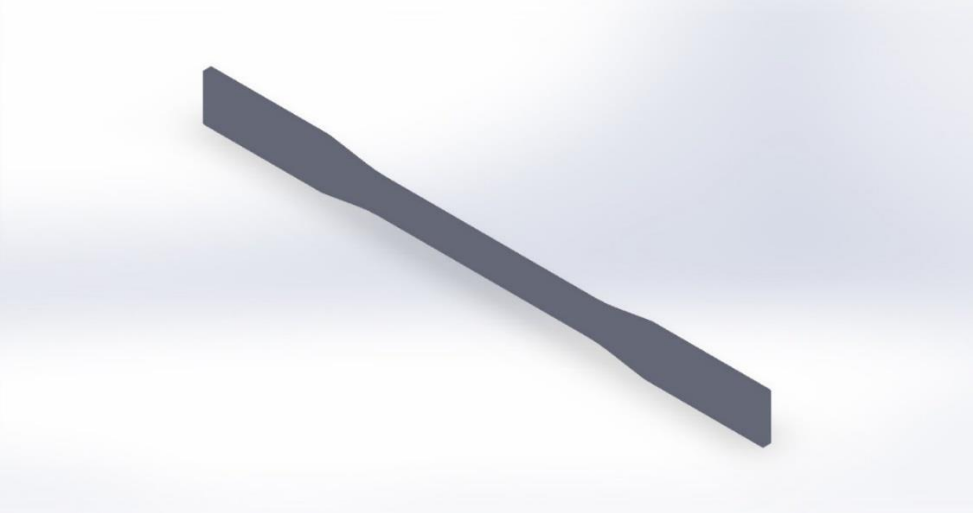

Fig. 5.2 The model of the testing part.

5.3.2 Experimental design and analysis for selection of the significant factors

From the first step, potential factors included (A) mold temperature, (B) injection time, (C) injection temperature, (D) injection pressure, (E) packing time, (F) packing pressure and (G) cooling time and their value ranges were shown in Table 5.1. For the selection step as an initial screening, a 1/4 fractional factorial design is selected with two levels for each factor and a good alternative to the full factorial design. In this fractional factorial design, the seven factors with 2 levels coded as -1, 1 were shown in Table 5.2.

Table 5.2 Factors and their levels of fractional factorial design.

Factors	Lower level (-1)	Upper level (+1)
(A) Mold temperature (℃)	40	50
(B) Injection time (s)	1	3
(C) Injection temperature (℃)	210	250
(D) Injection pressure (MPa)	4.5	7.5
(E) Packing time (s)	15	30
(F) Packing pressure (% $P_{injection}$)	80	90
(G) Cooling time (s)	10	20

This fractional factorial design only had 32 runs (refer to Table D.1 in Appendix D) instead of 128 runs as in a full factorial design. The results of shrinkage and warpage for this fractional factorial design for selection of the significant factors were shown in Table 5.3.

Table 5.3 The Results of shrinkage and warpage for the fractional factorial design.

Run	A	B	C	D	E	F	G	Warpage(mm)	Shrinkage (%)
1	40	1	210	4.5	15	90	20	0.3025	9.602
2	40	1	210	7.5	15	80	10	0.3167	9.602
3	50	3	210	7.5	15	80	10	0.3137	8.962
4	40	1	250	4.5	30	80	10	0.3178	6.650
5	40	3	210	4.5	30	80	20	0.2869	6.682
6	50	1	210	4.5	15	80	10	0.3314	10.10
7	40	1	250	4.5	15	80	20	0.3802	14.00
8	40	3	250	4.5	15	90	10	0.3850	12.65
9	50	1	250	4.5	30	90	20	0.2972	6.006
10	50	3	250	4.5	30	80	10	0.3384	7.851
11	50	3	210	4.5	15	90	20	0.3205	8.922
12	50	1	210	7.5	15	90	20	0.3118	10.10
13	50	3	250	7.5	30	90	20	0.3091	7.049
14	50	3	210	7.5	30	80	20	0.2825	6.348
15	50	1	210	7.5	30	90	10	0.2810	5.426
16	40	3	210	7.5	30	90	10	0.2755	6.656
17	40	1	210	7.5	30	80	20	0.2741	5.446
18	40	3	250	7.5	15	80	20	0.3850	12.66
19	50	1	250	4.5	15	90	10	0.3827	12.26
20	50	1	210	4.5	30	80	20	0.2833	5.702
21	40	3	250	4.5	30	90	20	0.3080	7.183
22	40	1	210	4.5	30	90	10	0.2810	5.426
23	40	1	250	7.5	15	90	10	0.3767	14.00

24	50	3	250	4.5	15	80	20	0.3950	13.41
25	40	1	250	7.5	30	90	20	0.2922	6.116
26	50	3	210	4.5	30	90	10	0.2954	6.338
27	40	3	210	7.5	15	90	20	0.2979	8.429
28	40	3	250	7.5	30	80	10	0.3347	7.914
29	50	1	250	7.5	15	80	20	0.3854	12.26
30	50	1	250	7.5	30	80	10	0.3177	6.538
31	50	3	250	7.5	15	90	10	0.3780	13.40
32	40	3	210	4.5	15	80	10	0.3130	8.433

Based on the data in Table 5.3, analysis of the fractional factorial design was conducted by MINITAB. The results were shown in Fig. 5.3 to Fig. 5.7

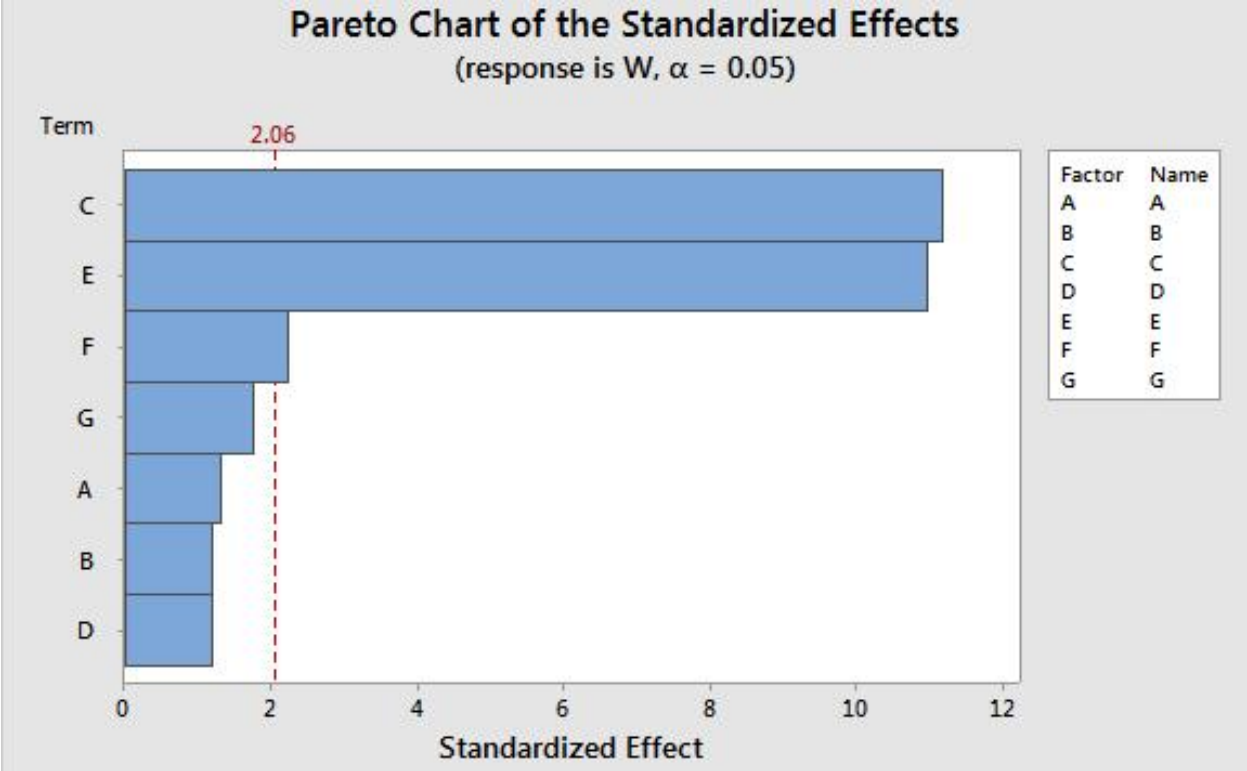

Fig. 5.3 Pareto chat of the standardized effects for warpage.

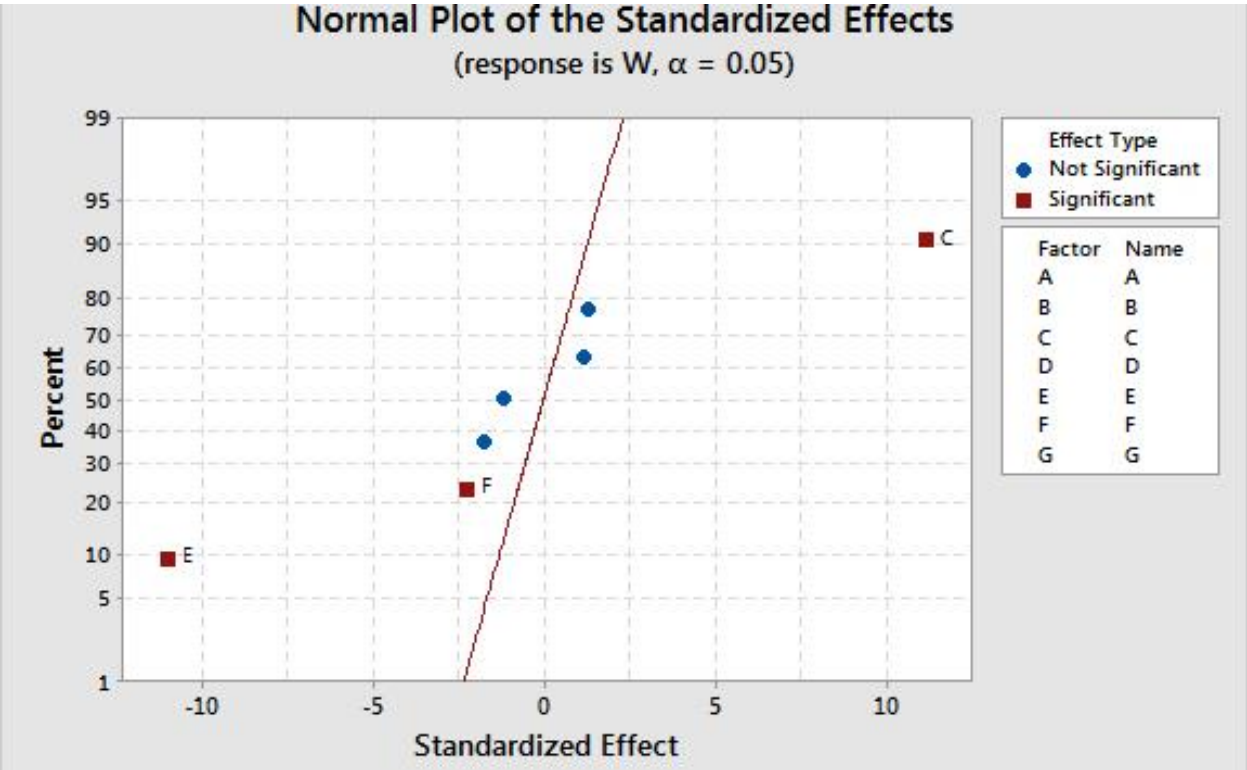

Fig. 5.4 Normal Plot of standardized effects for warpage.

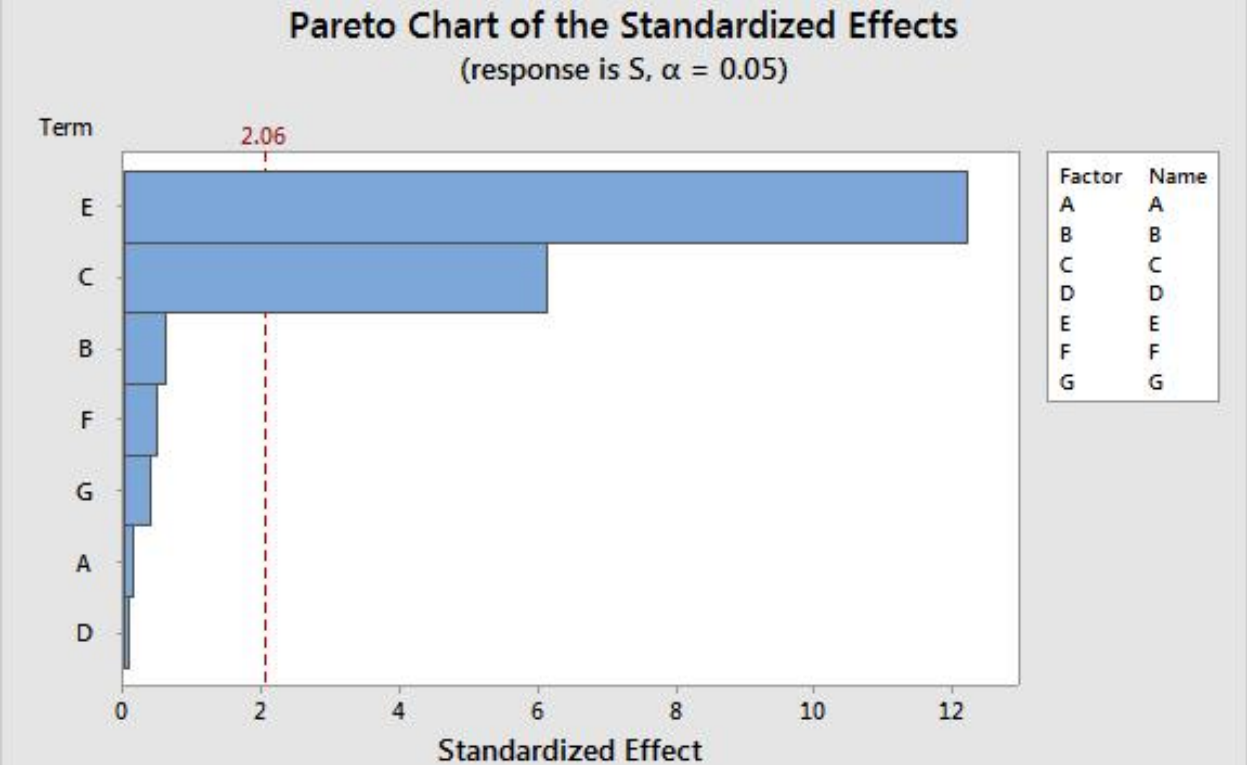

Fig. 5.5 Pareto chat of the standardized effects for shrinkage.

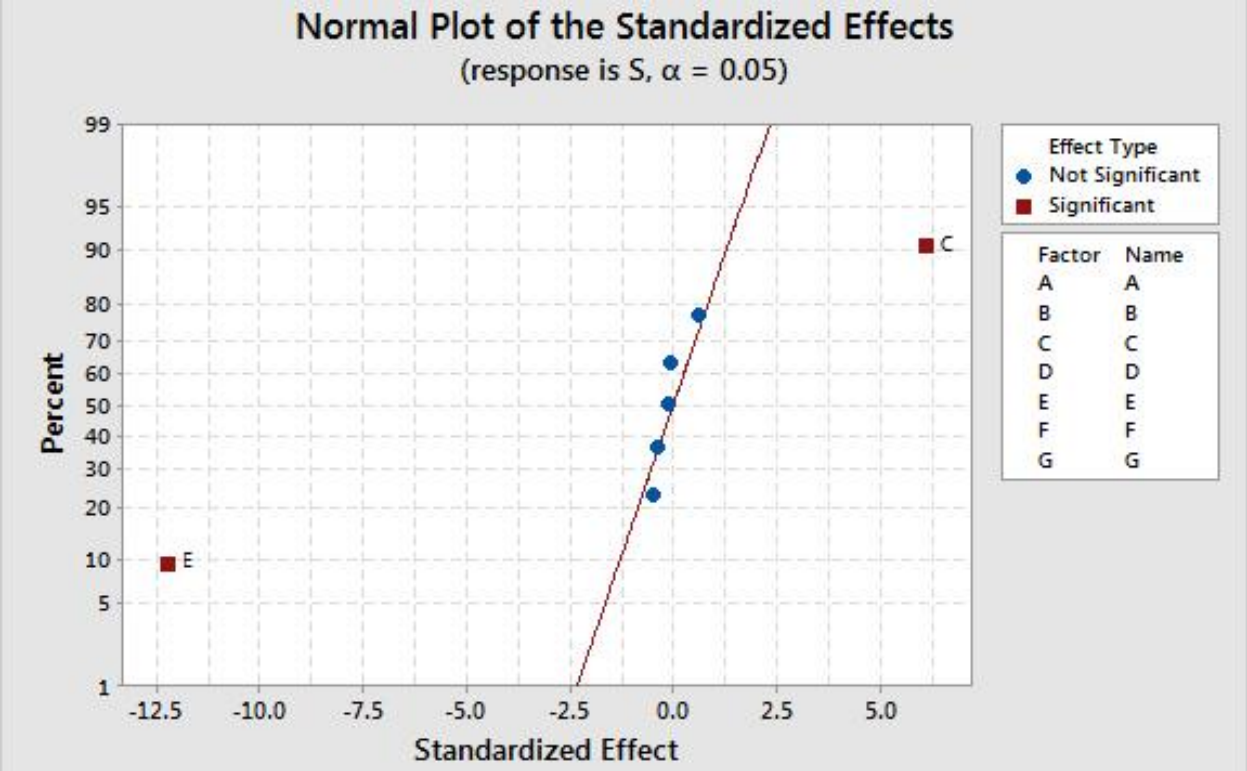

Fig. 5.6 Normal Plot of standardized effects for shrinkage.

Fig. 5.3 and Fig. 5.5 showed, respectively, the rank of the effect of seven factors on shrinkage and warpage. Fig 5.4 and Fig. 5.6 showed the same and gave the significant factors of shrinkage and warpage. Therefore, the significant factors were determined as follows: (C) injection temperature, (E) packing time, and (F) packing pressure. The other potential factors had a lower effect on the shrinkage and warpage and thus were excluded for the analysis of RSM in the third step.

5.3.3 Experimental design for RSM

The significant factors selected by the second step were considered as the variables in RSM, and they were (C) injection temperature, (E) packing time, and (F) packing pressure. According to the analysis in Section 5.2.3, BBD was selected as the simulation experimental design for RSM. In this study, there are three variables, and each had three levels coded as -1, 0, 1 (shown in Table 5.4). The BBD had 15 runs for three variables with three levels (refer to Table D.2 in Appendix D).

Table 5.4 Variables and their levels of simulation experimental design for RSM.

Variables	Level 1 (-1)	Level 2 (0)	Level 3 (1)
(C) Injection temperature (℃)	210	230	250
(E) Packing time (s)	15	22.5	30
(F) Packing pressure (% $P_{injection}$)	80	85	90

5.4 Results and discussion

5.4.1 RSM identification

The simulation experiments were conducted by following to the BBD matrix (refer to Table D.3 to D.8 in Appendix D). The results of the warpage and the shrinkage of injection molded biocomposites were shown in Table 5.5.

Table 5.5 The results of shrinkage and warpage for BBD simulation experiments.

Run	Injection temperature (℃)	Packing time (s)	Packing pressure (% $P_{injection}$)	Warpage (mm)	Shrinkage (%)
1	210	15	85	0.3328	10.21
2	210	22.5	90	0.3062	4.939
3	250	22.5	80	0.3325	6.625
4	230	30	90	0.2921	4.835
5	250	15	85	0.407	12.25
6	250	30	85	0.3052	5.195
7	230	15	90	0.3683	12.41
8	210	30	85	0.2902	4.953
9	230	22.5	85	0.3256	7.078

10	230	30	80	0.2992	5.176
11	250	22.5	90	0.3231	6.602
12	210	22.5	80	0.3018	4.966
13	230	15	80	0.3721	12.46
14	230	22.5	85	0.3256	7.078
15	230	22.5	85	0.3256	7.078

Based on the experimental data of BBD, the regression models were generated through analyzing response surface design in MINITAB (refer to Table D.3 to d.8 in Appendix D). Two second order polynomial equation were developed for shrinkage and warpage, as follows.

Warpage:

$$W = -2.95 + 0.01108C + 0.00958E + 0.0440F - 0.000011C^2 + 0.000224E^2 - 0.000211F^2 - 0.000099CE - 0.000034CF - 0.000022EF \quad (5.4)$$

where W is the warpage of injection molded biocomposites (mm);

C is the injection temperature (℃);

E is the packing time (s);

F is the packing pressure (% $P_{injection}$).

Shrinkage:

$$S = -219.0 + 1.173C - 1.203E + 2.50F - 0.002329C^2 + 0.03566E^2 - 0.01453F^2 - 0.00300CE + 0.00001CF - 0.00194EF \quad (5.5)$$

where S is the shrinkage of injection molded biocomposites (%).

5.4.2 Optimization for the shrinkage and warpage

Once the relationships between the shrinkage and warpage and the significant factors were built, the problem is finally generalized to be the problem of the multi-objective optimization. In the view of industry, this problem can be solved by considering the shrinkage as a constraint and the warpage as the goal. This multi-objective optimization could be transferred to a single objective

(minimizing the warpage) optimization with a constraint (assuming the shrinkage = 4.5% for this study), which is expressed as follows:

$$\min W \tag{5.6}$$

$$\text{Constraint} = S - 4.5 \tag{5.7}$$

$$210 \leq C \leq 250 \tag{5.8}$$

$$15 \leq E \leq 30 \tag{5.9}$$

$$80 \leq F \leq 90 \tag{5.10}$$

where W is the warpage (mm);

S is the shrinkage (%);

C is the injection temperature (℃);

E is the packing time (s);

F is the packing pressure (% $P_{injection}$).

This problem can be solved by Constrained Nonlinear Optimization Algorithms in MATLAB. The results were shown in Fig. 5.7.

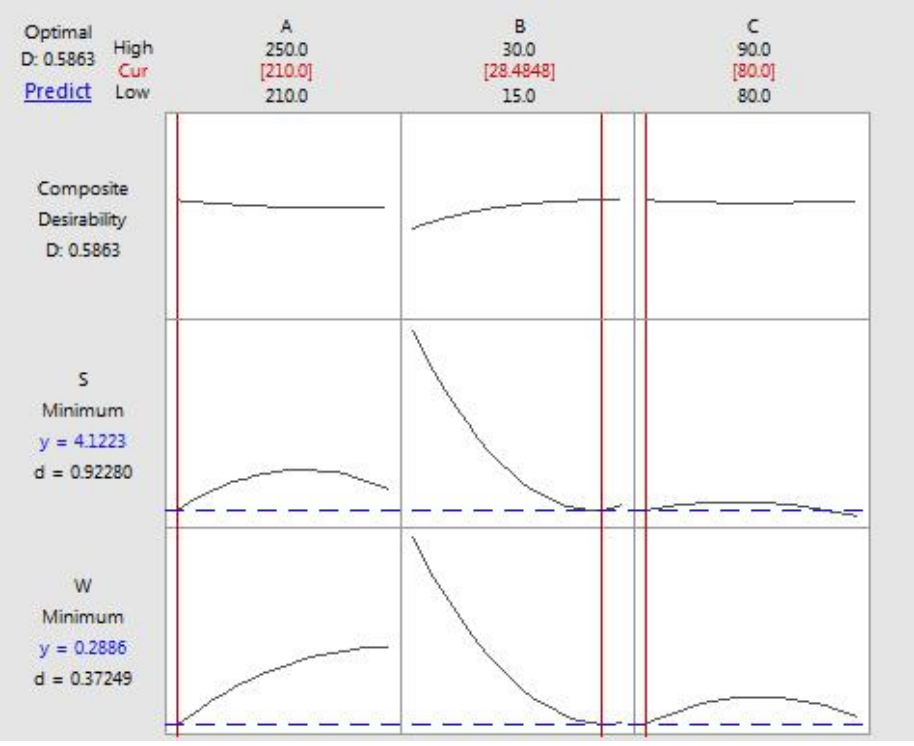

Fig. 5.7 The result of the optimization for shrinkage and warpage.

According to the above figure, the minimum warpage is 0.2886 mm and the minimum shrinkage is 4.12%. Therefore, the optimal set of the processing parameters for the minimization of shrinkage and warpage was obtained (shown in Table 5.6).

Table 5.6 The optimal values of processing parameters.

Variables	Values
(C) Injection temperature (℃)	210
(E) Packing time (s)	28.5
(F) Packing pressure (% $P_{injection}$)	80

5.5 Conclusion

This chapter proposed a systematic approach on simulation analysis and optimization of injection molding for minimizing the shrinkage and warpage of biocomposites. The proposed approach includes three steps, which are identification of potential factors, selection of the significant factors and determination of the optimal set of processing parameters, and integrates DOE, CAE simulation, statistical analysis and optimization methods.

Following this approach, the significant factors on the shrinkage and warpage of biocomposites were determined as injection temperature, packing time, and packing pressure and their optimal values were obtained. The proposed approach could be widely used to improve the quality of newly developed materials by injection molding and to quickly obtain the optimal set of the processing parameters.

CHAPTER 6 CONCLUSIONS AND FUTURE WORK

6.1 Overview

Flax fibers have the advantages of low density, low cost, and recyclability is thus considered as potential materials to reinforce plastic materials. Though Canada is one of the largest seed flax growing countries in the world, the utilization of flax fibers as reinforcement in composites in Canada is not as developed as in Europe. Indeed, in Canada, a large amount of flax straws is left in the fields and burned by farmers each year, because flax stalk requires a much longer time to degrade on its own right than many other agricultural residues. Therefore, the development of technologies to make use of flax straw for reinforcement in biocomposites and so on will have huge benefits to both the material industries and flax farmers in Canada.

This thesis presented a study of flax fibers reinforced biocomposites by injection molding through modeling and optimization. The focus of the study was to understand the relationships between the properties of biocomposites and the processing conditions through the experiment and improve the qualities of biocomposites by optimizing the processing conditions.

In the current literature, studies of how the injection molding parameters influence the properties of natural fiber reinforced biocomposites are very limited. Particularly, there is rare literature on the shrinkage and warpage of injection molded products made of natural fiber reinforced biocomposites. Additionally, the current methods rarely consider the influence of the rheological behavior of melts in injection molding and hinders its effective optimization, because of the lack of integration of practical experience, DOE approach and CAE process simulation.

This study was motivated by overcoming these limitations. The overall objective of the study is to develop injection molding technologies for biocomposites to achieve their best geometrical and properties and to maximize their usage in machinery (e.g., agricultural machinery and automotive machinery). To achieve this overall objective, the following specific objectives are defined for this study.

Objective 1: Establish a test-bed with an effective method to process flax fiber reinforced biocomposites with injection molding such that all the factors or parameters in the process can be covered

Objective 2: Understand and build the relationship between the process or operating parameters including the material composition of parts and the properties of the parts

Objective 3: Identify the main factors influencing the rheological properties of biocomposites during the processing

Objective 4: Develop an effective approach to improve the quality of injection molded biocomposites

These objectives have been achieved. An overview of each chapter is given as follows. A literature review (Chapter 2) was presented to confirm the validity of the proposed objectives. In Chapter 3, biocomposites were successfully produced by injection molding and the processing scheme were presented. The influence of flax fiber loading and processing conditions including injection temperature and pressure on the mechanical properties (tensile properties and flexural properties) and water absorption of biocomposites were investigated. Chapter 4 investigated the effect of the processing conditions (fiber content and temperature) on the rheological properties of biocomposites and then employed Cross – WLF model to determine the rheological information of biocomposites for implement of simulation analysis of injection molding for biocomposites. Chapter 5 proposed a systematic approach on simulation analysis and optimization of injection molding to minimize the shrinkage and warpage of biocomposites and to improve the qualities of injection molded biocomposites.

6.2 Conclusions

The study presented in this thesis concludes:

1. Influence of the processing conditions on the properties of biocomposites.

a) Fiber content is the most significant impact factor of influencing the mechanical properties of biocomposites compared with the other two processing conditions (injection temperature and injection pressure) and the tensile properties and flexural properties of biocomposites dreamingly increased with flax fiber content.
b) Biocomposites with various fiber contents (from 0 to 30 wt%) processed by lower injection temperature has higher tensile properties and flexural properties.
c) Water absorption of biocomposites is significantly dependent on fiber content and injection temperature and their effects on water absorption of biocomposites are almost the same.
d) Injection pressure has no significant effect on either mechanical properties or water absorption.

2. The rheological characteristics

a) The shear viscosity of biocomposites increases with fiber content, but at very high shear rates (from 5,000 to 10,000 S^{-1}), the shear viscosities of biocomposites with various fiber content (from 0 to 30%) all tend to be the same.
b) The shear viscosity of biocomposites decreases with temperature, and at higher shear rate, all the shear viscosity variations as function of shear rates followed the same rate for different temperatures.
c) At high shear rate, the shear viscosity mostly depends on the shear rate rather than fiber content and temperature.
d) A method is presented to determine the seven parameters of the Cross-WLF model for biocomposites.

3. Minimization of the shrinkage and warpage of injection molded biocomposites

a) The significant factors on the shrinkage and warpage of biocomposites by injection molding are injection temperature, packing time, and packing pressure.
b) The optimization of the injection molding of biocomposites for reducing the shrinkage and warpage of biocomposites is successful by integrating DOE and simulation technique.

6.3 Contributions

This work was focused on manufacturing of biocomposites. The main contributions of this work are described below:

- In the field of biocomposites reinforcement, the study has shown a great promise to use flax fibers to enhance the mechanical properties of the thermoplastics, in particular an increase of 41.83% in tensile strength and an increase of 47.13% in flexural strength. In addition, this work has provided a mathematical relationship between the processing condition of injection molding and the mechanical properties of biocomposites, which is important to control the manufacturing process to reach desired mechanical properties.
- In the field of optimal design and manufacturing of flax fiber biocomposites, this work has provided: (a) an effective method to determine the parameters in the rheology model of the biocomposites melt, which is an important step in simulating the process, and this method has a generalized implication to other types of biocomposites; and (b) a systematic approach to the optimization of the injection molding process for minimizing the shrinkage and warpage of biocomposites, which are the two most important quality issues in biocomposites.

6.3 Future work

Several future endeavors could potentially improve this thesis work further.

First, this study focused on the mechanical properties of biocomposites. The other properties of and biocomposites, such as impact properties, thermal stability, and ultraviolet resistance, should be studied in future. This will help in finding more applications of biocomposites.

Second, the maximum fiber content in this study was 30% because of the limitation of experimental conditions. However, the study showed fiber content could dramatically increase the mechanical properties of biocomposites. Higher fiber content (such as 40%, or more) should be studied in future when the experimental conditions are available.

Third, for biocomposites manufacturing, besides injection molding, the extrusion is also very important process. The effect of extrusion on the properties of biocomposites are suggested to study in future. This may help to obtain the biocomposite product with better properties

REFERENCES

Albano, C., Gonzalez, J., Ichazo, M., & Kaiser, D. (1999). Thermal stability of blends of polyolefins and sisal fiber. *Polymer Degradation and Stability, 66(2),* 179-190.

Alix, S., Lebrun, L., Morvan, C., & Marais, S. (2011). Study of water behaviour of chemically treated flax fibres-based composites: A way to approach the hydric interface. *Composites Science and Technology, 71(6),,* 893-899.

Andersons, J., Joffe, R., Spārniņš, E., & Weichert, D. (2011). Modeling the effect of reinforcement discontinuity on the tensile strength of UD flax fiber composites. *Journal of Materials Science, 46(15),* 5104-5110.

Andersons, J., Spārniņš, E., & Joffe, R. (2006). Stiffness and strength of flax fiber/polymer matrix composites. *Polymer Composites, 27(2),* 221-229.

Ansari, M., Alabbas, A., Hatzikiriakos, S. G., & Mitsoulis, E. (2010). Entry flow of polyethylene melts in tapered dies. *nternational Polymer Processing, 25(4),* 287-296.

Ansari, M., Hatzikiriakos, S. G., & Mitsoulis, E. (2012). Slip effects in HDPE flows. *Journal of Non-Newtonian Fluid Mechanics, 167,* 18-29.

Arbelaiz, A., Fernandez, B., Ramos, J. A., Llano-Ponte, R., & Mondragon, I. (2005). Mechanical properties of short flax fibre bundle/polypropylene composites: Influence of matrix/fibre modification, fibre content, water uptake and recycling. *Composites Science and Technology, 65(10),* 1582-1592.

Arbelaiz, A., Fernández, B., Valea, A., & Mondragon, I. (2006). Mechanical properties of short flax fibre bundle/poly (ε-caprolactone) composites: Influence of matrix modification and fibre content. *Carbohydrate Polymers, 64(2),* 224-232.

Assarar, M., Scida, D., El Mahi, A., Poilâne, C., & Ayad, R. (2011). Influence of water ageing on mechanical properties and damage events of two reinforced composite materials: Flax–fibres and glass–fibres. *Materials & Design, 32(2),* 788-795.

ASTM International. (2014). *D638 − 14: Standard Test Method for Tensile Properties of Plastics.*

ASTM International. (2015). *ASTM D790-15e2 Standard Test Methods for Flexural Properties of Unreinforced and Reinforced Plastics and Electrical Insulating Materials.*

Baley, C. (2004). Influence of kink bands on the tensile strength of flax fibers. *Journal of materials science, 39(1)*, 331-334.

Barghash, M. A., & Alkaabneh, F. A. (2014). Shrinkage and warpage detailed analysis and optimization for the injection molding process using multistage experimental design. *Quality Engineering, 26(3)*, 319-334.

Bledzki, A. K., Faruk, O., & Sperber, V. E. (2006). Cars from Bio-Fibres. *Macromolecular Materials and Engineering, 291(5)*, 449-457.

Bledzki, A. K., Fink, H. P., & Specht, K. (2004). Unidirectional hemp and flax EP-and PP-composites: Influence of defined fiber treatments. *Journal of Applied Polymer Science, 93(5)*, 2150-2156.

Bledzki, A. K., Franciszczak, P., & Meljon, A. (2015). High performance hybrid PP and PLA biocomposites reinforced with short man-made cellulose fibres and softwood flour. *Composites Part A: Applied Science and Manufacturing, 74*, 132-139.

Bos, H. L. (2004). *The potential of flax fibres as reinforcement for composite materials.* Eindhoven, Netherlands: Eindhoven University of Technology.

Box, G. E., & Behnken, D. W. (1960). Some new three level designs for the study of quantitative variables. *Technometrics, 2(4)*, 455-475.

Box, G. E., & Wilson, K. B. (1992). On the experimental attainment of optimum conditions. In *Breakthroughs in Statistics* (pp. 270-310). New York: Springer.

Cantero, G., Arbelaiz, A., Llano-Ponte, R., & Mondragon, I. (2003). Effects of fibre treatment on wettability and mechanical behaviour of flax/polypropylene composites. *Composites Science and Technology, 63(9)*, 1247-1254.

Carreau, P. J., MacDonald, I. F., & Bird, R. B. (1968). A nonlinear viscoelastic model for polymer solutions and melts—II. *Chemical Engineering Science, 23(8)*, 901-911.

Chabba, S., & Netravali, A. N. (2005). Green composites part 1: characterization of flax fabric and glutaraldehyde modified soy protein concentrate composites. *Journal of Materials Science, 40(23)*, 6263-6273.

Chang, R. Y., & Tsaur, B. D. (1995). Experimental and theoretical studies of shrinkage, warpage, and sink marks of crystalline polymer injection molded parts. *Polymer Engineering & Science, 35(15)*, 1222-1230.

Chen, C. P., Chuang, M. T., Hsiao, Y. H., Yang, Y. K., & Tsai, C. H. (2009). Simulation and experimental study in determining injection molding process parameters for thin-shell plastic parts via design of experiments analysis. *Expert Systems with Applications, 36(7),* 10752-10759.

Cheng, J., Liu, Z., & Tan, J. (2013). Multiobjective optimization of injection molding parameters based on soft computing and variable complexity method. *The International Journal of Advanced Manufacturing Technology, 66(5-8),* 907-916.

Cherizol, R., Sain, M., & Tjong, J. (2015). Review of Non-Newtonian Mathematical Models for Rheological Characteristics of Viscoelastic Composites. *Green and Sustainable Chemistry, 5(01), 6*.

Courbebaisse, G. (2005). Numerical simulation of injection moulding process and the pre-modelling concept. *Computational materials science, 34(4),* 397-405.

Cross, M. M. (1979). Relation between viscoelasticity and shear-thinning behaviour in liquids. *Rheologica Acta, 18(5),* 609-614.

Davies, G. C., & Bruce, D. (1998). Effect of environmental relative humidity and damage on the tensile properties of flax and nettle fibers. *Textile Research Journal, 68(9),* 623-629.

Dealy, J. M., & Wissbrun, K. F. (2012). *Melt rheology and its role in plastics processing: theory and applications.* Springer Science & Business Media.

Dhakal, H. N., Zhang, Z. Y., Guthrie, R., MacMullen, J., & Bennett, N. (2013). Development of flax/carbon fibre hybrid composites for enhanced properties. *Carbohydrate polymers, 96(1),* 1- 8.

Facca, A. G., Kortschot, M. T., & Yan, N. (2006). Predicting the elastic modulus of natural fibre reinforced thermoplastics. *Composites Part A: Applied Science and Manufacturing, 37(10),* 1660-1671.

Facca, A. G., Kortschot, M. T., & Yan, N. (2007). Predicting the tensile strength of natural fibre reinforced thermoplastics. *Composites Science and Technology, 67(11),* 2454-2466.

FCC. (2015). *Canada – A Flax Leader*. Retrieved from Flax Council of Canada Web site: http://flaxcouncil.ca/about-flax/canada-a-flax-leader/

FCC. (2015). *Production of Flax by Province Canada*. Retrieved in September, 2015 from Flax Council of Canada Web site: http://flaxcouncil.ca/resources/statistics/

Ferreira, S. C., Bruns, R. E., Ferreira, H. S., Matos, G. D., David, J. M., Brandao, G. C., & Dos Santos, W. N. (2007). Box-Behnken design: an alternative for the optimization of analytical methods. *Analytica chimica acta, 597(2),* 179-186.

Ferry, J. D. (1980). *Viscoelastic properties of polymers.* New York: John Wiley & Sons.

Fischer, J. (2012). *Handbook of molded part shrinkage and warpage.* William Andrew.

Gava, A., & Lucchetta, G. (2012). On the performance of a viscoelastic constitutive model for micro injection moulding simulations. *eXPRESS Polymer Letters, 6(5),* 417–426.

Gerhart, P. M., & Gross, R. J. (1985). *Fundamentals of fluid mechanics.* Addison-Wesley.

Girault, V., & Raviart, P. A. (1979). *Finite element approximation of the Navier-Stokes equations(Book).* Berlin: Springer-Verlag(Lecture Notes in Mathematics., 749.

Godard, F., Vincent, M., Agassant, J. F., & Vergnes, B. (2009). Rheological behavior and mechanical properties of sawdust/polyethylene composites. *Journal of applied polymer science, 112(4),* 2559-2566.

Guo, W., Mao, H. J., & Xu, Q. (2011). Warpage and Structural Analysis of Automotive Trim Based on FFD and CAE in Plastic Injection Molding. *In Advanced Materials Research Vol. 314,* 1282-1286.

Hajiha, H., Sain, M., & Mei, L. H. (2014). Modification and Characterization of Hemp and Sisal Fibers. *Journal of Natural Fibers, 11(2),* 144-168.

Halimin, N. A., Zain, A. M., & Azman, M. F. (2015). Warpage Prediction in Injection Molding Using Artificial Neural Network. *Journal of Soft Computing and Decision Support Systems, 2(5),* 7-9.

Hieber, C. A., & Chiang, H. H. (1992). Shear-rate-dependence modeling of polymer melt viscosity. *Polymer Engineering & Science, 32(14),* 931-938.

Hieber, C. A., & Shen, S. F. (1980). A finite-element/finite-difference simulation of the injection-molding filling process. *Journal of Non-Newtonian Fluid Mechanics, 7(1),* 1-32.

Hindle, C. (2015, November). *Polypropylene (PP).* Retrieved from British Plastics Federation: http://www.bpf.co.uk/plastipedia/polymers/pp.aspx#processing

Ho, M. P., Wang, H., Lee, J. H., Ho, C. K., Lau, K. T., Leng, J., & Hui, D. (2012). Critical factors on manufacturing processes of natural fibre composites. *Composites Part B: Engineering, 43(8),* 3549-3562.

Holbery, J., & Houston, D. (2006). Natural-fiber-reinforced polymer composites in automotive applications. . *Jom, 58(11)*, 80-86.

Huda, M. S., Drzal, L. T., Mohanty, A. K., & Misra, M. (2006). Chopped glass and recycled newspaper as reinforcement fibers in injection molded poly (lactic acid)(PLA) composites: a comparative study. *Composites Science and Technology, 66(11),*, 1813-1824.

Huda, M. S., Mohanty, A. K., Drzal, L. T., Schut, E., & Misra, M. (2005). "Green" composites from recycled cellulose and poly (lactic acid): Physico-mechanical and morphological properties evaluation. *Journal of Materials Science, 40(16),* , 4221-4229.

Hughes, M., Carpenter, J., & Hill, C. (2007). Deformation and fracture behaviour of flax fibre reinforced thermosetting polymer matrix composites. *Journal of Materials Science, 42(7)*, 2499-2511.

Hughes, M., Sèbe, G., Hague, J., Spear, M., & Mott, L. (2000). An investigation into the effects of micro-compressive defects on interphase behaviour in hemp-epoxy composites using half-fringe photoelasticity. *Composite Interfaces, 7(1)*, 13-29.

Jansen, K. M., Van Dijk, D. J., & Husselman, M. H. (1998). Effect of processing conditions on shrinkage in injection molding. *Polymer Engineering & Science, 38(5)*, 838-846.

Joshi, S. V., Drzal, L., Mohanty, A., & Arora, S. (2004). Are natural fiber composites environmentally superior to glass fiber reinforced composites? *Composites Part A: Applied science and manufacturing, 35(3)*, 371-376.

Jou, Y. T., Lin, W. T., Lee, W. C., & Yeh, T. M. (2014). Integrating the Taguchi method and response surface methodology for process parameter optimization of the injection molding. . *Applied Mathematics & Information Sciences, 8(3)*, 1277.

Kaith, B. S., & Kalia, S. (2007). Grafting of flax fiber (Linum usitatissimum) with vinyl monomers for enhancement of properties of flax-phenolic composites. *Polymer journal, 39(12)*, 1319-1327.

Kim, K. J., Bumm, S., Gupta, R. K., & White, J. L. (2008). Interfacial adhesion of cellulose fiber and natural fiber filled polypropylene compounds and their effects on rheological and mechanical properties. *Composite Interfaces, 15(2-3)*, 301-319.

Kraber, S. L. (1998). Keys to successful designed experiments. *In ASQ World Conference on Quality and Improvement Proceedings* (p. 119). American Society for Quality.

Kramschuster, A., Cavitt, R., Ermer, D., Chen, Z., & Turng, L. S. (2005). Quantitative study of shrinkage and warpage behavior for microcellular and conventional injection molding. *Polymer Engineering & Science, 45(10),* 1408-1418.

Kromer, K. H. (2009). Physical properties of flax fibre for non-textile-use. *Res Agric Eng, 55(2),* 52-61.

Kusić, D., Kek, T., Slabe, J. M., Svečko, R., & Grum, J. (2013). The impact of process parameters on test specimen deviations and their correlation with AE signals captured during the injection moulding cycle. *Polymer Testing, 32(3),* 583-593.

Le Duigou, A., Davies, P., & & Baley, C. (2012). Replacement of glass/unsaturated polyester composites by flax/PLLA biocomposites: is it justified? *Journal of biobased materials and bioenergy, 5(4),* 466-482.

Le Duigou, A., Davies, P., & Baley, C. (2011). Environmental impact analysis of the production of flax fibres to be used as composite material reinforcement. *Journal of biobased materials and bioenergy, 5(1),* 153-165.

Li, T. Q., & Wolcott, M. P. (2005). Rheology of wood plastics melt. Part 1. Capillary rheometry of HDPE filled with maple. *Polymer Engineering & Science, 45(4),* 549-559.

Li, X., Tabil, L. G., Panigrahi, S., & Crerar, W. J. (2006). The influence of fiber content on properties of injection molded flax fiber-HDPE biocomposites. *In 2006 ASAE Annual Meeting (p. 1).* American Society of Agricultural and Biological Engineers.

Liholt, H., & Madsen, B. (2012). Properties of flax and hemp composites. In CELC, *flax and hemp fibres: a natural solution for the composite industry* (pp. 119-140). Paris, France: JEC Composite.

Mallick, P. K. (2007). *Fiber-reinforced composites: materials, manufacturing, and design.* CRC press.

Manfredi, L. B., Rodríguez, E. S., Wladyka-Przybylak, M., & Vázquez, A. (2006). Thermal degradation and fire resistance of unsaturated polyester, modified acrylic resins and their composites with natural fibres. *Polymer Degradation and Stability, 91(2),* 255-261.

Marynowski, K. (2006). Two-dimensional rheological element in modelling of axially moving viscoelastic web. *European Journal of Mechanics-A/Solids, 25(5),* 729-744.

Miettinen, K. (2012). *Nonlinear multiobjective optimization (Vol. 12).* Springer Science & Business Media.

Modniks, J., & Andersons, J. (2010). Modeling elastic properties of short flax fiber-reinforced composites by orientation averaging. *Computational Materials Science, 50(2)*, 595-599.

Mohanty, A. K., Misra, M., & Drzal, L. T. (2001). Surface modifications of natural fibers and performance of the resulting biocomposites: an overview. *Composite Interfaces, 8(5)*, 313-343.

Mohanty, A. K., Misra, M., & Hinrichsen, G. (2000). Biofibres, biodegradable polymers and biocomposites: an overview. *Macromolecular materials and Engineering, 276(1)*, 1-24.

Monteiro, S. N., Lopes, F. P., Ferreira, A. S., & Nascimento, D. C. (2009). Natural-fiber polymer-matrix composites: cheaper, tougher, and environmentally friendly. *Jom, 61(1)*, 17-22.

Myers, R. H., & Carter, W. H. (1973). Response surface techniques for dual response systems. *Technometrics, 15(2)*, 301-317.

Nair, K. M., Thomas, S., & Groeninckx, G. (2001). Thermal and dynamic mechanical analysis of polystyrene composites reinforced with short sisal fibres. *Composites Science and Technology, 61(16)*, 2519-2529.

Nyström, B., Joffe, R., & Långström, R. (2007). Microstructure and strength of injection molded natural fiber composites. *Journal of reinforced plastics and composites, 26(6)*, 579-599.

Ogah, A. O., Afiukwa, J. N., & Nduji, A. A. (2014). Characterization and Comparison of Rheological Properties of Agro Fiber Filled High-Density Polyethylene Bio-Composites. *Open Journal of Polymer Chemistry*.

Ota, W. N., Amico, S. C., & Satyanarayana, K. G. (2005). Studies on the combined effect of injection temperature and fiber content on the properties of polypropylene-glass fiber composites. *Composites science and technology, 65(6)*, 873-881.

Owens, R. G., & Phillips, T. N. (2002). *Computational rheology (Vol. 14)*. London: Imperial College Press.

Pervaiz, M., & Sain, M. M. (2003). Carbon storage potential in natural fiber composites. *Resources, conservation and Recycling, 39(4)*, 325-340.

Pickering, K. L., Efendy, M. A., & Le, T. M. (2015). A review of recent developments in natural fibre composites and their mechanical performance. *Composites Part A: Applied Science and Manufacturing*.

Qatu, M. S. (2011). Application of kenaf-based natural fiber composites in the automotive industry. *SAE Technical Paper*.

Rocha, I. B., Parente, E., & Melo, A. M. (2014). A hybrid shared/distributed memory parallel genetic algorithm for optimization of laminate composites. *Composite Structures, 107*, 288-297.

Rosato, D. V., & Rosato, M. G. (2012). *Injection molding handbook.* Springer Science & Business Media.

Saheb, D. N., & Jog, J. P. (1999). Natural fiber polymer composites: a review. *Advances in polymer technology, 18(4)*, 351-363.

Serizawa, S., Inoue, K., & Iji, M. (2006). Kenaf-fiber-reinforced poly (lactic acid) used for electronic products. *Journal of Applied Polymer Science, 100(1)*, 618-624.

Sreekala, M. S., Kumaran, M. G., Joseph, S., Jacob, M., & Thomas, S. (2000). Oil palm fibre reinforced phenol formaldehyde composites: influence of fibre surface modifications on the mechanical performance. *Applied Composite Materials, 7(5-6)*, 295-329.

Stamboulis, A., Baillie, C. A., & & Peijs, T. (2001). Effects of environmental conditions on mechanical and physical properties of flax fibers. *Composites Part A: Applied Science and Manufacturing, 32(8)*, 1105-1115.

Tajvidi, M., Falk, R. H., & Hermanson, J. C. (2006). Effect of natural fibers on thermal and mechanical properties of natural fiber polypropylene composites studied by dynamic mechanical analysis. *Journal of Applied Polymer Science, 101(6)*, 4341-4349.

Thakur, V. K. (2013). *Green composites from natural resources.* CRC Press.

Thakur, V. K., Thakur, M. K., & Gupta, R. K. (2014). Review: raw natural fiber–based polymer composites. *International Journal of Polymer Analysis and Characterization, 19(3)*, 256-271.

Twite-Kabamba, E., Mechraoui, A., & Rodrigue, D. (2009). Rheological properties of polypropylene/hemp fiber composites. *Polymer Composites, 30(10)*, 1401-1407.

Van de Velde, K., & Kiekens, P. (2001). Thermoplastic polymers: overview of several properties and their consequences in flax fibre reinforced composites. *Polymer Testing, 20(8)*, 885-893.

Van de W., I., Truong, T. C., Vangrimde, B., & Verpoest, I. (2006). Improving the properties of UD flax fibre reinforced composites by applying an alkaline fibre treatment. *Composites Part A: Applied Science and Manufacturing, 37(9)*, 1368-1376.

Van Den Oever, M. J., & Snijder, M. H. (2008). Jute fiber reinforced polypropylene produced by continuous extrusion compounding, part 1: Processing and ageing properties. *Journal of Applied Polymer Science, 110(2)*, 1009-1018.

Van den Oever, M. J., Bos, H. L., & Van Kemenade, M. J. (2000). Influence of the physical structure of flax fibres on the mechanical properties of flax fibre reinforced polypropylene composites. *Applied Composite Materials, 7(5-6)*, 387-402.

Williams, M. L., Landel, R. F., & Ferry, J. D. (1955). The temperature dependence of relaxation mechanisms in amorphous polymers and other glass-forming liquids. *Journal of the American Chemical society, 77(14)*, 3701-3707.

Winterkorn, H. F. (2008). *Hygroscopicity, Hygroscopic Constant. In Encyclopedia of Soil Science (pp. 330-331).* Springer Netherlands.

Yan, L., Chouw, N., & Jayaraman, K. (2014). Flax fibre and its composites–A review. *Composites Part B: Engineering, 56*, 296-317.

Yan, L., Chouw, N., & Yuan, X. (2012). Improving the mechanical properties of natural fibre fabric reinforced epoxy composites by alkali treatment. *Journal of Reinforced Plastics, 31(6)*, 425–437.

APPENDIX A

Table A.1 Analysis of variance of the effect of processing conditions on tensile strength of biocomposites by SPSS

Source	Type III Sum of Squares	df	Mean Square	Sig. (P)
Corrected Model	942.529 (a)	35	26.929	<0.001
Intercept	61626.41	1	61626.41	<0.001
F	865.697	3	288.566	<0.001
T	66.326	2	33.163	<0.001
P	3.279	2	1.639	0.279
F * T	1.908	6	0.318	0.331
F * P	1.229	6	0.205	0.403
T * P	2.96	4	0.74	0.352
F * T * P	1.13	12	0.094	0.541
Error	3.17	11	.	
Total	62568.94	46		
Corrected Total	942.529	35		

Dependent variable: Tensile strength (MPa);

F: Fiber content (wt%);

T: Injection temperature (ºC);

P: Injection pressure (MPa);

(a) R Square = 94.57%.

Table A.2 Analysis of variance of the effect of processing conditions on Young's modulus of biocomposites by SPSS.

Source	Type III Sum of Squares	df	Mean Square	Sig. (P)
Corrected Model	6603762.750 (a)	35	188678.936	<0.001
Intercept	128085806.3	1	128085806.3	<0.001
F	6294750.972	3	2098250.324	<0.001
T	248359.5	2	124179.75	<0.001
P	2179.5	2	1089.75	0.417
F * T	28126.278	6	4687.713	0.076
F * P	5746.944	6	957.824	0.291
T * P	9919.5	4	2479.875	0.252
F * T * P	14680.056	12	1223.338	0.142
Error	1101.2	15	.	
Total	134689569	50		
Corrected Total	6603762.75	35		

Dependent variable: Young's modulus (MPa);

F: Fiber content (wt%);

T: Injection temperature (^{o}C);

P: Injection pressure (MPa);

(a) R Square = 96.57%.

Table A.3 Analysis of variance of the effect of processing conditions on flexural strength of biocomposites by SPSS

Source	Type III Sum of Squares	df	Mean Square	Sig. (P)
Corrected Model	2394.351 (a)	35	68.410	<0.001
Intercept	129902.576	1	129902.576	<0.001
F	2314.253	3	771.418	<0.001
T	74.649	2	37.324	<0.001
P	0.349	2	0.175	0.312
F * T	3.422	6	0.570	0.023
F * P	0.213	6	0.035	0.412
T * P	0.254	4	0.063	0.534
F * T * P	1.211	12	0.101	0.127
Error	1.021	9	.	
Total	132296.927	44		
Corrected Total	2394.351	35		

Dependent variable: Flexural strength (MPa);

F: Fiber content (wt%);

T: Injection temperature (^{o}C);

P: Injection pressure (MPa);

(a) R Square = 95.51%.

Table A.4 Analysis of variance of the effect of processing conditions on flexural modulus of biocomposites by SPSS.

Source	Type III Sum of Squares	df	Mean Square	Sig. (P)
Corrected Model	9985377.556 (a)	35	285296.502	<0.001
Intercept	122294108.400	1	122294108.400	<0.001
F	9518108.667	3	3172702.889	<0.001
T	452695.722	2	226347.861	<0.001
P	1519.056	2	759.528	0.412
F * T	5276.500	6	879.417	0.217
F * P	1309.833	6	218.306	0.501
T * P	1890.278	4	472.569	0.307
F * T * P	4577.500	12	381.458	0.275
Error	1321.761	17	.	
Total	132279486.000	52		
Corrected Total	9985377.556	35		

Dependent variable: Flexural modulus (MPa);

F: Fiber content (wt%);

T: Injection temperature (^{o}C);

P: Injection pressure (MPa);

(a) R Square = 94.25%.

Table A.5 Analysis of variance of the effect of processing conditions on water absorption of biocomposites by SPSS.

Source	Type III Sum of Squares	df	Mean Square	Sig. (P)
Corrected Model	0.003	26	0	<0.001
Intercept	0.962	1	0.962	<0.001
F	0.002	2	0	<0.001
T	0.003	2	0.001	<0.001
P	1.99E-06	2	9.94E-07	0.479
F * T	1.72E-05	4	4.30E-06	0.131
F * P	1.17E-05	4	2.92E-06	0.371
T * P	1.28E-05	4	3.19E-06	0.402
F * T * P	1.10E-05	8	1.38E-06	0.241
Error	0.134	8	.	
Total	0.965	35		
Corrected Total	0.003	26	0	

Dependent variable: Water absorption (%);

F: Fiber content (wt%);

T: Injection temperature (°C);

P: Injection pressure (MPa);

(a) R Square = 95.71%.

APPENDIX B

Table B.1 The coefficients of predicted model of tensile strength by linear regression.

Term	Coefficient	SE Coefficient	T-Value	P-Value	VIF
Constant	14	169	0.08	0.935	
F	1.062	0.401	2.65	0.013	738.25
T	0.33	1.54	0.21	0.834	5810.8
F*F	-0.01074	0.00165	-6.51	0	12.25
T*T	-0.00107	0.0035	-0.31	0.762	5809
F*T	-0.00144	0.00181	-0.8	0.433	728.8

Dependent Variable: tensile strength;

F = Fiber content (wt%); T= Injection temperature (ºC).

Table B.2 Analysis of Variance for fitting the model between tensile strength and F, T.

Source	DF	Adjusted SS	Adjusted MS	F-Value	P-Value
Regression	5	913.094	182.619	186.13	0
F	1	6.87	6.87	7	0.013
T	1	0.044	0.044	0.04	0.834
F*F	1	41.56	41.56	42.36	0
T*T	1	0.092	0.092	0.09	0.762
F*T	1	0.621	0.621	0.63	0.433
Error	30	29.435	0.981		
Lack-of-Fit	6	20.837	3.473	9.69	0
Pure Error	24	8.598	0.358		
Total	35	942.529			

Dependent Variable: Tensile strength.

Predictors: (Constant), F, T, F*F, T*T, F*T.

Table B.3 Model summary for predicting tensile strength.

S	R-square	R-square(adjusted)	R-square(predicted)
0.990531	96.88%	96.36%	95.63%

Table B.4 Matlab codes for the variation of tensile strength.

Lines	Codes
1	[x,y]=meshgrid(0:1:30,210:1:230);
2	z=14.001+1.062*x-0.011*x.*x-0.001*x.*y+0.327*y-0.001*y.*y;
3	figure
4	grid on
5	surface(x,y,z)
6	view(3)
7	shading faceted %interp
8	colormap('jet')
9	colorbar

Table B.5 The coefficients of predicted model of Young's modulus by linear regression

Term	Coefficient	SE Coefficient	T-Value	P-Value	VIF
Constant	3317	7384	0.45	0.656	
F	12	17.5	0.69	0.498	738.25
T	-26.5	67.2	-0.39	0.696	5810.8
F*F	-0.1153	0.0719	-1.6	0.12	12.25
T*T	0.079	0.153	0.52	0.61	5809
F*T	0.1312	0.0788	1.66	0.106	728.8

Dependent Variable: tensile strength;

F = Fiber content (wt%); T= Injection temperature (ºC).

Table B.6 Analysis of Variance for fitting the model between Young's modulus and F, T

Source	DF	Adjusted SS	Adjusted MS	F-Value	P-Value
Regression	5	6547864	1309573	702.83	0
F	1	876	876	0.47	0.498
T	1	289	289	0.16	0.696
F*F	1	4784	4784	2.57	0.12
T*T	1	496	496	0.27	0.61
F*T	1	5161	5161	2.77	0.106
Error	30	55899	1863		
Lack-of-Fit	6	23373	3895	2.87	0.03
Pure Error	24	32526	1355		
Total	35	6603763			

Dependent Variable: Young's Modulus;

Predictors: (Constant), F, T, F*F, T*T, F*T.

Table B.7 Model summary for predicting Young's modulus

S	R-square	R-square(adjusted)	R-square(predicted)
43.1659	99.15%	99.01%	98.77

Table B.8 Matlab codes for the variation of Young's modulus

Lines	Codes
1	[x,y]=meshgrid(0:1:30,210:1:230);
2	z=3317+12.0*x-0.1153*x.*x+0.1312*x.*y-26.5*y+0.078*y.*y;
3	figure
4	grid on
5	surface(x,y,z)
6	view(3)
7	shading faceted %interp
8	colormap('jet')
9	colorbar

Table B.9 The coefficients of predicted model of flexural strength by linear regression.

Term	Coefficient	SE Coefficient	T-Value	P-Value	VIF
Constant	118	265	0.44	0.66	
F	2.025	0.628	3.22	0.003	738.25
T	-0.51	2.41	-0.21	0.835	5810.8
F*F	-0.02171	0.00259	-8.4	0	12.25
T*T	0.00086	0.00548	0.16	0.876	5809
F*T	-0.00316	0.00283	-1.12	0.274	728.8

Dependent Variable: tensile strength;

F = Fiber content (wt%);

T= Injection temperature (ºC).

Table B.10 Analysis of Variance for fitting the model between flexural strength and F, T.

Source	DF	Adjusted SS	Adjusted MS	F-Value	P-Value
Regression	5	2322.16	464.431	192.99	0
F	1	25	25	10.39	0.003
T	1	0.11	0.107	0.04	0.835
F*F	1	169.69	169.694	70.51	0
T*T	1	0.06	0.06	0.02	0.876
F*T	1	2.99	2.993	1.24	0.274
Error	30	72.2	2.407		
Lack-of-Fit	6	70.17	11.695	138.48	0
Pure Error	24	2.03	0.084		
Total	35	2394.35			

Dependent Variable: Tensile strength.

Predictors: (Constant), F, T, F*F, T*T, F*T

Table B.11 Model summary for predicting flexural strength.

S	R-square	R-square(adjusted)	R-square(predicted)
1.55129	96.98%	96.48%	95.97%

Table B.12 Matlab codes for the variation of flexural strength.

Lines	Codes
1	[x,y]=meshgrid(0:1:30,210:1:230);
2	z=3317+12.0*x-0.1153*x.*x+0.1312*x.*y-26.5*y+0.078*y.*y;
3	figure
4	grid on
5	surface(x,y,z)
6	view(3)
7	shading faceted %interp
8	colormap('jet')
9	colorbar

Table B.13 The coefficients of predicted model of flexural modulus by linear regression.

Term	Coefficient	SE Coefficient	T-Value	P-Value	VIF
Constant	14848	3905	3.8	0.001	
F	75.66	9.25	8.18	0	738.25
T	-112.6	35.5	-3.17	0.004	5810.8
F*F	-0.3311	0.0381	-8.7	0	12.25
T*T	0.2279	0.0807	2.82	0.008	5809
F*T	-0.0902	0.0417	-2.16	0.039	728.8

Dependent Variable: tensile strength;

F = Fiber content (wt%); T= Injection temperature (ºC).

Table B.14 Analysis of Variance for fitting the model between flexural modulus and F, T.

Source	DF	Adjusted SS	Adjusted MS	F-Value	P-Value
Regression	5	9969741	1993948	3825.55	0
F	1	34890	34890	66.94	0
T	1	5237	5237	10.05	0.004
F*F	1	39468	39468	75.72	0
T*T	1	4156	4156	7.97	0.008
F*T	1	2439	2439	4.68	0.039
Error	30	15637	521		
Lack-of-Fit	6	6340	1057	2.73	0.036
Pure Error	24	9297	387		
Total	35	9985378			

Dependent Variable: Young’s Modulus;

Predictors: (Constant), F, T, F*F, T*T, F*T.

Table B.15 Model summary for predicting flexural modulus.

S	R-square	R-square(adjusted)	R-square(predicted)
22.8302	99.84%	99.82%	99.78%

Table B.16 Matlab codes for the variation of f modulus.

Lines	Codes
1	[x,y]=meshgrid(0:1:30,210:1:230);
2	z=3317+12.0*x-0.1153*x.*x+0.1312*x.*y-26.5*y+0.078*y.*y;
3	figure
4	grid on
5	surface(x,y,z)
6	view(3)
7	shading faceted %interp
8	colormap('jet')
9	colorbar

Table B.17 The coefficients of predicted model of water absorption by linear regression.

Term	Coefficient	SE Coefficient	T-Value	P-Value	VIF
Constant	-0.302	0.273	-1.1	0.282	
F	0.002356	0.000907	2.6	0.017	775
T	0.00292	0.00248	1.18	0.253	5815
F*F	0.000012	0.000006	2.09	0.049	49
T*T	-0.000003	0.000006	-0.57	0.574	5809
F*T	-0.000011	0.000004	-2.76	0.012	733

Dependent Variable: Water absorption;

F = Fiber content (wt%); T= Injection temperature (ºC).

Table B.18 Analysis of Variance for fitting the model between water absorption and F, T.

Source	DF	Adjusted SS	Adjusted MS	F-Value	P-Value
Regression	5	0.003281	0.000656	343.37	0
F	1	0.000013	0.000013	6.74	0.017
T	1	0.000003	0.000003	1.38	0.253
F*F	1	0.000008	0.000008	4.36	0.049
T*T	1	0.000001	0.000001	0.33	0.574
F*T	1	0.000015	0.000015	7.6	0.012
Error	21	0.00004	0.000002		
Lack-of-Fit	3	0.000003	0.000001	0.43	0.734
Pure Error	18	0.000037	0.000002		
Total	26	0.003321			

Dependent Variable: Tensile strength.

Predictors: (Constant), F, T, F*F, T*T, F*T

Table B.19 Model summary for predicting water absorption.

S	R-square	R-square(adjusted)	R-square(predicted)
0.0013823	98.79%	98.50%	98.01%

Table B.20 Matlab codes for the variation of water absorption.

Lines	Codes
1	[x,y]=meshgrid(0:1:30,210:1:230);
2	z=-0.302+0.002356*x+0.000012*x.*x-0.000011*x.*y+0.00292*y-0.000003*y.*y;
3	figure
4	grid on
5	surface(x,y,z)
6	view(3)
7	shading faceted %interp
8	colormap('jet')
9	colorbar

APPENDIX C

Table C.1 Parameter estimation of Equation 4.13 for biocomposites with 10 wt% flax fibers at 210 ℃ by SPSS nonlinear regression.

Parameter	Estimate	Std. Error	95% Confidence Interval	
			Lower Bound	Upper Bound
n0	2177.983	943.582	177.679	4178.288
t	23313.898	11544.241	-1158.801	47786.596

Dependent variable: the shear viscosity of the biocomposite melt (Pa/s);

n0: the zero shear viscosity (Pa/s);

t: the model constant (Pa).

Table C.2 ANOVA of parameter estimation in Table C.1.

Source	Sum of Squares	df	Mean Squares
Regression	2678818.997	2	1339409.498
Residual	128971.838	16	8060.740
Uncorrected Total	2807790.834	18	
Corrected Total	1397827.683	17	

Dependent variable: N

R squared = 1 - (Residual Sum of Squares) / (Corrected Sum of Squares) = 0.908.

Table C.3 Parameter estimation of Equation 4.13 for biocomposites with 20 wt% flax fibers at 210 ℃ by SPSS nonlinear regression.

Parameter	Estimate	Std. Error	95% Confidence Interval	
			Lower Bound	Upper Bound
n0	2724.549	515.783	1645.003	3804.095
t	29998.676	6078.832	17275.535	42721.816

Dependent variable: the shear viscosity of the biocomposite melt (Pa/s);

n0: the zero shear viscosity (Pa/s);

t: the model constant (Pa).

Table C.4 ANOVA of parameter estimation in Table C.3.

Source	Sum of Squares	df	Mean Squares
Regression	4102263.050	2	2051131.525
Residual	42809.692	19	2253.142
Uncorrected Total	4145072.743	21	
Corrected Total	2324065.869	20	

Dependent variable: N

R squared = 1 - (Residual Sum of Squares) / (Corrected Sum of Squares) = 0.908.

Table C.5 Parameter estimation of Equation 4.13 for biocomposites with 30 wt% flax fibers at 210 ℃ by SPSS nonlinear regression.

Parameter	Estimate	Std. Error	95% Confidence Interval	
			Lower Bound	Upper Bound
n0	2616.185	529.855	1507.185	3725.184
t	44077.044	10670.934	21742.522	66411.566

Dependent variable: the shear viscosity of the biocomposite melt (Pa/s);

n0: the zero shear viscosity (Pa/s);

t: the model constant (Pa).

Table C.6 ANOVA of parameter estimation in Table C.5.

Source	Sum of Squares	df	Mean Squares
Regression	5446875.821	2	2723437.910
Residual	104183.382	19	5483.336
Uncorrected Total	5551059.203	21	
Corrected Total	3134753.082	20	

Dependent variable: N

R squared = 1 - (Residual Sum of Squares) / (Corrected Sum of Squares) = 0.908.

Table C.7 Parameter estimation of Equation 4.13 for biocomposites with 10 wt% flax fibers at 220 ℃ by SPSS nonlinear regression.

Parameter	Estimate	Std. Error	95% Confidence Interval	
			Lower Bound	Upper Bound
n0	1533.284	442.581	877.791	3421.562
t	17312.761	9594.207	8518.347	23691.157

Dependent variable: the shear viscosity of the biocomposite melt (Pa/s);

n0: the zero shear viscosity (Pa/s);

t: the model constant (Pa).

Table C.8 ANOVA of parameter estimation in Table C.7.

Source	Sum of Squares	df	Mean Squares
Regression	2047613.619	2	1023806.809
Residual	1947.030	19	102.475
Uncorrected Total	2049560.648	21	
Corrected Total	1095571.422	20	

Dependent variable: N

R squared = 1 - (Residual Sum of Squares) / (Corrected Sum of Squares) = 0.908.

Table C.9 Parameter estimation of Equation 4.13 for biocomposites with 20 wt% flax fibers at 220 ℃ by SPSS nonlinear regression.

Parameter	Estimate	Std. Error	95% Confidence Interval	
			Lower Bound	Upper Bound
n0	2197.614	150.791	1882.005	2513.223
t	25177.610	1134.215	12803.671	27551.550

Dependent variable: the shear viscosity of the biocomposite melt (Pa/s);

n0: the zero shear viscosity (Pa/s);

t: the model constant (Pa).

Table C.10 ANOVA of parameter estimation in Table C.9.

Source	Sum of Squares	df	Mean Squares
Regression	2047613.619	2	1023806.809
Residual	1947.030	19	102.475
Uncorrected Total	2049560.648	21	
Corrected Total	1095571.422	20	

Dependent variable: N

R squared = 1 - (Residual Sum of Squares) / (Corrected Sum of Squares) = 0.908.

Table C.11 Parameter estimation of Equation 4.13 for biocomposites with 30 wt% flax fibers at 220 ℃ by SPSS nonlinear regression.

Parameter	Estimate	Std. Error	95% Confidence Interval	
			Lower Bound	Upper Bound
n0	2444.494	169.307	2090.130	2798.858
t	33587.698	945.814	11608.086	45567.311

Dependent variable: the shear viscosity of the biocomposite melt (Pa/s);

n0: the zero shear viscosity (Pa/s);

t: the model constant (Pa).

Table C.12 ANOVA of parameter estimation in Table C.11.

Source	Sum of Squares	df	Mean Squares
Regression	2000707.347	2	1000353.674
Residual	1471.907	19	77.469
Uncorrected Total	2002179.254	21	
Corrected Total	1081433.985	20	

Dependent variable: N

R squared = 1 - (Residual Sum of Squares) / (Corrected Sum of Squares) = 0.908.

Table C.13 Parameter estimation of Equation 4.13 for biocomposites with 10 wt% flax fibers at 230 ℃ by SPSS nonlinear regression.

Parameter	Estimate	Std. Error	95% Confidence Interval	
			Lower Bound	Upper Bound
n0	628.515	63.649	489.836	767.195
t	19756.617	4030.776	10974.310	28538.923

Dependent variable: the shear viscosity of the biocomposite melt (Pa/s);

n0: the zero shear viscosity (Pa/s);

t: the model constant (Pa).

Table C.14 ANOVA of parameter estimation in Table C.13.

Source	Sum of Squares	df	Mean Squares
Regression	440553.702	2	220276.851
Residual	2903.197	12	241.933
Uncorrected Total	443456.899	14	
Corrected Total	207311.110	13	

Dependent variable: N

R squared = 1 - (Residual Sum of Squares) / (Corrected Sum of Squares) = 0.908.

Table C.15 Parameter estimation of Equation 4.13 for biocomposites with 20 wt% flax fibers at 230 ℃ by SPSS nonlinear regression.

Parameter	Estimate	Std. Error	95% Confidence Interval	
			Lower Bound	Upper Bound
n0	947.267	129.789	661.603	1232.932
t	20778.967	2340.327	5627.941	25929.993

Dependent variable: the shear viscosity of the biocomposite melt (Pa/s);

n0: the zero shear viscosity (Pa/s);

t: the model constant (Pa).

Table C.16 ANOVA of parameter estimation in Table C.15.

Source	Sum of Squares	df	Mean Squares
Regression	490389.254	2	245194.627
Residual	2166.761	11	196.978
Uncorrected Total	492556.015	13	
Corrected Total	219646.642	12	

Dependent variable: N

R squared = 1 - (Residual Sum of Squares) / (Corrected Sum of Squares) = 0.908.

Table C.17 Parameter estimation of Equation 4.13 for biocomposites with 30 wt% flax fibers at 230 ℃ by SPSS nonlinear regression.

Parameter	Estimate	Std. Error	95% Confidence Interval	
			Lower Bound	Upper Bound
n0	864.609	97.204	652.819	1076.399
t	23076.133	2377.444	7896.128	28256.137

Dependent variable: the shear viscosity of the biocomposite melt (Pa/s);

n0: the zero shear viscosity (Pa/s);

t: the model constant (Pa).

Table C.18 ANOVA of parameter estimation in Table C.9-1.

Source	Sum of Squares	df	Mean Squares
Regression	490538.888	2	245269.444
Residual	2059.514	12	171.626
Uncorrected Total	492598.402	14	
Corrected Total	237427.687	13	

Dependent variable: N

R squared = 1 - (Residual Sum of Squares) / (Corrected Sum of Squares) = 0.908.

APPENDIX D

Table D.1 1/4 fractional factorial design for selection of the significant factors.

Run	A	B	C	D	E	F	G
1	-1	-1	-1	-1	-1	1	1
2	-1	-1	-1	1	-1	-1	-1
3	1	1	-1	1	-1	-1	-1
4	-1	-1	1	-1	1	-1	-1
5	-1	1	-1	-1	1	-1	1
6	1	-1	-1	-1	-1	-1	-1
7	-1	-1	1	-1	-1	-1	1
8	-1	1	1	-1	-1	1	-1
9	1	-1	1	-1	1	1	1
10	1	1	1	-1	1	-1	-1
11	1	1	-1	-1	-1	1	1
12	1	-1	-1	1	-1	1	1
13	1	1	1	1	1	1	1
14	1	1	-1	1	1	-1	1
15	1	-1	-1	1	1	1	-1
16	-1	1	-1	1	1	1	-1
17	-1	-1	-1	1	1	-1	1
18	-1	1	1	1	-1	-1	1

19	1	-1	1	-1	-1	1	-1
20	1	-1	-1	-1	1	-1	1
21	-1	1	1	-1	1	1	1
22	-1	-1	-1	-1	1	1	-1
23	-1	-1	1	1	-1	1	-1
24	1	1	1	-1	-1	-1	1
25	-1	-1	1	1	1	1	1
26	1	1	-1	-1	1	1	-1
27	-1	1	-1	1	-1	1	1
28	-1	1	1	1	1	-1	-1
29	1	-1	1	1	-1	-1	1
30	1	-1	1	1	1	-1	-1
31	1	1	1	1	-1	1	-1
32	-1	1	-1	-1	-1	-1	-1

(A) Mold temperature (℃);

(B) Injection time (s);

(C) Injection temperature (℃);

(D) Injection pressure (MPa);

(E) Packing time (s);

(F) Packing pressure (% $P_{injection}$);

(G) Cooling time (s).

Table D.2 Design matrix of BBD for RSM.

Run	Pt Type	Blocks	C	E	F
1	2	1	-1	-1	0
2	0	1	-1	0	1
3	2	1	1	-0	-1
4	2	1	0	1	1
5	0	1	1	-1	0
6	2	1	1	1	0
7	2	1	0	-1	1
8	0	1	-1	1	0
9	2	1	0	0	0
10	2	1	0	1	-1
11	2	1	1	0	1
12	2	1	-1	0	-1
13	2	1	0	-1	-1
14	2	1	0	0	0
15	2	1	0	0	0

(C) Injection temperature (℃);

(E) Packing time (s);

(F) Packing pressure (% $P_{injection}$).

Table D.3 NOVA of RSM regression for the warpage.

Source	DF	Adj SS	Adj MS	F-Value	P-Value
Model	9	0.014889	0.001654	37.02	0
Linear	3	0.013139	0.00438	98.01	0
C	1	0.002339	0.002339	52.35	0.001
E	1	0.010768	0.010768	240.96	0
F	1	0.000032	0.000032	0.71	0.439
Square	3	0.000824	0.000275	6.14	0.039
C*C	1	0.000072	0.000072	1.61	0.261
E*E	1	0.000587	0.000587	13.14	0.015
F*F	1	0.000103	0.000103	2.31	0.189
2-Way Interaction	3	0.000926	0.000309	6.91	0.031
C*E	1	0.000876	0.000876	19.61	0.007
C*F	1	0.000048	0.000048	1.07	0.349
E*F	1	0.000003	0.000003	0.06	0.815
Error	5	0.000223	0.000045		
Lack-of-Fit	3	0.000223	0.000074	*	*
Pure Error	2	0	0		
Total	14	0.015112			

Dependent variable: Warpage (mm);

(C) Injection temperature (℃);

(E) Packing time (s);

(F) Packing pressure (% $P_{injection}$).

Table D.4 Model summary for Table D.3.

S	R-sq	R-sq(adj)	R-sq(pred)
0.006685	98.52%	95.86%	92.34%

Table D.5 Predicted coefficients of RSM regression for the warpage.

Term	Effect	Coef	SE Coef	T-Value	P-Value	VIF
Constant		0.3256	0.00386	84.36	0	
C	0.0342	0.0171	0.00236	7.24	0.001	1
E	-0.07337	-0.03669	0.00236	-15.52	0	1
F	-0.00397	-0.00199	0.00236	-0.84	0.439	1
C*C	-0.00883	-0.00441	0.00348	-1.27	0.261	1.01
E*E	0.02523	0.01261	0.00348	3.63	0.015	1.01
F*F	-0.01057	-0.00529	0.00348	-1.52	0.189	1.01
C*E	-0.0296	-0.0148	0.00334	-4.43	0.007	1
C*F	-0.0069	-0.00345	0.00334	-1.03	0.349	1
E*F	-0.00165	-0.00083	0.00334	-0.25	0.815	1

Dependent variable: Warpage (mm);

(C) Injection temperature (℃);

(E) Packing time (s);

(F) Packing pressure (% $P_{injection}$).

Table D.6 ANOVA of RSM regression for the shrinkage.

Source	DF	Adj SS	Adj MS	F-Value	P-Value
Model	9	117.018	13.0019	67.67	0
Linear	3	96.233	32.0776	166.96	0
C	1	3.926	3.9256	20.43	0.006
E	1	92.283	92.2829	480.32	0
F	1	0.024	0.0243	0.13	0.737
Square	3	19.955	6.6518	34.62	0.001
C*C	1	3.205	3.2046	16.68	0.01
E*E	1	14.852	14.8524	77.31	0
F*F	1	0.488	0.4875	2.54	0.172
2-Way Interaction	3	0.829	0.2765	1.44	0.336
C*E	1	0.808	0.8082	4.21	0.096
C*F	1	0	0	0	0.997
E*F	1	0.021	0.0212	0.11	0.753
Error	5	0.961	0.1921		
Lack-of-Fit	3	0.961	0.3202	*	*
Pure Error	2	0	0		
Total	14	117.978			

Dependent variable: Shrinkage (%);

(C) Injection temperature (℃);

(E) Packing time (s);

(F) Packing pressure (% $P_{injection}$).

Table D.7 Model summary for Table D.6.

S	R-sq	R-sq(adj)	R-sq(pred)
0.438323	99.19%	97.72%	86.97%

Table D.8 Predicted coefficients of RSM regression for the shrinkage.

Term	Effect	Coef	SE Coef	T-Value	P-Value	VIF
Constant		7.078	0.253	27.97	0	
Constant	1.401	0.7	0.155	4.52	0.006	1
C	-6.793	-3.396	0.155	-21.92	0	1
E	-0.11	-0.055	0.155	-0.36	0.737	1
F	-1.863	-0.932	0.228	-4.08	0.01	1.01
C*C	4.011	2.006	0.228	8.79	0	1.01
E*E	-0.727	-0.363	0.228	-1.59	0.172	1.01
F*F	-0.899	-0.45	0.219	-2.05	0.096	1
C*E	0.002	0.001	0.219	0	0.997	1
C*F	-0.146	-0.073	0.219	-0.33	0.753	1

Dependent variable: Shrinkage (%);

(C) Injection temperature (℃);

(E) Packing time (s);

(F) Packing pressure (% $P_{injection}$).